UNIVERSITY OF NAPLES
"FEDERICO II"

Faculty of Mathematical, Physical and Natural Sciences

phD Thesis in Chemical Sciences
XXV cycle

Extremophile bacteria glycolipids: structure and biological activity

SARA CARILLO

Tutor
Ch.ma Prof.ssa Maria Michela Corsaro

Supervisor
Ch.mo Prof. Giovanni Palumbo

Alla mia famiglia…
quella vecchia e quella nuova

Summary

Introduction

Psychrophiles

Haloalkaliphiles

Experimental Part

Abbreviations

AA	Alditol Acetate
AFPs	Antifreeze Proteins
Ala	L-Alanine
AMG	acetylated *O*-methyl glycosides
CD14	Cluster of differentiation 14
Col	3,6-dideoxy-L-*xylo*-hexose
CPS	Capsular Polysaccharide
CSD	Capillary Skimmed Dissociation
D,D-Hep	D-*glycero*-D-*manno*-heptose
DOC-PAGE	DeOxyCholate PolyAcrylamide Gel Electrophoresis
DQF-COSY	Double Quantum Filter-Correlation SpectroscopY
EPS	Exopolysaccharide
ESI FT-ICR	ElectroSpray Ionization Fourier Transform-Ion Cyclotron Resonance
Et_3N	Triethilamine
GAG	GlycosAmino Glycans
Gal	D-galactose
GalA	D-galacturonic acid
GalN	2-deoxy-2-amino-D-galctose
GC-MS	Gas Chromatography interfaced with Mass Spectrometry
Glc	D-glucose
GlcA	D-glucuronic acid
GlcN	2-deoxy-2-amino-D-glucose
Gro	Glycerol
HMBC	Heteronuclear Multiple Bond Correlation
HPAEC-PAD	High Pressure Anion Exchange Chromatography – Pulsed Amperometric Detection
HPLC	High Performance Liquid Chromatography

HSQC	Heteronuclear Single Quantum Correlation
IL-6	Interleukin-6
IRMPD	InfraRed MultiPhoton Dissociation
Kdo	3-deoxy-D-manno-oct-2-ulosonic acid
L,D-Hep	L-*glycero*-D-*manno*-heptose
LOS	Lipooligosaccharide
LPS	Lipopolysaccharide
Mal	Myelin and lymphocyte protein
MALDI-TOF	Matrix Assisted Laser Desorption Ionization – Time Of Flight
Man	D-mannose
MD-2	myeloid differentiation factor 2
MPLA	monophosphoryl lipid A
MyD88	Myeloid differentiation primary response gene (88)
NMR	Nuclear Magnetic Resonance
NOE	Nuclear Overhauser Effect
P	$-PO_4^{-3}$
PAMPs	Pathogen Associated Molecular Patterns
PCP	Petroleum Ether/Chloroform/Phenol 90%
PMAA	Partially Methylated Alditol Acetate
Rha	6-deoxy-L-mannose
ROESY	Rotating frame Overhauser Effect Spectroscopy
SDS-PAGE	Sodium Dodecyl Sulphate PolyAcrylamide Gel Electrophoresis
TEM	Trasmission Electronic Microscopy
TFA	trifluoroacetic acid
THP-1	Human acute monocytic leukemia cell line
Thr	L-Threonine
TIR	Toll-IL-1 receptor
TLRs	Toll-like receptors
TNFα	Tumor necrosis factor α

TOCSY	Total Correlation Spectroscopy
TRAM	TRIF-related adaptor molecule
TRIF	TIR-domain-containing adapter-inducing interferon-β
ZPS	Zwitterionic polysaccharide

Abstract

Extremophile bacteria are able to survive in harsh life conditions, such as high or low temperatures (thermophiles and psychrophiles, respectively), high pressure (barophiles), high or low pH values (acidophiles or alkalophiles), environments characterized by high salt concentrations (halophiles).

Structural features of the macromolecules belonging to the external layer are fundamental in adaptation mechanisms, e.g. it is well known that halophiles membrane phospholipids showed an increased negative charge density, while in psychrophiles these molecules display shorter acyl chains and higher unsaturation degree.

In Gram-negative bacteria, 75% of the outer membrane is constituted by lipopolysaccharides (LPSs). Consequently they play a key role in the adaptation and survival in extreme life conditions. Nevertheless, very few LPSs isolated from extremophilic bacteria has been characterized so far.

LPS are constituted by three covalently linked regions:

- lipid A, which is the glycolipidic portion of the macromolecule. It is the most conservative region between bacteria belonging to the same genus and represents the minimal endotoxic structural motif;
- core region, which is an oligosaccharidic portion where it is possible to find LPSs peculiar monosaccharides, such as heptoses and Kdo (3-deoxy oct-2-oulosonic acid);
- O-chain, which is the polysaccharidic region, not always expressed by the bacterium. Moreover, O-chain is highly variable even among bacteria belonging to the same species.

Beside the structural characterization of LPS, aimed at adaptation mechanisms comprehension, also their biological activity is worth being investigated. In fact extremophilic

bacteria are rarely found to be pathogen, so they are source of lipid A with potential anti-inflammatory (antagonist) or adjuvant activity.

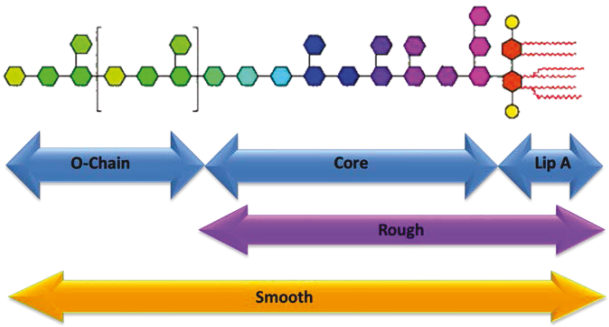

During this phD work, the LPSs from three haloalkaliphilic and two psychrophilic bacteria has been investigated.
Each LPS has been extracted from dried cells, then purified and analysed by chemical analysis, NMR spectroscopy and mass spectrometry.

As for the haloalkaliphilic bacteria, the LPSs belonging to *Halomonas alkaliantarctica* strain CRSS, *Halomonas stevensii* strain S18214 and *Salinivibrio sharmensis* strain BAG^T were completely characterized.

By comparing the structures obtained, especially for core oligosaccharides, it is possible to speculate that they are all characterized by high negative charge density, due to phosphate groups, usually linked to Kdo and lipid A saccharidic residues, or to uronic acids.

Such structural elements contribute to the tightness of the outer-membrane and decrease the ion permeability, due to the association of LPS molecules through divalent cations (Ca^{2+} and Mg^{2+}).

Moreover, lipid A structural characterization of lipid A from *H. stevensii* and *S. sharmensis* has been carried out.

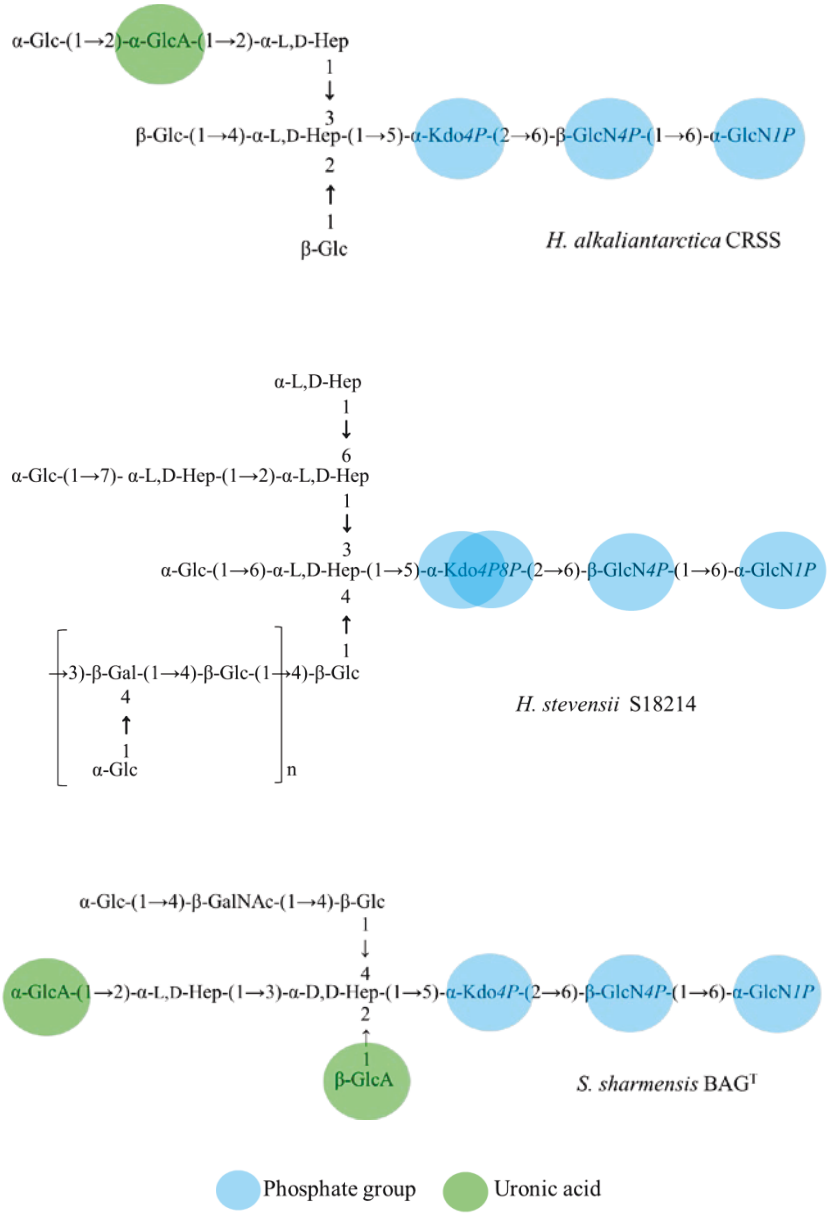

Both the psychrophilic bacteria *Pseudoalteromonas haloplanktis* strain TAB 23 and *Colwellia psychrerythraea* strain 34H expressed a rough-LPS. The core and lipid A

structures were obtained. Moreover, biological assays on both lipid A were performed.

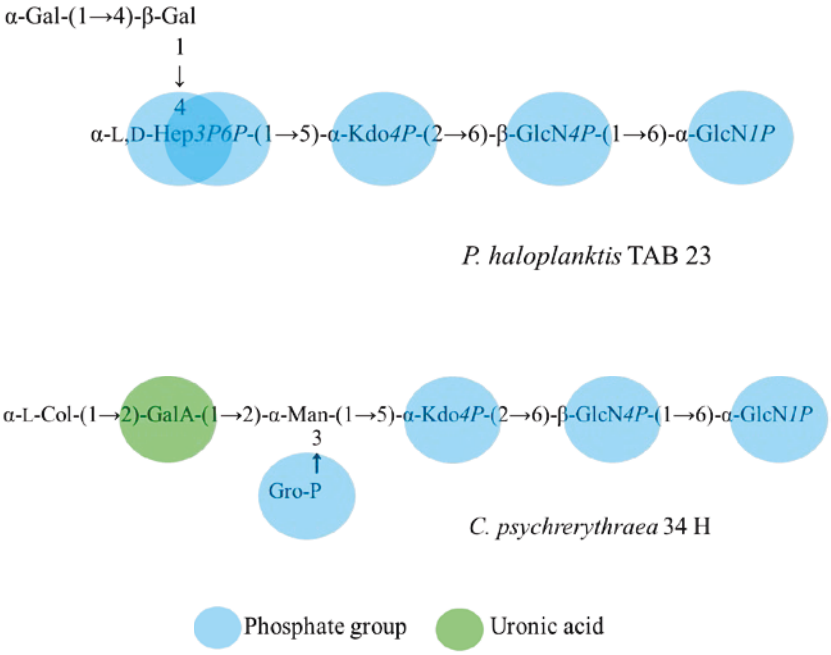

The structural common features of these two bacteria are the high negative charge density and the lack of the O-chain. The first helps membrane permeability, allowing bacterial survival in marine environment, where these microorganisms are often isolated. The second characteristic was found in all known LPS from psychrophiles and can be explained as a consequence of cell economy: O-chain biosynthesis is an energy-demanding process avoided by the organisms in low-temperature life conditions.

As for the lipid A structures, they both share the presence of short and unsaturated fatty acids chains, as already found in psychrophilic bacteria membrane phospholipids. Moreover, the

TNFα production was not elicited in both cases, and for *P. haloplanktis* TAB 23 lipid A an inhibitory activity was found.

These results led to a deeper knowledge of halo- and cold adaptation mechanisms in Gram-negative bacteria. Moreover, molecules with different and interesting physicochemical and biological properties has been isolated and characterized.

It is evident that extremophilic bacteria are an important source of biomolecules of which probably nowadays only the peak of the iceberg is known.

Papers related to this thesis work

1. "Structural characterization of the core oligosaccharide isolated from the lipopolysaccharide of the psychrophilic bacterium *Colwellia psychrerythraea* strain 34H."

Carillo S, Pieretti G, Lindner , Parrilli E, Sannino F, Tutino ML, Lanzetta R, Parrilli M, Corsaro MM.
Eur J Org Chem. *In press*

2. "The lipid A from the haloalkaliphilic bacterium *Salinivibrio sharmensis* strain BAG^T."

Carillo S, Pieretti G, Lindner B, Romano I, Nicolaus B, Lanzetta R, Parrilli M, Corsaro MM.
Marine Drugs. **2013**; 11(1): 184-93.

3. "Structural characterization of the core oligosaccharide isolated from the lipopolysaccharide of the haloalkaliphilic bacterium *Salinivibrio sharmensis* strain BAG^T."

Carillo S, Pieretti G, Lindner B, Romano I, Nicolaus B, Lanzetta R, Parrilli M, Corsaro MM.
Carbohydr Res. **2013**; 368: 61-7.

4. "Characterization of the core oligosaccharide and the O-antigen biological repeating unit from *Halomonas stevensii* lipopolysaccharide: the first case of O-antigen linked to the inner core."

Pieretti G, Carillo S, Lindner B, Kim KK, Lee KC, Lee JS, Lanzetta R, Parrilli M, Corsaro MM.
Chemistry. **2012**; 18(12):3729-35.

5. "Structural investigation and biological activity of the lipooligosaccharide from the psychrophilic bacterium *Pseudoalteromonas haloplanktis* TAB 23."

Carillo S, Pieretti G, Parrilli E, Tutino ML, Gemma S, Molteni M, Lanzetta R, Parrilli M, Corsaro MM.
Chemistry. **2011**; 17(25):7053-60.

6. "O-chain structure from the lipopolysaccharide of the human pathogen *Halomonas stevensii* strain S18214."

Pieretti G, Carillo S, Kim KK, Lee KC, Lee JS, Lanzetta R, Parrilli M, Corsaro MM.
Carbohydr Res. **2011**; 346(2):362-5.

7. "Structural characterization of the core region from the lipopolysaccharide of the haloalkaliphilic bacterium *Halomonas alkaliantarctica* strain CRSS."

Pieretti G, Carillo S, Nicolaus B, Poli A, Lanzetta R, Parrilli M, Corsaro MM.
Org Biomol Chem. **2010**; 8(23):5404-10.

Papers do not related to this thesis work

1. "Structural characterization of the O-chain polysaccharide from an environmentally beneficial bacterium *Pseudomonas chlororaphis* subsp. *aureofaciens* strain M71."

Pieretti G, Puopolo G, Carillo S, Zoina A, Lanzetta R, Parrilli M, Evidente A, Corsaro MM.
Carbohydr Res. **2011**; 346(17):2705-9.

2. "Structural determination of the O-specific polysaccharide from *Aeromonas hydrophila* strain A19 (serogroup O:14) with S-layer."

Pieretti G, Carillo S, Lanzetta R, Parrilli M, Merino S, Tomás JM, Corsaro MM.
Carbohydr Res. **2011**; 346(15):2519-22.

3. "A novel alpha-D-galactosynthase from *Thermotoga maritima* converts beta-D-galactopyranosyl azide to alpha-galacto-oligosaccharides."

Cobucci-Ponzano B, Zorzetti C, Strazzulli A, Carillo S, Bedini E, Corsaro MM, Comfort DA, Kelly RM, Rossi M, Moracci M.
Glycobiology. **2011**; 21(4):448-56.

4. "The complete structure of the core of the LPS from *Plesiomonas shigelloides* 302-73 and the identification of its O-antigen biological repeating unit."

Pieretti G, Carillo S, Lindner B, Lanzetta R, Parrilli M, Jimenez N, Regué M, Tomás JM, Corsaro MM.
Carbohydr Res. **2010**; 345(17):2523-8.

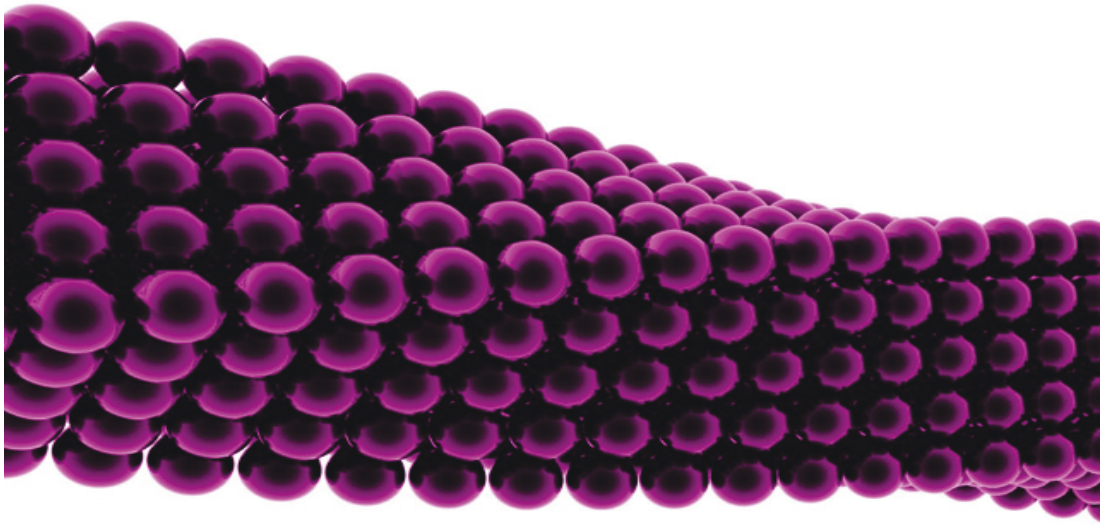

Introduction

Chapter 1

Life in Extreme Environments

Life is everywhere on earth, even where it was thought to be impossible. The anthropocentric way of considering "normal" the parameters required for human life, led to the conception of "extremophile" as an organism able to survive in inhuman habitat, such as natural niches characterized by high or low temperatures, high pressure, high salinity, high limits of pH range or desiccation. The term "extremophiles" was first coined by MacElroy in 1974 and since then many prohibitive habitat where life was able to proliferate were discovered.

Extremophilic organisms may be located in all the three dominia and include prokaryotic and eukaryotic cells.

To survive in these harsh life conditions, extremophiles have developed many adaptation strategies, including structural modification of their biomolecules. These changes concern mostly molecules belonging to the cellular membrane, being the first to come in contact with the external environment, or even molecules secreted outside the cell, like exopolysaccharides, which are able to protect the cell through biofilms formation.

These organisms have been classified on the basis of their optimal proliferation conditions; for example, an organism able to survive at high temperature (above 55°C) is called thermophilic as well as an organism which thrives in habitats characterized by low pH values (below pH 3) is called acidophile. Nevertheless, it is possible to deal with polyextremophiles (Rothschild and Mancinelli, 2001), which are isolated from environments where two or more extreme conditions are verified simultaneously (for example, marine Arctic and Antarctic habitats, characterized by low temperatures and high salt concentrations). The main types of

extremophiles are summarized in Table 1.1 (Rothschild and Mancinelli, 2001). Moreover, whether the extreme parameter is required for their proliferation or just tolerated, the organisms may be divided in obligate or facultative extremophiles.

The occurrence of extremophiles on earth has brought the studies on evolution into question. In fact, the majority of extremophilic microorganisms belongs to hyperthermophilic Archaea which are considered the most ancient form of life; the study of their cells constituents is mandatory to understand the origin and development of life. Moreover, extreme life conditions may be found elsewhere in the solar system (Canganella and Wiegel, 2011); as a consequence, the study of extremophiles could help the research of life outside the earth.

Table 1.1 – Classification of extremophilic microorganisms.

Environmental parameter	Type	Definition
Temperature	Hyperthermophiles	>80°C
	Thermophiles	60-80°C
	Mesophiles	15-60°C
	Psychrophiles	<15°C
Pressure	Barophiles	Weight-loving
	Piezophiles	Pressure-loving
Dessication	Xerophiles	Anhydrobiotic
Salinity	Halophiles	Salt-loving (2-5 M NaCl)
pH	Alkaliphiles	High pH-loving (pH>9)
	Acidophiles	Low pH-loving

Another important point is the new direction that extreme organisms, especially microorganisms, has given to biotechnology. In fact, enzymes able to work under peculiar conditions are very attractive for many industrial and biotechnological applications as demonstrated by the number of studies carried out about these

"extremozymes" during the last decades (Hough and Danson, 1999).

The present work was focused on the structural characterization of the saccharidic and glycolipid constituents of extremophilic Gram-negative bacteria membrane. In fact, besides membrane phospholipids and proteins, microorganisms exposed to the same external stressors should modify similarly their LPSs too.

In particular, psycrophiles and haloalkaliphiles bacteria were investigated. Consequently a deeper insight into these two classes of extremophiles is provided in next sections, as well as an overview on the architecture and saccharidic components of Gram-negative bacteria cell wall.

1.1 Psychrophiles

In 1975 Morita proposed the definition usually given to psychrophiles: microorganisms with optimum growth temperature below 15°C and upper cardinal temperatures of ~20°C. However, the temperature range does not correspond to any clear separation of biological process or environmental conditions. Moreover, there are some microorganisms named psychrotolerant with an optimum growth temperature above 20°C, but able to proliferate below 5°C. A great number of eukaryotic organisms are psychrophiles; among them polar fishes are the most studied to understand the molecular mechanisms involved in the adaptation to low temperatures (Verde *et al.*, 2008). However, Archaea and Bacteria represent the majority of psychrophilic organisms in terms of species diversity. To survive in Arctic and Antarctic habitats eukaryotic and prokaryotic cells have to face several difficulties, depending on the specific habitat they occupy (Casanueva *et al.*, 2010). For example, besides the resistance to low temperatures, Antarctic soil organisms experience desiccation, low nutrient level and high radiation, while marine microorganisms generally add to their stressors, high pressure and

salt concentration. In order to reduce the transition temperature from liquid to gel phase, they enhance membrane fluidity providing themselves with a number of unsaturated fatty acids, short or branched carbon chain fatty acids with a *-anteiso* to *-iso* ratio higher compared to mesophilic microorganisms (Chattopadhyay, 2006) (Figure 1.1).

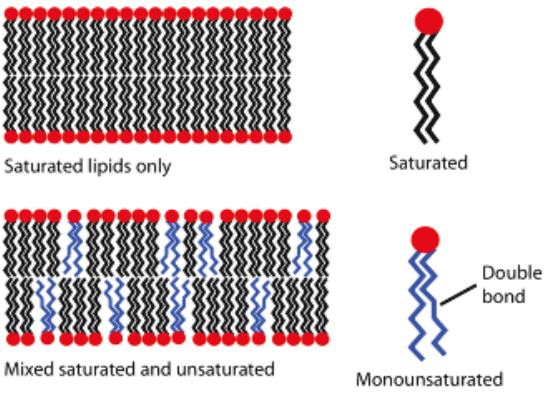

Figure 1.1 – Fatty acids in phospholipids bilayer in psychrophiles.

Such a lipid composition decrease packing efficiency of the phospholipids bilayer, increasing the membrane fluidity. Moreover, like other extremophiles (thermophiles, xerophiles) which need to preserve cells swelling, psychrophiles gather high intracellular concentration of some organic and inorganic small molecules named "compatible solute" (Welsh, 2000), such as K^+ ions or glycine, betaine, glycerol, trehalose, mannitol, sorbitol and other highly soluble poly-hydroxylated compounds, (Casanueva *et al.*, 2010) that also help to reduce the freezing point of cytoplasm and stabilize enzymes. In the adaptation to cold temperatures, an important role is carried out by several groups of proteins. Antifreeze proteins (AFPs, Figure 1.2) and Ice-binding proteins

(IBPs) are able to bind to ice thus preventing ice-crystal growth. Moreover, psychrophiles biosynthesise cold-shock proteins (Csps), the expression of which in mesophilic microorganisms is induced only through the exposure to low temperature.

Figure 1.2 - Structure of the *Tenebriomolitor* beta-helical antifreeze protein. (Adapted from: Daley ME, Spyracopoulos L, Jia Z, Davies PL, Sykes BD (April 2002). "Structure and dynamics of a beta-helical antifreeze protein". Biochemistry 41 (17): 5515–25)

Nevertheless, all proteins and enzymes face structural modifications in order to maintain their functionality, which is compromised by climatic situation as low temperatures decrease enzymatic reaction efficiency. In particular, by comparing proteins homologous from mesophilic and thermophilic microrganisms, it seems that this problem has been overcome increasing protein flexibility, especially in the active site pocket (Casanueva *et al.*, 2010).

1.2 Haloalkaliphiles

Usually haloalkaliphilic bacteria have been isolated from samples of soil, water, sediment and a number of other sources obtained from hypersaline soda lakes.

Halophiles microorganisms are present in all three dominia and have an optimum growth above 3% salt concentration; in particular

between 3 and 15% they are considered moderate halophiles, while above 15% and up to saturation, extreme halophiles. Moreover, hypersaline environments can be divided into two main types: thassohaline and athassohaline, depending on whether they originated from seawater or not. Soda lakes are among athassohaline environments which are widespread worldwide and they are the perfect habitat for haloalkaliphilic bacteria. In fact, in soda lakes water contains low amounts of Mg^{2+} and Ca^{2+} and is near-saturated with sodium salts, especially chloride, carbonate and bicarbonate; consequently, the pH is generally around 10. To survive in high pH and salt concentration conditions, microorganisms have to maintain an internal osmotic pressure equal to that of the surrounding medium. This condition may be achieved by accumulating non-toxic inorganic ions (true halophilic) or organic "compatible solute" (halotolerant microorganisms). Also proteins and enzymes structure and composition are regulated to face the elevated salt concentration: their primary structure presents an excess ratio of acidic to basic amino acids. Moreover, the stability of these proteins is achieved only in the presence of salts and their enzymes require salts for activity (Shivanand and Mugeraya, 2011). In addition, the cell envelope and the phospholipid bilayer are important for the survival in extreme haloalkaliphilic conditions. To manage the high salt concentration outside the cell the nature of lipids is modified in order to increase ion permeability of the cell; in particular, the presence of negatively charged phospholipids increases at the expense of neutral ones. Moreover, integral membrane proteins acting as ion pumps are present to contrast the constant influx of Na^{+} ions. (Ventosa *et al.*, 1998)

1.3 Industrial and biotechnological applications

Among the countless molecules derived from the bacteria world and with a potential use in industrial and biotechnological processes, certainly enzymes represent the majority. These 'extremozymes', offer new opportunities for biocatalysis, biotransformations and protein engineering (Hough and Danson, 1999). The typical example of extremophile-derived enzymes in biotechnology is the source of Taq polymerase (isolated from the thermophilic bacterium *Thermus aquaticus*, an organism discovered in 1969 in Yellowstone National Park, Wyoming) used in polymerase chain reaction (PCR) (Brock and Freeze, 1969).

A rapid look on the principal applications of psychrophiles and haloalkaliphiles derived molecules now will be given.

Cold-adapted enzymes are of great interest because their employment could avoid heating and consequently save energy. This is very important, especially in food industry since this could prevent heat-sensitive substrates from chemical degradation. Some examples of applications of psychrophile enzymes are reported in Table 1.2 (Cavicchioli *et al.*, 2002).

Table 1.2 –Biotechnological application of cold-active enzyme. (Cavicchioli *et al.*, 2002)

Enzyme	Organism	Applications	Refs
RNA polymerase	*Pseudomonas syringae*	Molecular biology	Uma *et al.*, 1999
DNA ligase	*Pseudoalteromonas haloplanktis*	Molecular biology	Georlette *et al.*, 2000
β-galactosidase	*Camobacterium piscicola* BA	Diary industries	Coombs *et al.*, 1999
Alcohol dehydrogenase	*Moraxella sp* TAE 123	Asymmetric chemical synthesis	Tsigos *et al.*, 1998
Metalloprotease	*Sphingomonas paucimobilis*	Food, detergents, molecular biology	Turkiewicz *et al.*, 1999

As for alkaliphilic microorganisms their proteases are widely used as additives in some detergents. In particular we are dealing with cellulases, amylases and lipases, which are produced from *Bacillus* species, the most characterized organisms among alkaliphiles. This kind of enzymes often show activities in a broad pH range, thermostability and increased tolerance to oxidants compared to neutral enzymes (Fujinami and Fujisawa, 2010).

Besides enzymes, many compatible solutes are of industrial interest as stabilizers. For example, molecules such as glycine betaine, glycerol, ectoines (Figure 1.2) are used. The latter is produced by a process called "bacterial milking" (Oren, 2010; Sauer and Galinski, 1998; Nagata *et al.*, 2007) from moderately halophiles (*Halomonas elongata*) and is used in cosmetic products.

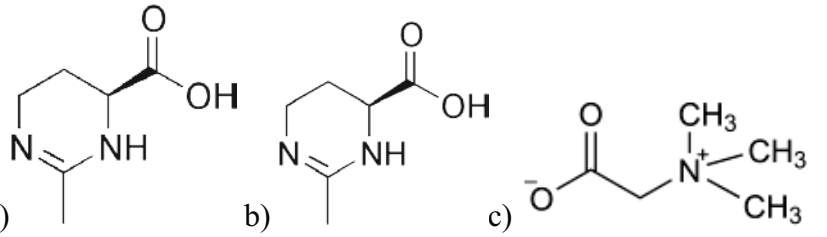

Figure 1.2 – Chemical structures of "compatible solute" ectoine (a), hydroxyectoine (b) and glycine betaine (c)

Another example of industrially relevant molecules obtained by halophiles is β-carotene, a pigment used as antioxidant, as a source of pro-vitamin A (retinol) and as a food colouring agent. It is derived by the green algae *Dunaliella salina* (Figure 1.3) and *D. bardawil* (Raj *et al.*, 2007).

Another class of molecules obtained from extremophilic bacteria and exploited in many industrial processes is that of biopolymers (polysaccharides, polyesters, polyamides). They enhance bacterial survival in harsh life conditions thanks to their physicochemical properties. These molecules are of great interest for industries because they could be employed in several fields ranging from

wastewater treatment to medical applications (tissue engineering, drug delivery) (see Section 2.3).

Figure 1.3 – Green algae *Dunaliella salina*

For example, poly-β-hydroxyalkanoate (PHA), a polymer containing β-hydroxybutyrate and β-hydroxyvalerate units, is accumulated by Bacteria as well as Archaea as a storage polymer. It is used for the production of biodegradable plastics ('biological polyesters') with properties resembling that of polypropylene and is currently produced using the bacterium *Cupravidus necator*. Another halophilic candidate for PHA production is *Halomonas boliviensis* (*Gammaproteobacteria*) (Quillaguamán *et al.*, 2006). It can accumulate the compound up to 88% of its dry weight. As for exopolysaccharides, among the halophilic representatives of the Bacteria, the *Halomonas* species (*H. maura*, *H. eurihalina*) shows considerable production of an extracellular polyanionic polysaccharide, a potent emulsifying agent that exhibits a pseudoplastic behaviour (Calvo *et al.*, 2002). Yet, another exopolysaccharide obtained from *H. maura* ('mauran') has also been shown to be an immunomodulator (Arias *et al.*, 2003).

Chapter 2

Gram-negative bacteria

Bacteria domain includes prokaryotic organisms that are ubiquitous. In fact, they can be found in all kind of habitats, for example in soil, water, glaciers, acid hot springs or organic matter. As bacteria are widespread, they always need to communicate or interact with the external environment or host organisms. In particular, bacteria can establish several types of relationships with an host organism, e.g. parasitism, mutualism and commensalism, mediated by molecules belonging to the cell walls; these are the reasons why in eukaryotes as well as in prokaryotes, the study of the cellular membrane constituents is of great interest.

The interaction between human and bacterial world has revealed good and bad aspects: for example, the spread of epidemic diseases and the development of vaccines is counterbalanced by the presence in digestive system of bacteria which are necessary to humans. Crop bacterial diseases destroyed food but, on the other side, bacteria are involved in the nitrogen-fixing process as well. “Good” bacteria are used in fermentation and pasteurization processes or in bioremediation as they are able to use toxic waste as organic source of carbon. Nevertheless, bacteria are more commonly associated with diseases and the research of the best strategy for defeating pathogenic microorganisms involves the majority of the studies.

However, both the fight against diseases and the exploitation of bacterial properties need a deep knowledge of their morphology, physiology and genetic.

2.1 The organization of the outer membrane

The main subdivision between bacteria is made on the basis of the structure of their cell wall, in particular, on the peptidoglycan content. In fact, two types of architecture exist. The Gram-positive bacteria are provided with a plasma membrane (Figure 2.1a) surrounded by a thick peptidoglycan layer which constitutes the outer barrier of the microorganisms; proteins, polysaccharides and teichoic acids are imbedded in the cell wall. The organization of the cell wall in Gram-negative bacteria (Figure 2.1b) exhibits two phospholipids bilayers. The external one is manly constituted (75%) by lipopolysaccharides. The peptidoglycan layer is much thinner than in Gram-positive bacteria and this is the reason why iodine stain during Gram test is not retained (Figure 2.2).

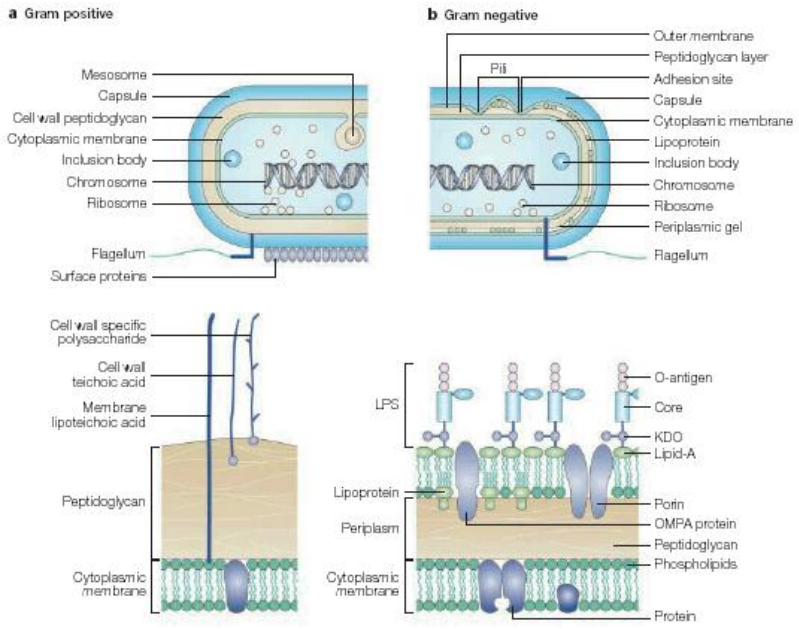

Figure 2.1 – Structural organization of Gram-positive (a) and Gram-negative (b) bacteria cell envelops.

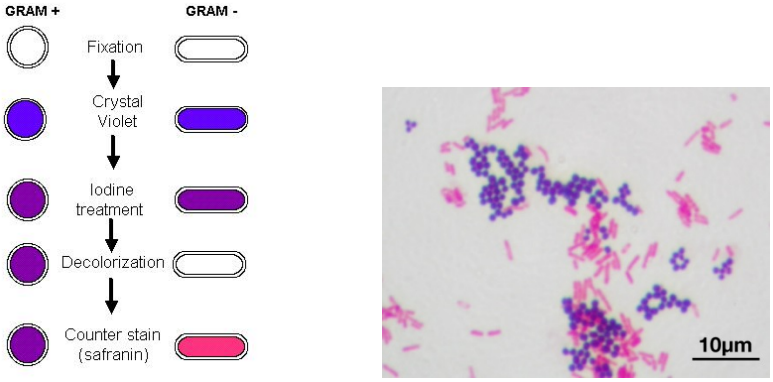

Figure 2.2 – Gram staining procedure and a Gram stain of mixed *Staphylococcus aureus* ATCC 25923 (Gram-positive cocci, in purple) and *Escherichia coli* ATCC 11775(Gram-negative bacilli, in red). Adapted from http://en.wikipedia.org/wiki/Gram_staining

Lipopolysaccharides and peptidoglycans are saccharidic macromolecules necessary for bacterium survival; in fact, the antibiotic mechanism of penicillin acts as an inhibitor of peptidoglycan biosynthesis.

Outside the cell some bacteria express other essential molecules such us S-layer, a rigid envelope constituted by proteins or glycoproteins, which provides the cells with bacteriophages resistance, stabilization of the membrane and capacity to adhere.

Another important extracellular component of bacterial cell wall is the capsular polysaccharide. It usually shows a complex structure and may be associated to the membrane or released in the surrounding medium (slime or exopolysaccharide). As structural elucidation and biological activity of capsule and lipopolysaccharides will be the aim of this thesis, their biological relevance and main features will be discussed in details in next sections.

2.2 Lipopolysaccharides: chemical features and structure

LPSs (Figure 2.3) are amphiphilic macromolecules characterized by a lipid portion, anchored in the phospholipid bilayer of the external membrane, and a saccharidic region of variable length and projected outside the cell.

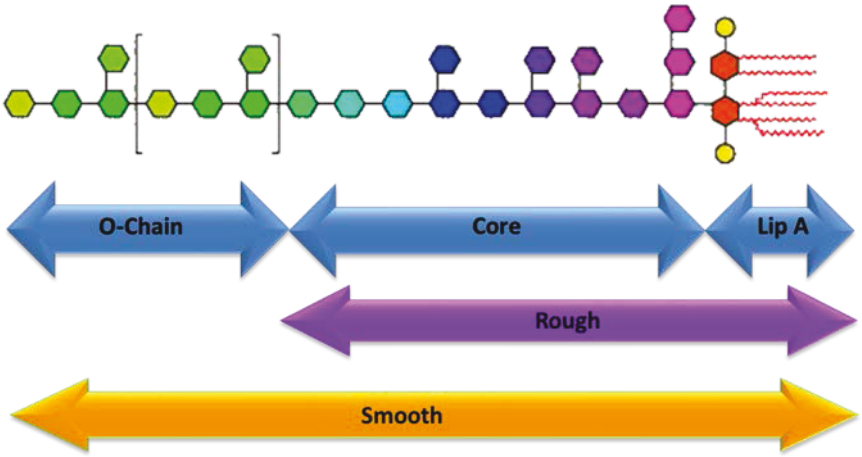

Figure 2.3 –General structure of bacterial lipopolysaccharides.

They are constituted by three regions biosynthetically and chemically different (Caroff and Karibian, 2003). The lipid A is the glycolipid portion of LPS. Being anchored in the phospholipid bilayer, it helps the assembly of cellular membrane.

Chemically, lipid A is constituted by a disaccharidic backbone in which two glucosamines are linked through a β(1→6) glycosidic bond (Figure 2.4). Generally, each glucosamine is substituted at positions 2 and 3 by 3-hydroxylated fatty acids with 10 to 30 carbon atoms; they are marker of LPSs and may bare secondary fatty acids. The lipid A structure comprises two phosphate monoester groups at position 1 of the reducing glucosamine and position 4 of the non-reducing one; additional substituents may be linked on phosphate groups by phosphodiester linkage.

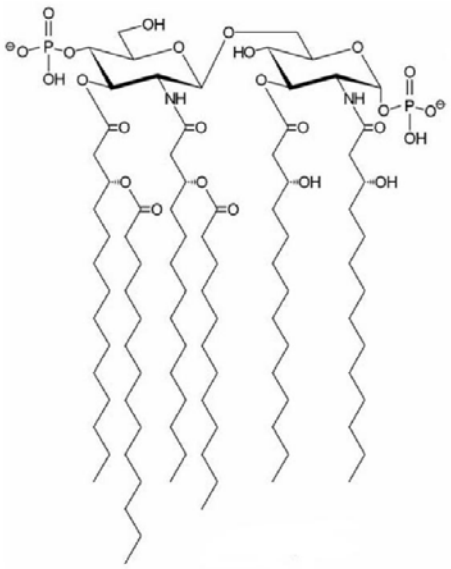

Figure 2.4 – The structure of lipid A portion from the LPS of *Escherichia coli.*

Lipid A is the most conservative portion of the lipopolysaccharides. In fact, lipid A isolated from bacteria belonging to the same species share most of the structural features: i.e. the type of fatty acids linked to the saccharidic backbone (especially 3-hydroxylated fatty acids) or the substituents on phosphate groups (Rietschel *et al.*, 1994). For example, bacteria belonging to *Burkholderia* genus share the presence of arabinosamine residues on lipid A phosphate groups (Holst and Molinaro, 2009).

Lipid A is constituted by a family of molecules with different acylation degrees, from tri- to hepta-acylated species, and different acyl chains length for secondary fatty acids.

The non-reducing glucosamine of lipid A is glycosylated at position 6 by the core oligosaccharidic region of the LPSs. This may be divided in inner and outer core. The inner core is characterized by the presence of peculiar monosaccharides constituted by eight or seven carbon atoms, such as Kdo (3-deoxy-

D-*manno*-oct-2-ulosonic acid) and heptoses (generally L-*glycero*-D-*manno* configured). Like lipid A, this portion is generally conserved between bacteria belonging to the same species. Organic and inorganic substituents (phosphate groups, ethanolamine) may decorate this region. The outer core generally contains hexoses, aminosugars and uronic acids and its chemical structure is more variable between the same genus.

A molecule formed by lipid A and core region is named lipooligosaccharide (LOS) or rough-LPS. Some bacteria express an additional polysaccharidic region (named O-chain), which is highly variable even among two strains of the same bacterium. It glycosylates the core region giving a lipopolysaccharide or smooth-LPS (Caroff and Karibian, 2003). The adjectives "smooth" and "rough" derived from the morphology the two type of LPSs confer to cells.

Each portion of the LPSs has a different biological function. For example, the lipid A and core regions are usually negatively charged in order to maintain the rigidity of cellular membranes by ionic interaction between two LPSs mediated by cations present in the surrounding medium. The same mechanisms seem to be involved in bacterial resistance to antimicrobial peptides, which are positively charged, or in bacterial resistance to hypersaline environment (see Section 1.2). Yet, the O-chain has an important biological role in protection of bacterial cells and it is one of the most important virulence factor in the interaction of bacteria with humans and animals (Knirel, 2009). In fact, being the outermost part of the LPS molecule expressed on bacteria, the O-chain is the major antigen targeted by host antibody responses. These responses can be highly O-chain specific, and for this reason the O-chain is often also referred to as the O-antigen (Erridge *et al.*, 2002).

2.3 Exopolysaccharides: slime and capsule

Some bacteria can produce polysaccharides secreted outside cell wall. Usually, the production of these polysaccharides is recognisable from the mucoid morphology of the colony, while in liquid medium, cultures may appear very viscous or even solidify as a gel. As mentioned above, this polysaccharidic material may remain associated to cellular membrane (capsule, CPS) or be released in the surrounding medium like a slime. Yet, exopolysaccharides may be part of a biofilm, a complex matrix of microorganisms in which living cells adhere to each other on a solid surface (Figure 2.5). The polymeric materials contained in the biofilm allow communication among the single cells and constitute a "food reservoir" by means of water channels that allow distribution of nutrients and signalling molecules (Hall-Stoodley, 2004).

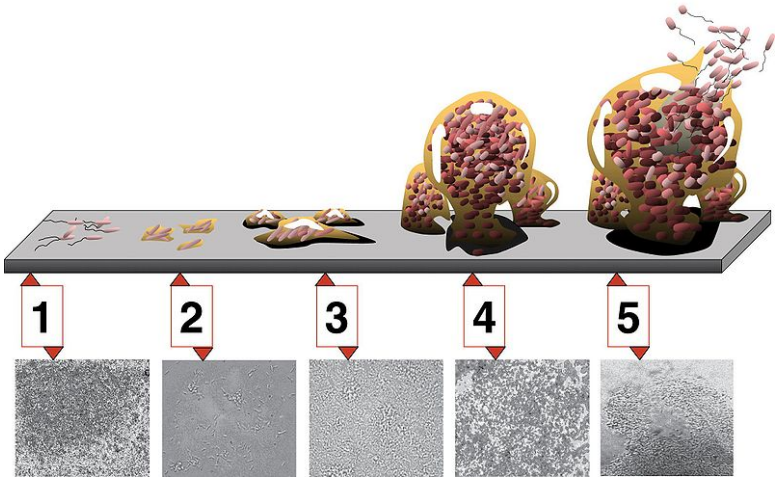

Figure 2.5 -5 stages of biofilm development. Stage 1, initial attachment; stage 2, irreversible attachment; stage 3, maturation I; stage 4, maturation II; stage 5, dispersion. Each stage of development in the diagram is paired with a photomicrograph of a developing *Pseudomonas aeruginosa* biofilm. Adapted from http://en.wikipedia.org/wiki/Biofilm

Capsule plays an important role both in protection and communication of the cell with the external environment. In fact, it contains water and ions which prevent bacteria desiccation or help them in hypersaline environments.

Moreover, they are involved in cell-cell recognition, as well as in aiding attachment to biotic (e.g. epithelial and endothelial cells) and abiotic (i.e. mineral surfaces or medical implant) surfaces. Capsular polysaccharide are considered as virulence factor because they enhance the ability of bacteria to cause disease, preventing phagocytosis and enhancing cell adhesion to host tissues (Bazaka *et al.*, 2011). For example, *Streptococcus pneumoniae* causes diseases such as otitis media, pneumonia, bacteraemia, and meningitis, or is carried by the host asymptomatically depending on the capsular serotype of bacterial strain (Bogaert *et al.*, 2004; Lipsitch and O'Hagan, 2007). As capsular polysaccharides of *S. pneumoniae* are often target of the immune system, (Janeway *et al.*, 2001) they are also used for vaccination. (Black *et al.*, 2000)

As a consequence of their properties, capsular polysaccharides are often studied to exploit them in industrial processes. One of the main application of EPS from marine bacteria is the decontamination of polluted sites, for example from heavy metals. This application exploit the anionic nature of EPS, which are able, consequently, to chelate pollutants.

Food, pharmaceutical and cosmetic industries are more interested in physical properties of EPS, like high viscosity, gelling capacity or high resistance in wide range of temperature and pH (Freitas *et al.,* 2011). Other EPS are appealing because of their biological activity. For example, xanthan, sulphated dextran and sulphated curdlan, are used as antiviral (Ghosh *et al.*, 2009) and anticancer agents (Takeuchi *et al.*, 2009)

Chemically, exopolysaccharides may have different nature. The monosaccharidic constituents range from neutral (glucans) to anionic (hyaluronan from *Pseudomonas aeruginosa*; Rehm, 2009), while the structure can be linear or highly branched. Though many

EPS are well characterized, the enormous structural diversity found in these polysaccharides requires the continuous search for novel structures with new features, especially in the almost unknown world of extremophiles.

2.4 The lipopolysaccharides: biological activity

Lipopolysaccharides are considered the endotoxin of pathogenic bacteria and they are one of the most important PAMPs (Pathogen Associated Molecular Patterns) in the interaction with the host organism.

To recognize the presence of a pathogenic guest, host organisms have developed an innate immune system.

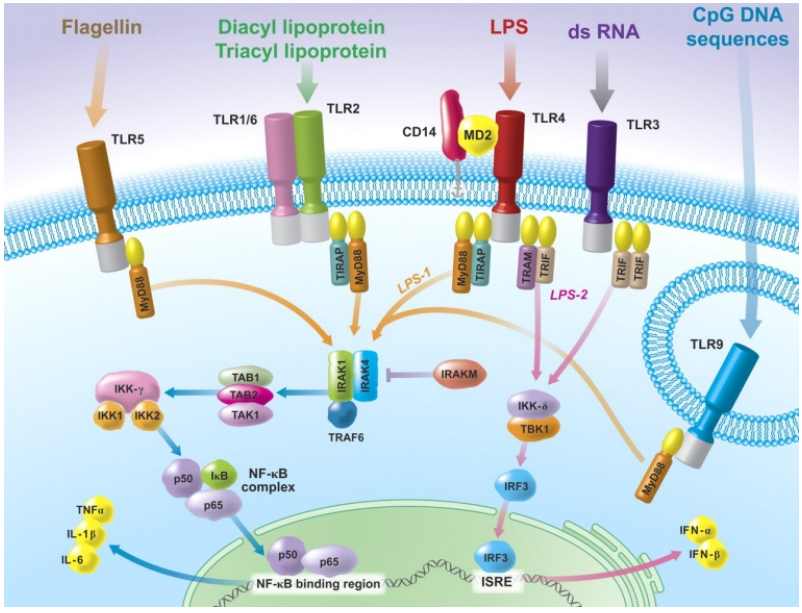

Figure 2.6 – Scheme of some TLR signaling pathways. (Adapted from Frevert*et al.* Innate immunity in the Lungs 2005.)

Toll-like receptors (TLRs) play a key role in innate immune system and are expressed on the surface of sentinel cells like macrophages and dendritic cells (Figure 2.6). TLRs are trans-membrane proteins divided in different classes of receptors depending on which PAMP they structurally recognize and their task is to communicate the presence of a non-self antigen to the internal part of the cell. TLRs together with the Interleukin-1 receptors form a receptor superfamily, known as the "Interleukin-1 Receptor/Toll-Like Receptor Superfamily"; all members of this family have in common a so-called TIR (Toll-IL-1 receptor) domain.

It is known that the receptors responsible for the recognition of LPSs is Toll-like Receptor 4 (TLR-4) together with the myeloid differentiation factor 2 (MD-2). When LPSs are released in the surrounding medium, the lipid A moiety is recognized by host cells receptors and may activate the immune system. Consequently the host response is strongly influenced by lipid A chemical structures. More in detail, LPSs are released from the bacterial membrane and transferred to the heterodimer TLR-4/MD-2 by two accessory proteins, LPS-binding protein and CD14 (Cluster of differentiation 14) (Takeda and Akira, 2004).

Actually, in the complex set of reactions regulating immune system responses to host infections, TLR-4 may activate two pathways. The first one is common to all TLRs and is mediated by the myeloid differentiation primary response gene (MyD88); this pathway finally activates the production of NF-κB and proinflammatory cytokines. The MyD88-indipendent pathway is used exclusively by TLR-3 and TLR-4. The intracellular domain of the receptor recruits TIR-domain-containing adapter-inducing interferon-β (TRIF) which leads to the production of type 1 interferons. The TRIF pathway is of particular interest for the development of vaccines. (Takeda and Akira, 2004)

To recognize bacterial LPSs belonging to different organisms, TLR-4 needs a common pattern, which can be identified in the lipid

A portion. Actually, even if the length and type of fatty acids constituting the lipid A may change, this is the most conserved portion. Nevertheless different LPSs trigger the immune system in different ways and maybe the structural characteristics of lipid A region are responsible for this feature; this implies a strong structure-function relationship between lipid A and biological activity. The degree of acylation seems to be important in the activation of immune system; hexa-acylated lipid A (*Escherichia coli, Salmonella minnesota*) excites the innate response and causes pathogenicity and septic shock. On the other side, under acylated lipid A (*Rhodobacter sphaeroides*, *Porphyromonas gingivalis*) acts as antagonist and induces markedly less host defence responses and can inhibit in a dose-dependent manner the strong endotoxic response triggered by hexa-acylated LPS.

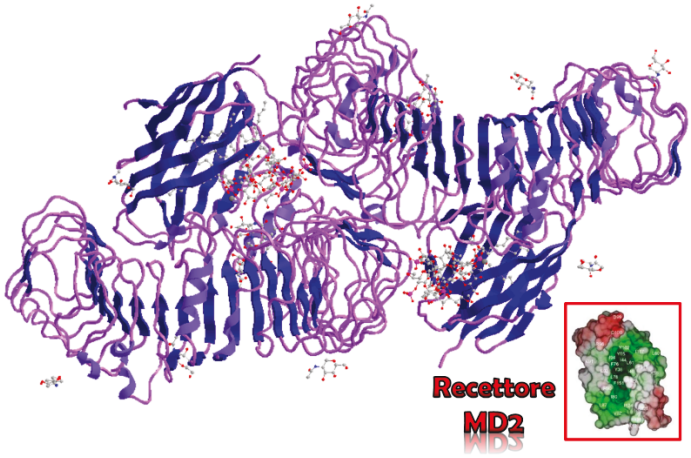

Figure 2.7 –TLR-4 horseshoe-like structure. Adapted from Park *et al*., 2009

In 2009 Park *et al.* finally succeeded in obtaining the crystal structure of the TLR-4/MD-2/LPS complex (Figure 2.7), thus providing a deeper insight on the molecular basis of this interaction. The authors deduced that LPS binds MD-2 in an

hydrophobic pocket in which fatty acids chains are buried. Moreover, the LPS induces a dimerization of the complex so that the active receptor is formed by two copies symmetrically arranged. Actually, TLR-4 forms hydrophobic and hydrophilic bonds directly with LPS and two loops of MD-2. In particular, the hydrophobic connections are made by acyl chains exposed to the surface, as they cannot enter in MD-2 pocket, while hydrophilic interactions are established between ester and amide linkage of the fatty acids to the disaccharidic backbone and hydrophilic side chains of MD-2 and TLR-4. Moreover the phosphate groups are involved in the binding with positively charged residues.

From structural data, Park *et al.* concluded that the number, length and distribution of fatty acids seems to be crucial in the dimerization step which determines the type of immune response excited by the LPS. Another important factor is the presence of both phosphate groups on the saccharidic backbone. In fact, only a weak activation of the immune system is exerted after deletion of either of these phosphate (Rietschel *et al.*, 1994; Rietschel *et al.*, 1993). Consequently, the monophosphoryl lipid A (MPLA) of *Salmonella minnesota* is used in formulation of vaccines as it selectively activates the TLR-4/TRAM/TRIF signalling pathway but not the TLR-4/Mal/MyD88 pathway (Mata-Haro *et al.*, 2007).
It is easy to deduce that many other LPSs with interesting and exploitable biological activities have not been discovered yet. Moreover, the great variety of chemical structures found for LPSs together with their several interactions with host organisms implies that a good knowledge of the structure-function relationships needs further studies.

Chapter 3

Methodology in the study of lipopolysaccharides

The first "task" in the structural elucidation of lipopolysaccharides from bacterial cells is the isolation of an amphiphilic molecule that can be defined as "pure". The extremely variable nature of LPSs does not allow the implementation of a unique methodology for the extraction and the chemical study. So it is a sort of trial-and-error process, especially when the nature of LPSs is completely unknown.

However, the methodologies exploited in the study of carbohydrates and fatty acids remain valid, as well as chromatographic, spectroscopic and spectrometric methods.

3.1. Isolation and purification of LPSs

The extraction of LPSs from bacterial cells is conventionally achieved by two complementary procedures, that may lead to selective isolation of R-LPS and S-LPS (Figure 3.1). The first one is specific for R-LPS or S-LPS with a marked hydrophobic O-chain and follows the Petroleum Ether/Chloroform/Phenol 90% procedure optimized by Galanos *et al.* in 1969. With this procedure, the lipophilic LPS is extracted within the solvent mixture and, after removal of light solvents by evaporation, it is precipitated with water from residual phenol. Usually, the sample obtained from this procedure is free from nucleic and cytoplasmatic contaminants. The residual cells are extracted with a second procedure that implies cellular lysis. Cells are treated with a 90% Phenol/Water 1:1 mixture (Westphal and Jahn, 1965) obtaining two

phases, both recovered and dialysed against water. Usually, sample obtained from this procedure needs preliminary purification by enzymatic digestion with nucleases (DNase and RNase) and protease. This method is used for the isolation of capsular polysaccharides too, when present; their high hydrophilic nature allows their extraction in the water phase.

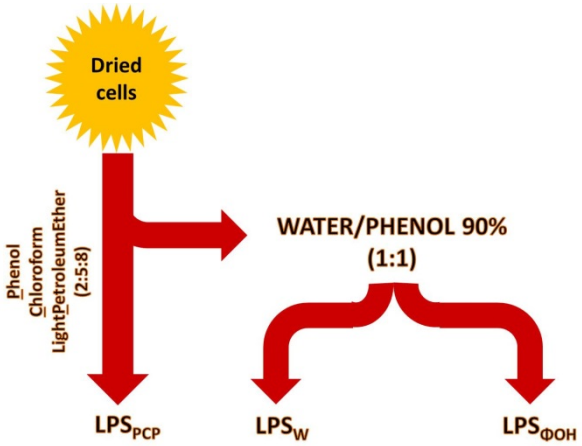

Figure 3.1 –Scheme of the main extraction methods for LPSs.

Finally, the three phases (PCP extract, water phase and phenol phase) are subjected to SDS or DOC polyacrylamide gel electrophoresis (PAGE) analysis followed by silver nitrate staining (Kittelberger and Hilbink, 1993) for the detection of the presence of LPS and the determination of the type (smooth or rough) of LPS (Figure 3.2).

Figure 3.2 –16% SDS-PAGE analysis of LPS from *E.coli* O55:B5 and *E.coli* Δ*waa*L mutant lacking O-chain region.

In Figure 3.2 both rough and smooth LPS are analysed. In particular, lane A shows the presence of a "ladder-like" migration pattern, which suggests the presence of a S-LPS where molecules differing for the number of repeating units are revealed. On the contrary, in lane B the presence of a R-LPS is proved by the presence of a unique or few bands with high migration. Moreover, alternative stainings, such as Alcian blue staining, allow to reveal the presence of anionic LPS and polysaccharides (EPS, capsule).

3.2. Chemical analysis and reaction on LPSs

After extraction and purification, the complete structure elucidation of LPSs is achieved through a sequence of steps aimed to the definition of the molecular features of both lipid and saccharidic moiety of the molecule. Chemical analysis performed on the whole LPSs allow a qualitative determination of monosaccharides, as well as their absolute configuration, the ring size and the glycosylation site for each residue. Usually, these analysis are performed by GC-MS; this is the reason why they can only be achieved after conversion of the monosaccharides into volatiles derivatives. The qualitative analysis of the

monosaccharides is obtained by means of two procedures. Treating the LPSs with hydrochloric anhydrous methanol leads to solvolysis of the molecule and to the formation of the *O*-methyl glycosides from each monosaccharide. Subsequent acetylation with acetic anhydride in pyridine leads to the formation of acetylated *O*-methyl glycosides (AMG) that are volatile enough to be analysed by GC-MS (Figure 3.3). The identification of each monosaccharide is achieved by the comparison of the GC retention times and of the MS fragmentation pattern with that of authentic standards. Several isomers can be obtained for each monosaccharide (i.e. pyranose and furanose either α and β anomers) and each corresponds to a peak in the chromatogram. This can be a problem, especially if a quantitative analysis is needed. The derivatization of monosaccharides into their acetylated alditols (AA) avoids this drawback. In this second procedure the LPSs undergoes a strong acid hydrolysis with trifluoroacetic acid (TFA) followed by reduction of the carbonyl moiety with $NaBH_4$ and acetylation of the residue. This leads to a single peak in the GC analysis for each monosaccharide. Moreover, when a phosphate group is present on the monosaccharide, a preliminary dephosphorylation with acqueous 48% HF is necessary to reveal the residue.

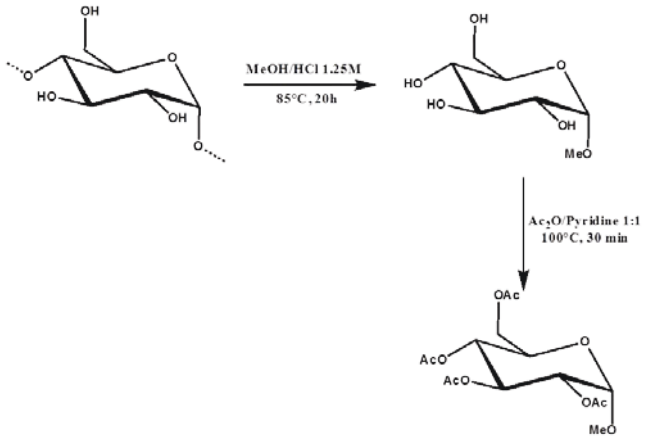

Figure 3.3 –Acetylated O-methyl glycosides formation.

For the determination of the absolute configuration for each monosaccharide the sample is solvolysed with an optical pure chiral alcohol, usually (+)-2-octanol or (+)-2-butanol (Leontein *et al.*, 1978). The diasteroisomeric molecules obtained during the derivatization can be acetylated and identified by GC by comparison with authentic standards.

Chemical analysis can help in the determination of the ring size and the glycosylation sites of the monosaccharides. To obtain these data, LPSs is extensively methylated with CH_3I in DMSO in alkaline conditions. Then, the sample is hydrolysed in acidic conditions and reduced with a marked reagent ($NaBD_4$). The alditols obtained have free hydroxyl groups at the positions previously involved in glycosidic linkage and cyclization that can be acetylated forming the partially methylated acetylated alditos (PMAA) (Ciucanu and Kerek, 1984, Figure 3.4).

The fragments observed in the MS spectra from the GC-MS analysis are diagnostic for specific substitution pattern of acetyl and methoxyl groups. In fact, the fragment ions which bear a methoxyl group are more stable, due to a resonance effect (Figure 3.4). In this thesis work we demonstrated that PMAA may be useful in the determination of phosphorylation sites; comparing the results obtained before and after 48% HF treatment, it is possible to determine phosphate groups positions (Carillo *et al.*, 2011). When LPSs is treated with hydrochloric anhydrous methanol *O*-methyl-esters derivatives of fatty acids are formed too. They can be easily extracted with hexane and analysed directly by GC-MS. The identification is performed on the basis of retention times and fragmentation patterns compared with those of authentic standards.

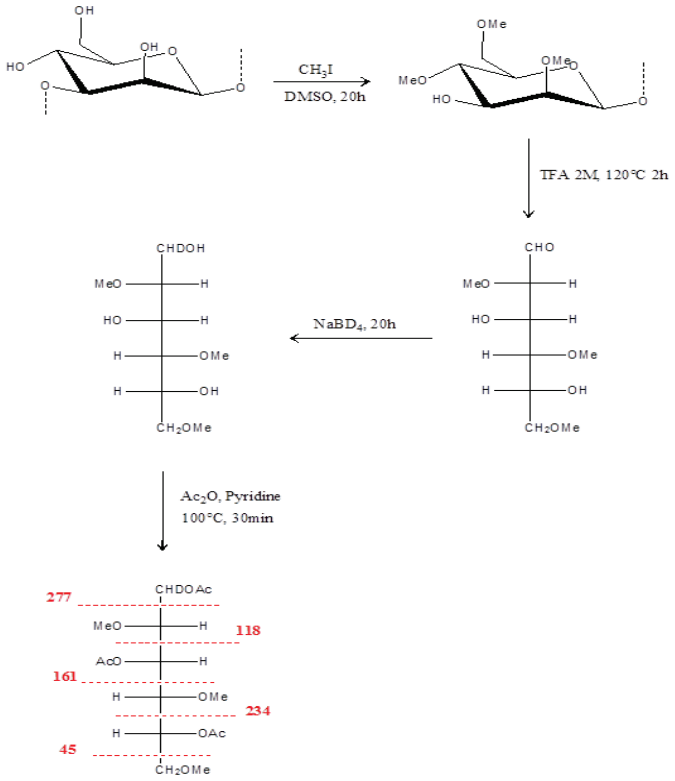

Figure 3.4 – PMAA procedure on a 3-α-D-mannose. Reactions and mass fragmentation pattern.

All the information obtained by chemical analysis will help in the structural elucidation and have to be confirmed by spectroscopic methods.

For the study of LPSs, the first problem is represented by the low yield obtained from extractions (~1-3%) and the poor solubility of glycolipids that usually form micelles that make difficult the analysis both in water and organic solvents. As a consequence, portions with a different nature are studied separately and then all the data collected contribute to the definition of a unique structure.

3.2.1. O-chain structure determination

The structural study of the O-chain is achieved by the splitting of lipid A from the other saccharidic regions. In fact, a mild acid hydrolysis with 1% acetic acid or acetic acid buffer allows the cleavage of the acid-labile linkage between Kdo and the saccharidic backbone of lipid A (de Castro *et al.*, 2010). As a consequence, lipid A and polysaccharidic moieties increase their hydrophobic and hydrophilic behaviour, respectively, so that, in the aqueous phase used for the reaction, the lipid A is completely insoluble and is recovered as precipitate while in the supernatant is dissolved the saccharidic fraction. O-chain structural study is easily achieved by chemical analysis and NMR spectroscopic techniques (see Section 3.5) as, usually, only the monosaccharides of the O-chain repeating units are revealed thanks to their high relative abundance compared to the residues belonging to core region.

3.2.2. Lipid A structure determination

The analysis on the precipitate fraction allow the structural determination of lipid A with chemical analysis and mass spectrometry techniques (see Section 3.4).The actual distribution of fatty acids on the disaccharidic backbone is achieved by a puzzling study of negative ions mass spectra and positive ions IRMPD-MS/MS spectra of the intact lipid A and NH_4OH treatment product (Silipo *et al.*, 2002). In particular, negative ions mass spectra furnish the acylation and phosphorylation degree of the molecules and the fatty acids linked at position C2 and C2' when NH_4OH product is investigated. Positive ion IRMPD-MS/MS spectra of lipid A can reveal the type of fatty acids linked to the non-reducing glucosamine of disaccharidic backbone in whole lipid A as well as in NH_4OH product.

3.2.3. Core region structure determination

A disadvantage of mild acid hydrolysis is that the reducing Kdo unit released establishes an equilibrium among its various conformation (α and β anomers of pyranose and furanose rings, condensed or anhydrous forms; Banoub *et al.*, 2004). This leads to heterogeneous samples with particularly disadvantageous effects in NMR experiments on short oligosaccharides. Therefore, this procedure is avoided for the structural determination of core region or R-LPSs. So, a complete delipidation of lipid A portion is mandatory for the study of the core oligosaccharide moiety.

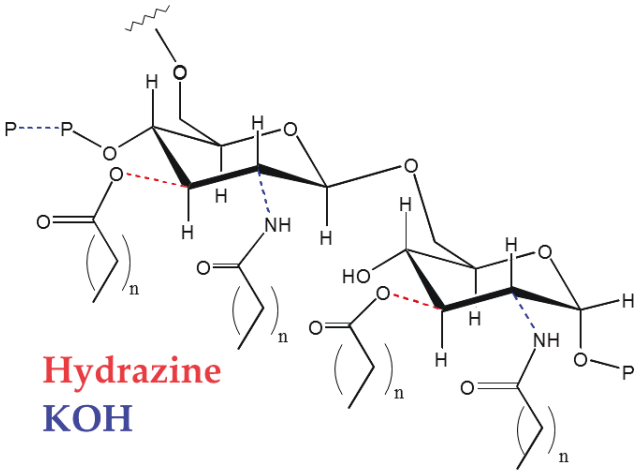

Figure 3.6 – Alkaline deacylation product of LPS (the linkage cleaved by N_2H_4 are shown in red, while the linkage cleaved by KOH 4M are shown in blue).

This technique implies two consecutive treatments (Masoud *et al.*, 1994; Figure 3.6). The first one is a mild alkaline hydrolysis using anhydrous hydrazine, which removes all ester-linked fatty acids. The increased hydrophilic nature of the molecule sometimes is adequate to obtain some structural information by NMR and does not implies the loss of basic-labile substituents. However, in the majority of the cases a complete deacylation is necessary to obtain

a water-soluble oligosaccharides mixture. This is achieved by a strong alkaline treatment with KOH 4M, which leaves intact the phosphate groups but removes many other substituents. The fraction obtained is suitable for chemical, mass spectrometry and NMR spectroscopy analysis. Nevertheless, sometimes the mixture is too complex and the overlapping of NMR signals compels the purification of the single glycoforms. This is achieved by chromatographic methods, such as gel permeation chromatography or HPLC (see Section 3.3). The fractions so obtained can be extensively studied by means of mono and bidimensional NMR techniques.

3.3. Chromatography in the study of LPSs

Chromatography techniques are exploited in all fields of chemical and biological research. In the study of lipopolysaccharides the purification of the samples is important to simplify further analysis, while some chromatographic instruments are used to obtain structural information. Low pressure chromatography and gas-chromatography interfaced with mass spectrometry (GC-MS) are widespread for purification and chemical analysis of LPSs, respectively. However, few chromatographic supports are suitable for separation of oligosaccharides mixture where species differ for a single monosaccharide or phosphate group. Consequently in this Section the attention will be focused on High Pressure Anion Exchange Chromatography (HPAEC), a peculiar HPLC instrument used during the overall thesis work.

HPAEC coupled with pulsed amperometric detection (PAD) permits direct quantification of nonderivatized carbohydrates at low picomole levels (Townsend *et al.*, 1988; Hardy *et al.*, 1988). HPAEC-PAD exploits the weakly acidic nature of carbohydrates

and furnishes highly selective separations at high pH using a strong anion exchange stationary phase. In fact, at high pH values even neutral sugars are partially ionized and thus they can be separated by anion exchange mechanisms.

Dionex® is the instrument of election for this chromatographic technique. It uses CarboPac columns that are packed with a unique polymeric, nonporous, MicroBead™ pellicular resin, which exhibit rapid mass transfer, high pH stability and excellent mechanical resistance (Figure 3.7). Moreover, using pulsed amperometry, carbohydrates are detected by measuring the electrical current generated by their oxidation at the surface of a gold electrode. This implies an excellent signal-to-noise ratio.

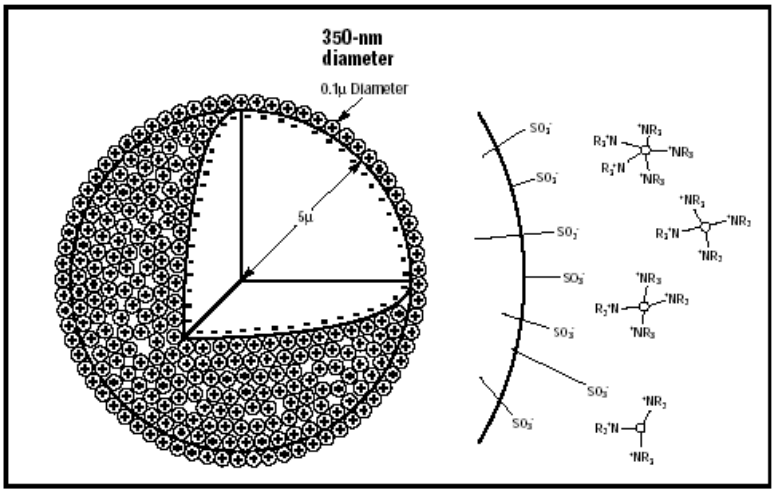

Figure 3.7 – Pellicular anion exchange resin bead.

The peculiarity of this method allows the separation of oligosaccharides on the basis of small molecular mass differences, such as one monosaccharide unit or a single phosphate group. In fact, the retention time depends on the charge to mass ratio, allowing the separation of species with the same saccharidic

backbone, but differing for phosphate content. However, the optimization of the gradient used for the separation and the following desalting purification require a sufficient amount of oligosaccharides mixture (depending from the number of species present in the mixture) not always compatible with the low yield of LPSs extraction and deacylation reactions. As a consequence, only the most abundant species are usually recovered for further analysis.

3.4. Mass spectrometry in the study of LPSs

Mass spectrometry is extensively used in LPSs structural determination, as it can provide information about the intact molecule without any derivatization or degradation. Moreover, lipid A structure is inferred only on the basis of chemical analysis and mass spectrometry experiments, as its amphiphilic nature and high heterogeneity makes the NMR study in solution quite difficult. For LPS analysis MALDI-TOF or ESI FT-ICR instrument are suitable. In fact, they use soft ionization techniques that allow the determination of the molecular mass of the intact molecule. Moreover, the number of species present in the sample will be obtained.

In addition, MALDI-TOF permits the analysis of fragment ions generated by the precursor ions in the flight tube if a higher laser intensity is applied and the detector parameters are correctly set (Post Source Decay experiment).

FT-ICR analyser interfaced with ESI source can achieve a mass resolving power higher than 100000 and a mass accurancy less than 1ppm. ESI FT-ICR has some good applications for LPSs structural determination. CSD (Capillary Skimmed Dissociation) experiments allows the cleavage of the labile linkage between lipid A portion and Kdo residue (Kondakov and Lindner, 2005). As a consequence, it is possible to gain information on the molecular mass of intact

LPS, lipid A and saccharidic regions simultaneously with a single experiment. Moreover IRMPD-MS/MS (InfraRed MultiPhoton Dissociation) gives important structural information using controlled fragmentation of the samples, as already reported for the structural elucidation of lipid A moiety (see Section 3.2.2).

3.5. NMR spectroscopy in the study of LPSs

Nuclear Magnetic Resonance has provided the most useful tool in the field of structure determination of carbohydrates. In fact, the samples are analysed in solution in a native situation, due to the good solubility observed for oligo- and polysaccharides in aqueous systems. The nuclei of interest when studying a LPS are ^{1}H, ^{13}C as well as ^{31}P, to detect phosphate groups and unusual phosphorus containing substituents.

A typical carbohydrate ^{1}H-NMR spectrum present signals divided in three regions:

- The region of anomeric proton signals located between 5.5 and 4.0 ppm;
- The region of ring proton signals between 4.6 and 2.5 ppm;
- The region of deoxy position signals between 2.5 and 1.0 ppm.

For molecules greater than a trisaccharide the region of ring proton signals becomes overcrowded so that is impossible to identify all chemical shifts. This problem is overcome by homonuclear two-dimensional experiments; in particular, TOCSY and DQF-COSY. The COSY pulse sequence shows crosspeak for vicinal scalar coupled protons. The TOCSY experiment permits the identification of all protons belonging to the same spin system. This is achieved by a series of soft pulses that transfer the magnetization in a measure that depends on the $^{3}J_{H,H}$ coupling constant. As a consequence, a *gluco* configured monosaccharide will show a good transfer of magnetization and in the TOCSY

spectrum all the signals of the residue will be present. On the contrary, *manno* or *galacto* configured residues present small coupling constant between H2-H3 and H4-H5 protons respectively, showing only 2 or 3 crosspeak correlated to anomeric proton signals.

To obtain the sequence of monosaccharides constituting the poly- or oligosaccharides, homonuclear and heteronuclear experiments are needed, such as ROESY, ^{1}H-^{13}C HSQC, HSQC-TOCSY and HMBC.

ROESY shows dipolar coupling between protons; signals present in this spectrum may derive from *intra*-residue (giving information about the anomeric configurations of the residues) or *inter*-residue correlations.

To confirm this data the study of ^{1}H-^{13}C HSQC, HSQC-TOCSY and HMBC spectra is needed.

The first one shows directly correlated protons and carbons. The second one shows correlations between one proton and all carbon signals belonging to the same spin system. HMBC experiment is mandatory for the determination of linkage positions since it displays scalar correlations between protons and carbons.

From the study of all above spectra, the complete assignment of all proton and carbon chemical shift values is possible. Then, by comparison with reference values of unsubstituted monosaccharides the glycosylated positions can be deduced. In fact, the glycosydic linkage causes the "glycosylation shift": the carbons involved in the linkage undergo a downfield shift of 8-10 ppm, while the adjacent carbons will be upfield shifted of 1-3 ppm.

Table 3.1 –Coupling constant values for α and β anomers.

anomer	$^{3}J_{H1,H2}$(Hz)	$^{3}J_{H1,C1}$(Hz)
α	2-3	>170
β	8-10	<165

Finally, from the study of monodimensional spectrum, from ROESY sequence and from 2D *F2*-coupled HSQC information about the anomeric configuration of each residue can be obtained. In fact, the measurement of $^{3}J_{H1,H2}$ and $^{3}J_{H1,C1}$ coupling constant from ^{1}H and 2D *F2*-coupled HSQC experiments, respectively, can indicate the presence of an α or β anomeric proton (Table 3.1).

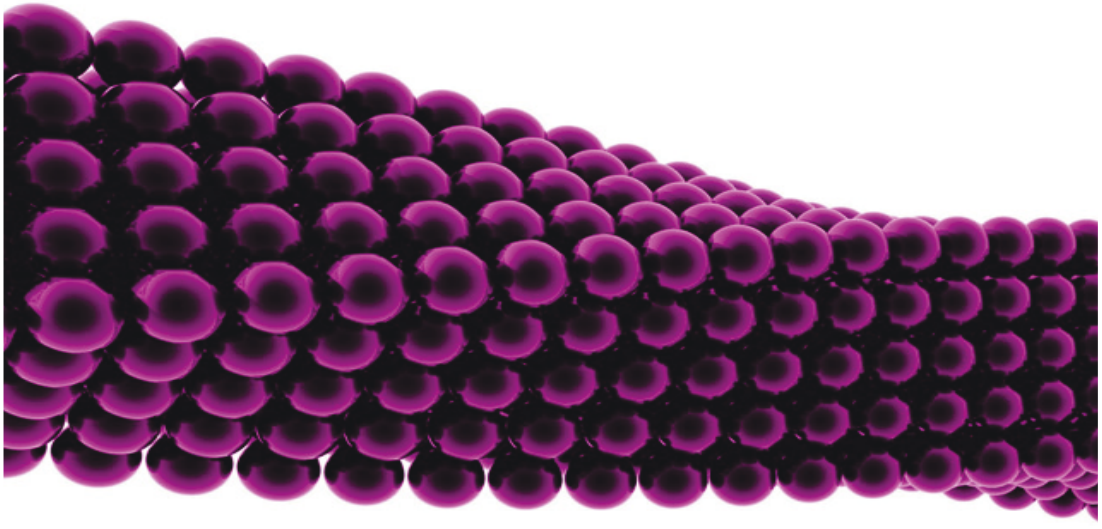

Psychrophiles

In this thesis work, the LPS from two psychrophilic bacterium has been investigated.

The first one, which contains about 40 validly described species, belongs to the genus *Pseudoalteromonas*, including some reclassified former *Alteromonas* species. Gram-negative bacteria of the genus *Pseudoalteromonas* are widespread obligatory marine micro-organisms that require seawater for their growth and produce a wide range of biologically active compounds. Although *Pseudoalteromonas* species are frequently found in association with eukaryotic hosts in the marine environment, the mechanisms involved in such associations have not yet been elucidated. For this reason the characterization of the surface molecules, which may play an important role in microbe-host relationship, is of great interest. Moreover many of these species produce biologically active metabolites which target a range of organisms (Holmström *et al.*, 1999). In particular, many *Pseudoalteromonas* species have been demonstrated to produce anti-bacterial products, such as agarases, toxins, bacteriolytic substances and other enzymes which may assist the bacterial cells in their competition for nutrients and space as well as in their protection against predators grazing at surfaces (Holmström *et al.*, 1999).

Although all bacteria belonging to genus *Pseudoalteromonas* are marine, not all of them are psychrophilic. Among these the LPS from the psychrophilic *Pseudoalteromonas haloplanktis* TAC 125 has already been characterized, revealing a rough-type LPS (Corsaro *et al.*, 2001; Corsaro *et al.*, 2002).

The second psychrophile belongs to genus *Colwellia*. All characterized members of genus *Colwellia* are facultative anaerobes, strictly psychrophilic and sometimes barophilic which possess a requirement for elevated sodium and magnesium ions to maintain cell wall and cytoplasmic membrane integrity (Bowman *et al.*, 1998).

Moreover, many of them produce extracellular polymeric substances relevant to biofilm formation and cryoprotection (Krembs *et al.*, 2002; Huston 2003) and enzymes capable of degrading high-molecular-weight organic compounds. Studies indicate that strains of *Colwellia* and *Vibrio marinus* synthesize ω3 polyunsaturated fatty acids (PUFAs), in particular docosahexaenoic acid (22: 6ω3, DHA) (DeLong and Yayanos, 1986; DeLong *et al.*, 1997) which is commonly found in cold water fatty fish, such as salmon and is even required for maintenance of normal brain function in human adults. (Horrocks and Yeo, 1999).

Chapter 4

Pseudoalteromonas haloplanktis TAB 23

Pseudoalteromonas haloplanktis TAB 23 is an Antarctic psychrophilic Gram-negative bacterium isolated from the Antarctic costal sea (Feller *et al.*, 1992).

In this thesis the structural elucidation of the LPS obtained from *P. haloplanktis* TAB 23 is illustrated.

Moreover, the bioactivity of lipid A obtained from *P. haloplanktis* TAB 23 was investigated in *vitro* in a human monocytic cell line, using the release of the pro-inflammatory mediators TNFα and IL-6, as markers of cell activation.

4.1 Isolation and compositional analysis of the LOS fraction.

P. haloplanktis TAB 23 was grown as reported in Experimental Section (par. 9.1.4). The dried cells were treated following the PCP procedure (Galanos *et al.*, 1969) to obtain the crude LPS. This was analysed by 18% DOC-PAGE experiment (Figure 4.1), using *P. haloplanktis* TAC 125 LOS as standard (Corsaro *et al.*, 2001)

The experiment revealed the presence of different glycoforms with a high mobility, that indicated the absence of the O-chain portion suggesting the rough nature of the LPS from *P. haloplanktis* TAB 23. In particular one of these glycoforms showed the same migration as TAC 125 LOS indicating a similar molecular mass for the two samples. The sugar composition was obtained by GC-MS analysis and revealed the occurrence of D-Gal, D-GlcN, D,D-Hep and Kdo. The presence of the latter residue was revealed only after HF treatment of the LPS, suggesting its phosphorylation

(Pieretti *et al.*, 2008). The finding of D,D-Hep in *P. haloplanktis* TAB 23 prompted us to revise the configuration of the heptose residue in *P. haloplanktis* TAC 125, which resulted to be D,D-configured.

Figure 4.1 - DOC-PAGE 18% analysis of the LOS from *P. haloplanktis* TAB 23. Lanes A and B represent the LOS from *P. haloplanktis* TAC 125 and the PCP extract from *P. haloplanktis* TAB 23, respectively.

Absolute configurations were inferred by comparison of the GC-MS retention times of the sugar 2-(+)-octylglycosides derivatives with those of authentic standards. Methylation analysis indicated the presence of terminal Gal, 4-substituted Gal, 4-substituted Hep and 6-substituted GlcN. The fatty acids composition was obtained by GC-MS analysis of their methyl ester derivatives. It showed that 3-hydroxydodecanoic acid [C12:0(3OH)] was the most abundant fatty acid and was present in minor amount also in the *iso*- series. Moreover, 3-hydroxyundecanoic acid [C11:0(3OH)], its corresponding isomer of the *iso*- series, 3-hydroxydecanoic [C10:0(3-OH)], 3-hydroxytridecanoic [C13:0(3-OH)], dodecanoic (C12:0), dodecenoic (C12:1) and tridecenoic (C13:1) acids were found. The high heterogeneity and the nature of the fatty acids were in agreement with that found, up to now, in the lipid A isolated from other bacteria belonging to *Pseudoalteromonas* genus (Corsaro *et al.*, 2002; Krasikova *et al.* 2003; Silipo *et al.*, 2004a).

4.2 Isolation and characterization of the acid hydrolysis products.

Mild acid hydrolysis of the LOS sample allowed the isolation of the lipid A and the core region (see Section 9.2.4). With regard to the lipid A moiety the negative ions reflectron MALDI-TOF mass spectrum (Figure 4.2) showed the presence of a main cluster of signals (**A1**) corresponding to penta-acylated diphosphorylated glycoforms differing for fatty acids composition.

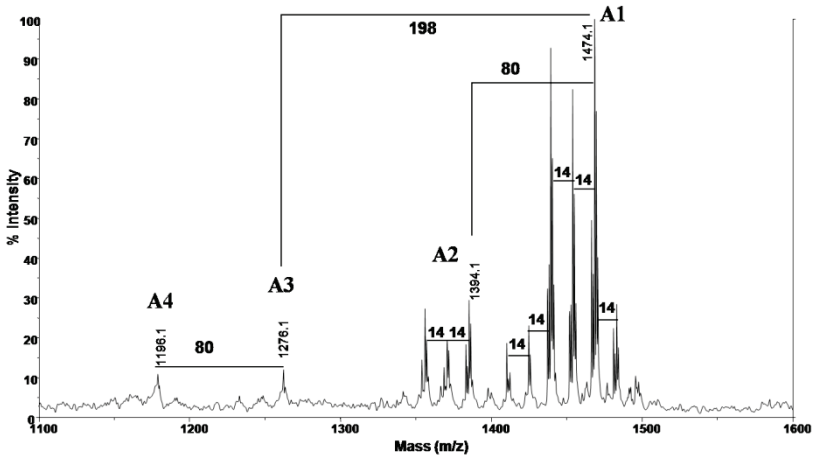

Figure 4.2 - Negative ions reflectron MALDI-TOF mass spectrum of the lipid A from *P. haloplanktis* TAB 23.

The main one occurred at *m/z* 1474.11 which was in agreement with the following composition: $[C12:0(3OH)]_4(C12:0)GlcN_2P_2$ (calculated $[M-H]^-$ =1473.90 Da). Besides this, a cluster of signals was present at 80 u lower (**A2**), suggesting the presence of monophosphorylated species. In addition, two minor clusters (**A3** and **A4**) at 198 u lower respect to **A1** and **A2**, respectively, were present, which were attributed to di- and mono-phosphorylated

tetra-acylated species lacking one 3-hydroxydodecanoic acid. This spectrum was quite similar to that already published of *P. haloplanktis* TAC 125 lipid A (Corsaro *et al.*, 2002). This was not surprising as the lipid A structure is the most conservative portion of LPSs belonging to bacteria of the same species. The nature and the positions of the secondary fatty acids were determined by treating the lipid A with NH_4OH (Silipo *et al.*, 2002). The negative ions reflectron MALDI-TOF mass spectrum of the product revealed the presence of three main species. The most abundant one occurred at *m/z* 1077.13 and corresponded to the following composition: $[C12:0(3OH)]_2C12:0GlcN_2P_2$, while the others contained one C12:0 and one phosphate less, respectively. The positive ions MALDI-TOF mass spectrum, displayed a signal at *m/z* 640.4, attributed to the oxonium ion in which the GlcN*4P* was substituted at position C-2 by a C12:0(3OH) primary fatty acid in turn substituted by a C12:0 secondary fatty acid (calculated oxonium ion mass 640.4 Da). On the basis of these data the main lipid A species was depicted as reported in Scheme 4.1.

We can conclude that the only difference between the lipid A main structures from *P. haloplanktis* TAB 23 and TAC 125 is the position of the secondary fatty acid. Actually, in both cases it is localized on GlcN*4P*, being acyloxyamide and acyloxyacyl in TAB 23 and TAC 125 lipid A, respectively.

The core oligosaccharide obtained from the mild acid hydrolysis was analysed by ^1H NMR. Despite the shortness of the sugar chain, evinced in the DOC-PAGE experiment, the NMR spectrum of this fraction appeared very complex due to the presence of the Kdo at the reducing end, that in the reaction conditions lead to the formation of its *anhydro* forms (Banoub *et al.*, 2004; Auzanneau *et al.*, 1991). For this reason NMR analysis was performed on the oligosaccharides obtained after LOS alkaline treatment.

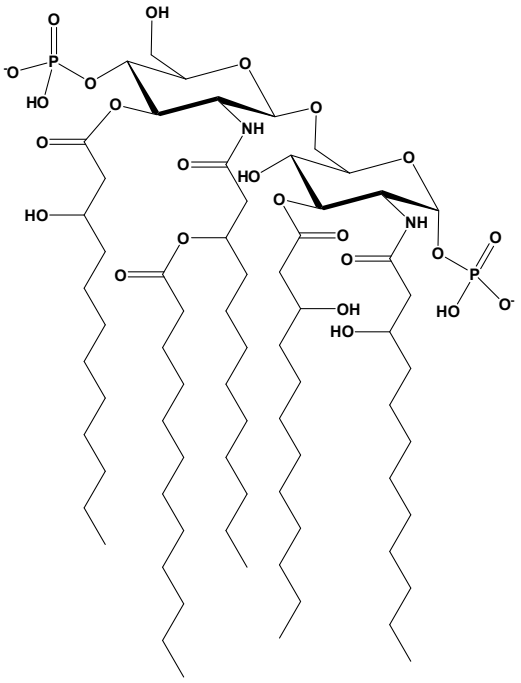

Scheme 4.1 – Lipid A structure from *Pseudoalteromonas haloplanktis* TAB 23.

4.3 De-O-acylation of the LOS

The LOS was de-*O*-acylated with anhydrous hydrazine (Holst, 2000). The negative ions reflectron MALDI-TOF MS spectrum of this fraction (LOS-OH) showed the presence of a complex mixture of glycoforms, due to both core and lipid A heterogeneity. Starting from low values of molecular masses the spectrum showed the presence of a signal occurring at *m/z* 1467.61 (**B1**, Table 4.1), corresponding to the following composition: $KdoHepGlcN_2P_4[C12:0(3OH)]_2$ (calculated molecular mass 1468.46 Da).

Beside this, a signal at 80 u more (**B2**) was present in the spectrum. Moreover two adduct ions (**B3** and **B6**) occurring at 162

u and 324 u higher masses respect to **B1,** suggested the presence of species containing one or two additional hexoses.

Table 4.1 - Composition of the main species present in the negative ions MALDI-TOF mass spectrum of the LOS-OH.

Fraction	$[M-H]^-_{obs}$	$[M-H]^-_{acc}$	Composition
B1	1467.61	1467.46	$HepKdoHexN_2P_4[C12:0(3OH)]_2$
B2	1547.54	1547.42	$HepKdoHexN_2P_5[C12:0(3OH)]_2$
B3	1629.55	1629.51	$HexHepKdoHexN_2P_4[C12:0(3OH)]_2$
B4	1709.61	1709.47	$HexHepKdoHexN_2P_5[C12:0(3OH)]_2$
B5	1711.59	1711.59	$Hex_2HepKdoHexN_2P_3[C12:0(3OH)]_2$
B6	1791.56	1791.59	$Hex_2HepKdoHexN_2P_4[C12:0(3OH)]_2$

To species **B4** and **B5** were attributed the same sugar composition as **B3** and **B6**, respectively, the mass difference being due to the phosphorylation degree.

4.4 De-N-acylation of the LOS-OH

The LOS-OH was fully deacylated with KOH. The oligosaccharides mixture was fractionated by HPAEC-PAD, obtaining three main fractions named **OS1**, **OS2** and **OS3**. ^{1}H NMR spectra showed, by anomeric signals integration, that **OS1** contained two glycoforms, while **OS2** and **OS3** were pure.^{1}H-NMR of **OS1** fraction (Figure 4.3, Table 4.2) showed the presence of seven anomeric signals (**A-E**, **B'**, **C'**) between 5.4 and 4.2 ppm.
The assignment of ^{1}H resonances was achieved by tracing the spin-connectivities, showed in the DQF-COSY and TOCSY contour maps, starting from the anomeric and some other diagnostic ring protons, such as axial and equatorial proton (H-3) of Kdo residue at

1.81-2.18 ppm. The ^{13}C chemical shifts values were assigned on the basis of the $^{1}H,^{13}C$ DEPT-HSQC experiment (Figure 4.4, Table 4.3). The anomeric configurations were deduced from the $^{1}J_{C1,H1}$ coupling constants measured in a 2D *F2*-coupled HSQC experiment.

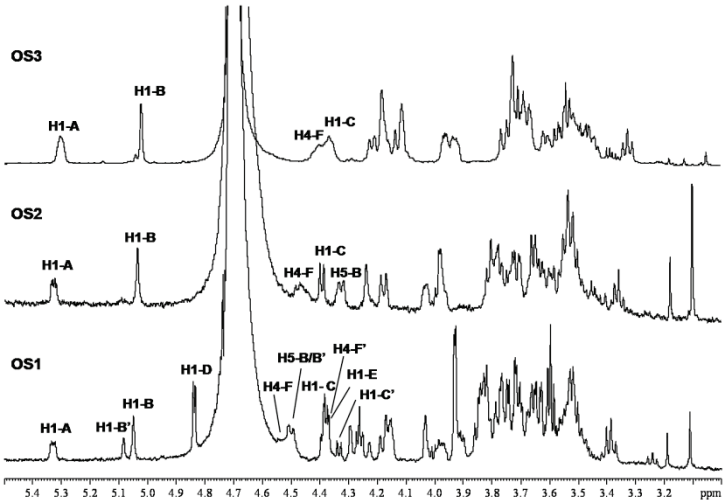

Figure 4.3 -^{1}H NMR of **OS1**, **OS2** performed at 298K and **OS3** performed at 293K. The spectra were recorded in D_2O at 600 MHz. The letters refer to the residues as described in Table 4.2-4.3.

Residue **A** was attributed to the 6-substituted α-Glc*p*N1*P* residue of lipid A on the basis of the multiplicity of the anomeric proton signal due to its phosphorylation ($^{3}J_{H,P}$ = 7.6 Hz), of the C-2 chemical shift at 56.8 ppm, which indicated a nitrogen-bearing carbon atom, and of the C-6 chemical shift, which was downfield shifted at 70.0 ppm due to its glycosylation. Residue **C** with C-1/H-1 signals at 104.7/4.37 ppm ($^{1}J_{C1,H1}$ = 169 Hz) was attributed to the 6-substituted β-Glc*p*N*4P* residue as a result of its C-2 chemical shift at 56.8 ppm and its linkage to *O*-6 of **A**. This structural feature was inferred by the *inter*-residue connectivity between H-1of **C** and H-6a,b of **A** identified in the ROESY experiment.

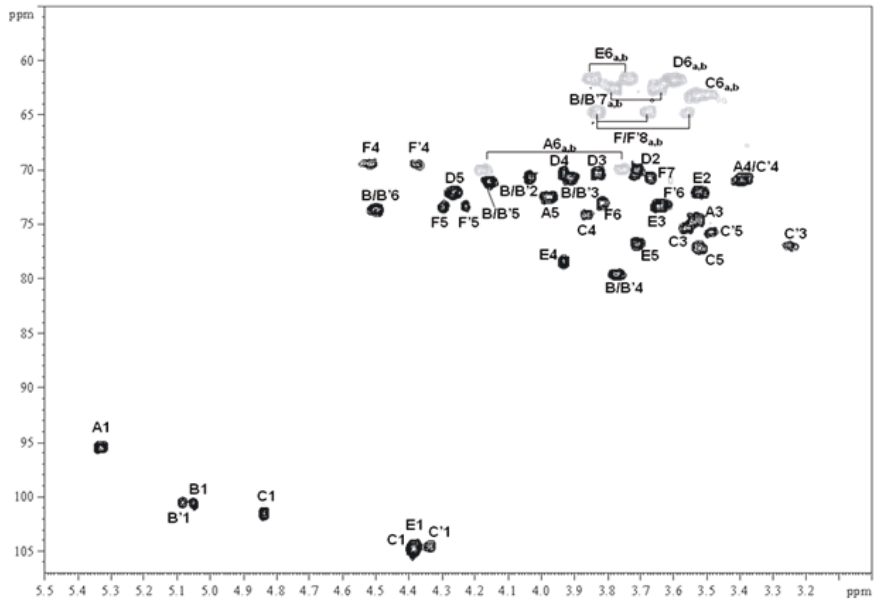

Figure 4.5 – Anomeric region and primary and secondary alcohol groups region of $^{1}H,^{13}C$ DEPT-HSQC spectrum of **OS1**. The spectrum was performed at 600 MHz in D_2O at 298K. The letters refer to the residues as described in Table 4.2 and 4.3.

Moreover, the H-4 and C-4 downfield shifts are diagnostic for the presence of a phosphate group linked at *O*-4 (Holst *et al.*, 1993). Residue **B** with C-1/H-1 signals at 100.6/5.05 ppm was assigned to a 4-substituted α-heptose as its $^{1}J_{C1,H1}$ was 174 Hz and its C-4 carbon atom occurred at 79.6 ppm, due to the glycosylation shift (Suesskind *et al.*, 1998; Vinogradov *et al.*, 1999).

Table 4.2 - ^{1}H NMR assignments of **OS1**, **OS2** and **OS3**

Residue	*OS*	*H-1*	*H-2*	*H-3*	*H-4*	*H-5*	*H-6a*	*H-7a H-6b*	*H-8a,b H-7b*
A 6-α-GlcN*p1P*	1	5.33	2.62	3.53	3.39	3.98	4.17	3.75	
	2	5.33	2.67	3.53	3.36	3.97	4.18	3.74	
	3	5.30	2.67	3.51	3.32	3.91	4.11	3.70	
B 4-α-Hep*p*	1	5.05	4.03	3.90	3.77	4.15	4.50	3.65	3.77
t-α-Hep*p*	2	5.04	3.98	3.80	3.57	4.04	4.32	3.61	3.72
	3	5.02	4.10	4.21	3.70	4.17	3.96	3.55	3.67
B' 4-α-Hep*p*	1	5.08	4.03	3.92	3.78	4.15	4.50	3.65	3.77
C 6-β-GlcN*p4P*	1	4.37	2.64	3.56	3.86	3.52	3.51	3.52	
	2	4.39	2.66	3.55	3.78	3.52	3.51	3.53	
	3	4.37	2.61	3.47	3.68	3.51	3.44	3.53	
C' 6-β-GlcN*p*	1	4.34	2.61	3.25	3.40	3.49	n.d.	n.d.	
F 5-α-Kdo*4P*	1	-	-	1.81-2.18	4.53	4.29	3.80	3.67	3.67-3.88
	2	-	-	1.83-2.15	4.46	4.25	3.78	3.66	3.66-3.81
	3	-	-	1.88-2.10	4.40	4.17	3.72	3.71	3.60-3.75
F' 5-α-Kdo*4P*	1	-	-	1.83-2.20	4.37	4.22	3.62	n.d.	3.55-3.82
D *t*-α-Gal*p*	1	4.83	3.71	3.83	3.93	4.26	3.59	3.59	
E 4-β-Gal*p*	1	4.38	3.52	3.64	3.93	3.71	3.84	3.73	

Table 4.3 - ^{13}C NMR assignments of **OS1, OS2** and **OS3**

Residue	*OS*	*C-1*	*C-2*	*C-3*	*C-4*	*C-5*	*C-6*	*C-7*	*C-8*
A 6-α-GlcN*p1P*	1	95.5	56.8	74.6	70.8	72.5	70.0		
	2	94.6	56.1	74.0	70.4	72.2	69.8		
	3	94.7	56.3	73.9	70.8	72.7	69.9		
B 4-α-Hep*p*	1	100.6	70.6	70.8	79.6	71.0	73.6	62.5	
t-α-Hep*p*	2	100.8	70.8	71.5	68.1	72.0	73.8	62.4	
	3	101.2	70.7	74.5	68.5	75.1	72.2	62.7	
B' 4-α-Hep*p*	1	100.5	70.6	70.8	79.6	71.0	73.6	62.5	
C 6-β-GlcN*p4P*	1	104.7	56.8	75.2	74.1	77.0	63.1		
	2	103.5	56.2	74.8	72.6	76.4	63.0		
	3	103.7	57.1	76.6	74.0	75.3	63.8		
C' 6-β-GlcN*p*	1	104.5	56.8	77.0	70.8	75.7	n.d.		
F 5-α-Kdo*4P*	1	182.4		35.4	69.4	73.4	73.1	70.7	64.7
	2			34.9	69.1	73.3	73.6	70.3	64.2
	3			35.4	69.8	73.9	72.9	70.5	64.6
F' 5-α-Kdo*4P*	1	182.4	-	35.4	69.4	73.2	73.0	n.d.	64.6
D *t*-α-Gal*p*	1	101.6	70.1	70.3	70.3	72.1	61.7		
E 4-β-Gal*p*	1	104.7	72.0	73.3	78.5	76.8	61.6		

Moreover its C-6/H-6 chemical shift values occurred at 73.6/4.50 ppm, respectively, indicating the presence of a phosphate group at position *O*-6 (Grzeszczyk *et al.*, 1996). Kdo residue (**F**) resulted to be glycosylated at *O*-5 position, as suggested by the downfield shift of its C-5 carbon signal at 73.4 ppm compared to the reference value for an unsubstituted Kdo residue that occurs at 67.4 ppm (Brade *et al.*, 1984).

Moreover, the H-4 and C-4 chemical shifts, downfield shifted at 4.53 and 69.4 ppm, respectively, indicated the Kdo phosphorylation at position *O*-4 (Müller-Loennies *et al.*, 2002). Residues **D** and **E** were attributed to *galacto* configured residues on the basis of the vicinal proton coupling constant values. In particular residue **D** (C-1/H-1 at 101.6/4.83 ppm) was assigned to a terminal non-reducing α-galactose unit since its $^{1}J_{C1,H1}$ coupling constant measured 174 Hz and none of its carbon atoms was shifted downfield. Galactose **E** with C-1/H-1 signals at 104.7/4.38 ppm was attributed to a 4-substituted residue, as its C-4 chemical shift value was shifted downfield (78.5 ppm) respect to that of an unsubstituted galactose unit (Bock and Pedersen, 1983). The β anomeric configuration for this residue was inferred by the *intra*-residue NOE contacts between H-1 and H-3, H-1 and H-5, and by the value of $^{1}J_{C1,H1}$ = 169 Hz. The sequence of the residues was inferred by proton-carbon long range scalar correlations showed in the HMBC spectrum between H-1 of **D** and C-4 of **E**, H-1 of **E** and C-4 of **B**, H-1 of **B** and C-5 of **F** and C-2 of **F** and H-6 of **C**. These results were confirmed also by dipolar couplings observed in the ROESY experiment between H-1 of **D** and H-4 of **E**, H-1 of **E** and H-4 of **B,** and H-1 of **B** and H-5 of **F**. Finally the NOE contact between H-5 of **B** and H-3ax of **F** suggests a D configuration for Kdo (Bock *et al.*, 1994), while the α-configuration for this residue was inferred by the difference (Δ= 0.37) between $H\text{-}3_{ax}$ and $H\text{-}3_{eq}$ (Agrawal *et al.*, 1994). The anomeric signal at 4.34 ppm (**C'**) was attributed to the non-phosphorylated lipid A β-GlcN, in fact its C-4/H-4 occurred at 70.8/3.40 ppm, respectively. This phosphate

heterogeneity determines the splitting of chemical shifts values belonging to residue **F** (**F'**) and to the heptose **B** (**B'**). As for the fractions **OS2** and **OS3** the ^{1}H NMR spectra (Figure 4.3) clearly showed the lack of the disaccharide α-Gal-(1→4)-β-Gal. Both were analyzed by one- and two-dimensional NMR spectroscopy. All the spin systems were assigned (Table 4.2 and 4.3) and the chemical shifts values indicated that residue **B** in **OS2** was a terminal α-Hep*6P*, while in **OS3** this residue was attributed to a terminal α-Hep*3P* as its C-3/H-3 chemical shifts occurred at 74.5/4.21 ppm, respectively (Grzeszczyk *et al.*, 1996). Moreover its C-6/H-6 chemical shift values occurring at 72.2/3.96 ppm confirmed the D,D configuration for this residue (Brisson *et al.*, 2002). These data were all confirmed by GC-MS methylation analysis. In particular, in order to confirm the position of the phosphate groups, the permethylation reaction was followed by a dephosphorylation with 48% aqueous HF. After acid hydrolysis, reduction and acetylation, the GC-MS chromatogram showed, besides the 4-substituted and the terminal heptose, a 3-substituted heptose, thus confirming the phosphorylation at position *O*-3 of this residue. The signal corresponding to 6-substituted heptose (Hep*6P*) was not found probably because phosphate group at position *O*-6 is not susceptible to hydrolysis (Grzeszczyk *et al.*, 1998). In conclusion, on the basis of all the collected data, the structure of the core region from *P. haloplanktis* TAB 23 LOS was determined as reported in Scheme 4.2.

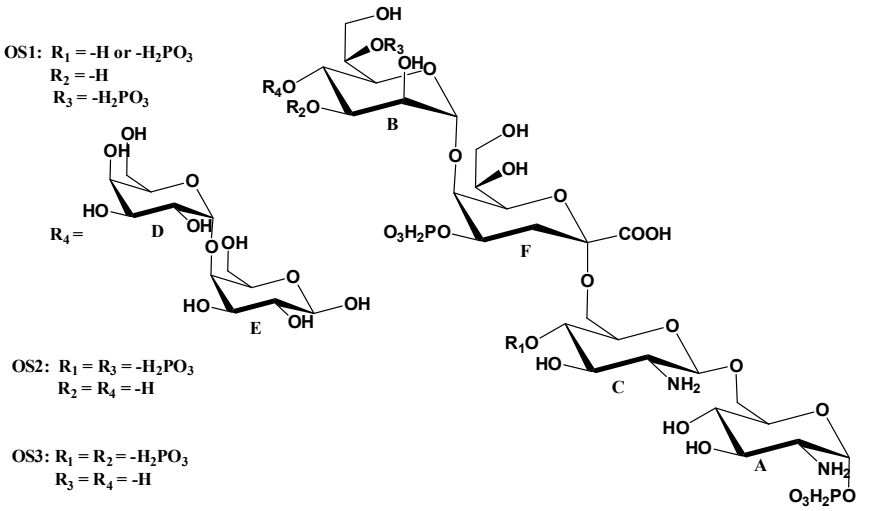

Scheme 4.2 – Structure of the core region oligosaccharides from *P. haloplanktis* TAB 23.

4.5 Biological activities of Lipid A

It is well known that the ability of bacterial LPS to stimulate the innate immune system depends on the lipid A moiety, which is recognized as a pathogen-associated molecule by TLR4 and induces the immune cells to activate the release of pro-inflammatory cytokines. Since lipid A from *P. haloplanktis* strains revealed a unique chemical structure, different from that of other Gram-negative bacteria whose immune-stimulatory activity has been widely studied (Erridge *et al.*, 2002), we evaluated whether this structure could have a significant impact on the immunological response *in vitro*.

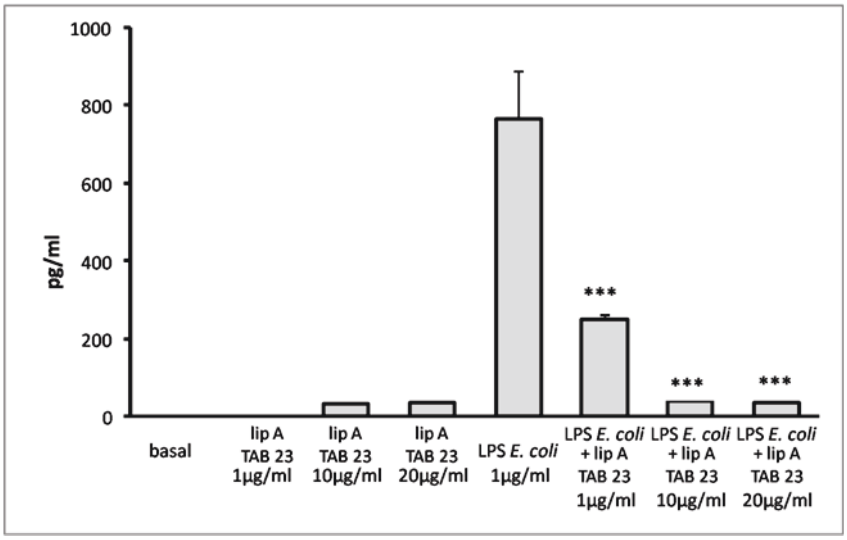

Figure 4.5 – TNFα production in THP-1 cells stimulated with *P. haloplanktis* strain TAB 23 lipid A with or without *E. coli* LPS. The results are expressed as means ± SD of triplicate data of one experiment of two performed with independent lipid A preparations. ***P<0.001 versus LPS alone (One way ANOVA with Dunnet correction).

In order to verify if lipid A was able to modulate the innate immune response, a human monocytic cell line (THP-1) was incubated with *P. haloplanktis* TAB 23 lipid A at different concentrations (1, 10 and 20 µg/mL) and the amounts of TNFα and IL-6 were measured in the culture supernatants. LPS from highly endotoxic bacteria (*E. coli* O111:B4) was used as a positive control. The results, shown in Figure 4.5, clearly demonstrated that *P. haloplanktis* TAB 23 lipid A failed to stimulate the production of TNFα.

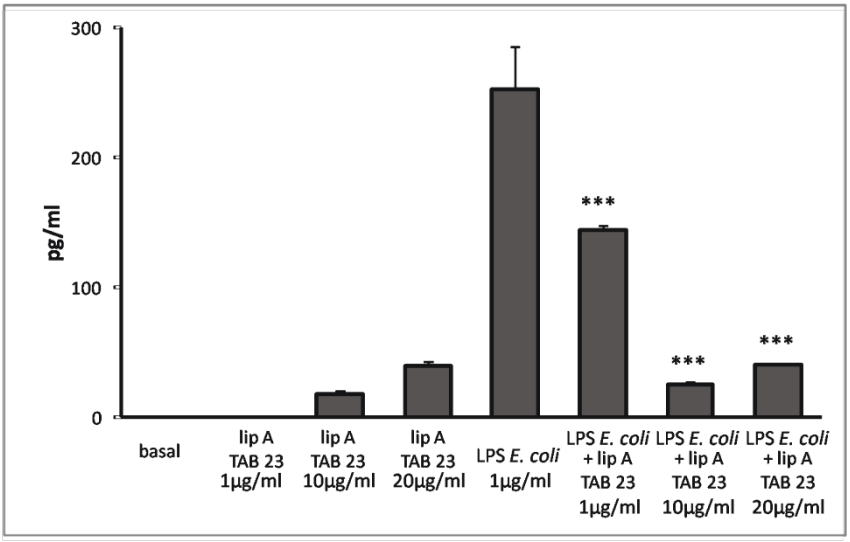

Figure 4.6 - IL-6 production in THP-1 cells stimulated with *P. haloplanktis* strain TAB 23 lipid A with or without *E. coli* LPS. The results are expressed as means ± SD of triplicate data of one experiment of two performed with independent lipid A preparations. ***P<0.001 versus LPS alone (One way ANOVA with Dunnet correction).

The production of IL-6 was slightly increased with lipid A at the highest concentration (20 µg/mL); however this production represented only 15% of the production induced by 1 µg/mL of *E. coli* LPS (Figure 4.6). When added in culture with LPS from *E. coli*, *P. haloplanktis* TAB 23 lipid A exerted a significant inhibitory effect on the LPS-induced pro-inflammatory cytokine production. *P. haloplanktis* TAB 23 lipid A was able to almost completely inhibit LPS-induced up-regulation of both TNFα (Figure 4.5) and IL-6 (Figure 4.6), reaching the maximum inhibition (95% inhibition for TNFα and 90% for IL-6, respectively) in cultures with 10 µg/mL lipid A added.

These results indicated that *P. haloplanktis* TAB 23 lipid A, which is mainly characterized by penta-acylated diphosphorylated

glycoforms, does not elicit a pro-inflammatory response *in vitro*, in terms of TNFα and IL-6 production.

4.6 Conclusions

In this work the core oligosaccharide from *P. haloplanktis* TAB 23 was structurally characterized (Scheme 4.2).
This strain belongs to the same species of *P. haloplanktis* TAC 125 and, for this reason, it was not surprising to find that LOSs have similar structures. As for the glycosyl composition the only difference was the presence of a terminal galactose unit in TAB 23 instead of a *N*-acetyl-mannosamine in TAC 125.

But the structure similarities are not limited to bacteria belonging to the same species. In fact, as already reported, bacteria belonging to genus *Pseudoalteromonas* are obligate marine and all characterized core structures present a high charge density. Moreover, the monosaccharides sequence has a common motif (Leone *et al.*, 2007), reported in Scheme 4.3.

β-Gal-(1→4)-α-L,D-Hep*3P*-(1→5)-α-Kdo*4P*-(2→6)-β-GlcN*4P*-(1→6)-α-GlcN*1P*

Scheme 4.3 – Oligosaccharide structure of *Pseudoalteromonas* genus.

As for lipid A moiety, the particular fatty acids composition is probably crucial for the biological activity. Interestingly, lipid A from *P. haloplanktis* TAB 23 exerts a potent antagonistic effect on cytokine up-regulation induced by *E. coli* LPS. This activity is not surprising since it has been demonstrated that other natural lipid A, with unique structures, obtained from Gram-negative photosynthetic bacteria, as *Rhodobacter sphaeroides* and *Rhodobacter capsulatus*, or from extremophilic and alkaliphilic bacteria, as *Halomonas magadiensis*, can antagonize cytokine release induced by endotoxic LPS both *in vitro* and *in vivo* (Rose *et*

al., 1995; Loppnow *et al.*, 1990; Ialenti *et al.*, 2006). On the other hand, it is noteworthy that the lipid A from *P. haloplanktis* TAC 125 exhibits a significant production of TNFα and IL-6 when tested on a human monocytic cell line (THP-1). This means that although the lipid A from strain TAC 125 and TAB 23 showed high structure similarity, the difference in the fatty acids distribution can influence biological activity.

Paper related to this chapter:

Carillo S, Pieretti G, Parrilli E, Tutino ML, Gemma S, Molteni M, Lanzetta R, Parrilli M, Corsaro MM.
"Structural investigation and biological activity of the lipooligosaccharide from the psychrophilic bacterium *Pseudoalteromonas haloplanktis* TAB 23."
Chemistry. **2011**; 17(25):7053-60.

Chapter 5

Colwellia psychrerythraea strain 34H

An intensively investigated steno-psychrophilic bacterium is *Colwellia psychrerythraea* strain 34H, a Gram-negative bacterium isolated from Arctic marine sediments (Huston *et al.*, 2000). It shows cardinal growth temperatures (optimum of 8°C, maximum of 19°C, and extrapolated minimum of -14.5°C) (Methè *et al.*, 2005) ranking among the lowest of all characterized bacteria which makes this bacterium an attractive model to study adaptive strategies to subzero lifestyle. In fact, thanks to *C. psychrerythraea* strain 34H, low temperatures tolerance, the motility and survival at -10°C in sea ice brines was proved (Junge *et al.*, 2003). As a consequence, the concept that liquid inclusions in the frozen environments of Earth provide adequate habitats for active microbial populations extends the discussion of the possibility of life elsewhere in the solar system.

The study of *C. psychrerythraea* strain 34H genome also showed that this bacterium is able to uptake or synthetise compounds that may confer cryotolerance, including polyhydroxyalkanoate (PHA) compounds (a family of polyesters that serve as intracellular carbon and energy reserves, of which some forms have been involved in pressure adaptation (Martin *et al.*, 2002)), cyanophycin-like compounds, and glycine betaine, as well as extracellular enzymes and polysaccharides (Methè *et al.*, 2005). Recently, the production of EPS from *C. psychrerythraea* strain 34H was tested in extreme life conditions (up to -14°C, 200 atm and 100‰ of salinity); the results obtained from Marx *et al.* in 2009 showed a dramatic increase of EPS production when the life conditions get worse, according to previous studies performed on

EPS belonging to *Pseudoalteromonas* species (Mancuso Nichols *et al.*, 2004; Nevot *et al.*, 2008).

Here the structural characterization of the LOS and CPS from *C. psychrerythraea* 34H and its lipid A biological activity are reported.

5.1. LPS extraction and preliminary analysis

C. psychrerythraea strain 34H cells were aerobically grown and recovered cell pellet was extracted by PCP to obtain crude LPS (Galanos *et al.*, 1969). When analysed by DOC-PAGE electrophoresis the latter showed positive silver staining. In particular a rough LPS (LOS_{PCP}) was revealed (Figure 5.1). Subsequent extraction by the phenol/water method (Westphal and Jann, 1965), yielded only a low amount of the lipooligosaccharide (LOS_W), the purity of which was worse than the LOS_{PCP}. The sugar composition of the LOS_{PCP} was obtained by GC-MS analysis of the acetylated methyl glycosides and revealed the occurrence of Man, GalA, GlcN, colitose (Col) and Kdo. The latter residue was revealed only after dephosphorylation of the LOS_{PCP}, which was achieved by HF treatment. This result suggested the presence of a phosphate group on this residue, that did not allow the detection of Kdo by GC-MS (Corsaro *et al.*, 2008). Methylation analysis indicated the presence of terminal Col, 6-substituted GlcN, 2-substituted GalA and 2,3-disubstituted Man. The methylation data also revealed a pyranose ring for all the residues.

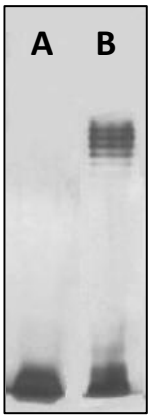

Figure 5.1 - 14% DOC-PAGE analysis of *Colwellia psychrerythraea* strain 34H LOS_{PCP} (lane A) and *Escherichia coli* O55:B5 LPS used as standard (lane B).

Absolute configurations of the sugar residues were determined by the GC-MS analysis of the corresponding acetylated 2-(+)-octyl glycosides (Leontein *et al.*, 1978). The GC-MS analysis of fatty acids methyl ester revealed the presence of decanoic (C10:0), dodecanoic (C12:0), 3-hydroxydodecanoic [C12:0(3OH)], tetradecenoic (C14:1), tetradecanoic (C14:0), pentadecenoic (C15:1), pentadecanoic (C15:0), 3-hydoxytetradecenoic [C14:1(3OH)], esadecenoic (C16:1), esadecanoic (C16:0), octadecenoic (C18:1) and octadecanoic (C18:0) acids.

5.2. Mass spectrometric analysis of the O-deacylated LOS_{PCP}

The LOS_{PCP} was *O*-deacylated by anhydrous hydrazine (Holst, 2000) and the product obtained (LOS-OH) was analysed by ESI FT-ICR MS. The charge deconvoluted spectrum displayed the presence of one main species (**M**) at 1844.607 Da. Other signals were attributed to potassium and sodium adducts (Figure 5.2). To

obtain further structural information the LOS-OH was subjected to capillary skimmer dissociation (CSD) which generated the Y and B fragments (Domon and Costello, 1988) resulting from the cleavage of the Kdo/lipid A linkage (Kondakov and Lindner, 2005). The CSD spectrum (Figure 5.3) showed the presence of a fragment at 922.176 *m/z* assigned to the core oligosaccharide and a second one at 922.423 *m/z* attributed to the lipidA-OH. In particular, the following composition was attributed to the core oligosaccharide: GroColGalAManKdoP_2 (accurated mass 922.175 Da) where Gro represents a glycerol residue. On the other hand, the lipidA-OH resulted to have the following composition: GlcN_2P_2[C12:0(3-OH)][C14:1(3-OH)] (accurated mass 922.426 Da), in agreement with the information obtained by chemical analysis.

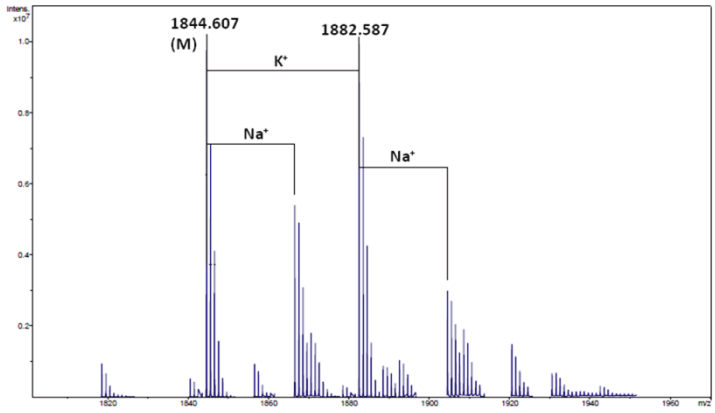

Figure 5.2 - Charge deconvoluted ESI FT-ICR mass spectrum of the LOS-OH isolated from *Colwellia psychrerytraea* strain 34H. The spectrum was acquired in the negative ions mode.

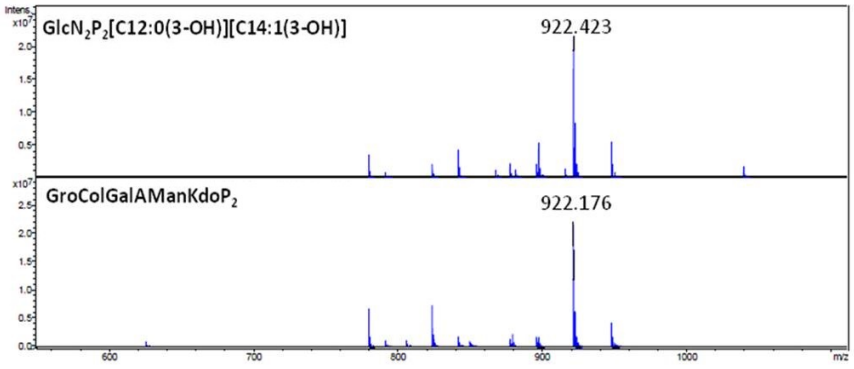

Figure 5.3 - Charge deconvoluted CSD mass spectrum of the LOS-OH isolated from *Colwellia psychrerytraea* strain 34H. The spectrum was acquired in the negative ions mode.

5.3. NMR analysis of the fully deacylated LOS$_{PCP}$

In order to characterize the core oligosaccharide the LOS-OH was further *N*-deacylated by strong alkaline hydrolysis and the obtained oligosaccharide (**OS**) was analysed by one- and two-dimensional NMR spectroscopy (Figures 5.4-5.6).

In particular ^{1}H-^{1}H DQF-COSY, ^{1}H-^{1}H TOCSY, ^{1}H-^{1}H ROESY, ^{1}H-^{13}C DEPT-HSQC, ^{1}H-^{13}C HSQC-TOCSY, ^{1}H-^{13}C HMBC, 2D *F2*-coupled HSQC and ^{31}P NMR were performed

The ^{1}H-NMR spectrum (Figure 5.4) of the fully deacylated LOS$_{PCP}$ showed the presence of five anomeric proton signals (**A**-**E**) between 4.7 and 5.7 ppm. By taking into account all the 2D NMR experiments the spin systems of all the monosaccharides were identified (Figure 5.5, Table 5.1).

.

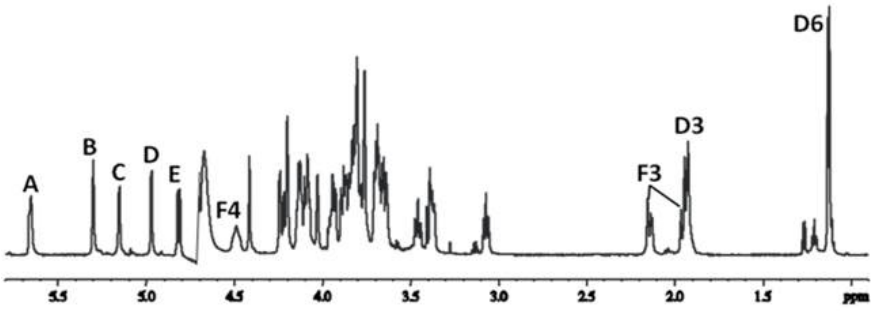

Figure 5.4 - ^{1}H-NMR spectrum of the oligosaccharide (**OS**) obtained by strong alkaline hydrolysis of the LOS_{PCP}. The spectrum was recorded in D_2O at 302 K at 600 MHz. The letters refer to the residues as described in Table 5.1 and in Scheme 5.1.

Residue **A** was attributed to the 6-substituted α-GlcpN*1P* of lipid A on the basis of the multiplicity of the anomeric proton signal due to its phosphorylation ($^{3}J_{H,P}$= 6.1 Hz). Moreover the C-2 chemical shift occurred at 55.3 ppm, which indicated a nitrogen-bearing carbon while the C-6 chemical shift was downfield shifted by glycosylation at 70.3 ppm.

Residue **E** with C-1/H-1 signals at 99.9/4.82 ppm ($^{1}J_{C1,H1}$= 166.3 Hz) was attributed to the lipid A 6-substituted β-GlcpN*4P* residue, as a result of its C-2 chemical shift at 56.8 ppm and its linkage to *O*-6 of **A**. In fact H-1of **E** displayed a long range scalar coupling with C-6 of **A** in the HMBC spectrum. The β-anomeric configuration was corroborated by the *intra*-residue NOE connectivities occurring between H-1 and both H-3 and H-5 protons in the ROESY spectrum. Moreover, the H-4 and C-4 downfield shifts were diagnostic for the presence of a phosphate group linked at *O*-4 (Holst *et al.*, 1993).

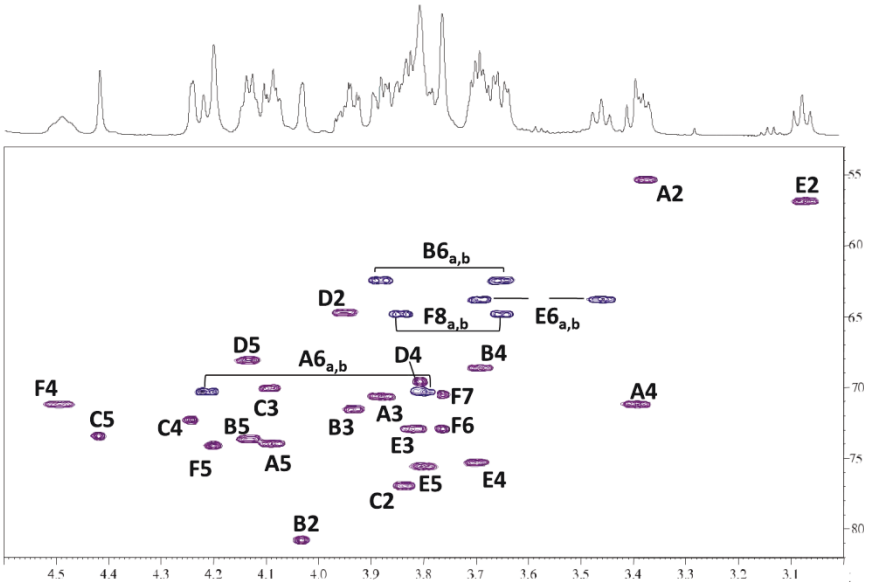

Figure 5.5 - Carbinolic signals region (3.0-4.6 ppm) of ^{1}H-^{13}C HSQC spectrum of **OS**. The spectrum was recorded in D_2O at 302 K at 600 MHz using acetone as internal standard (δ_H 2.225 ppm and δ_C 31.45 ppm). The letters refer to the residues as described in Table 5.1 and in Scheme 5.1.

Table 5.1 - ^{1}H and ^{13}C assignments of the fully deacylated oligosaccharide of the LOS_{PCP} from *Colwellia psychrerythraea* strain 34H. All the values are referred to acetone as internal standard (^{1}H 2.225 ppm; ^{13}C 31.45 ppm). Spectra were recorded at 302 K.

Residue	H1 C1	H2 C2	H3 C3	H4 C4	H5 C5	H6a C6	H6b/H7 C7	H7b/H8 C8
A α-GlcN*p1P*	5.56 92.8	3.38 55.3	3.88 70.6	3.39 71.1	4.09 73.9	3.80 70.3	4.21	
B 2-α-Man*p*	5.30 100.2	4.03 80.8	3.93 71.5	3.69 68.6	4.14 73.6	3.88 62.4	3.65	
C 2-α-GalA*p*	5.16 101.7	3.84 76.9	4.09 70.0	4.24 72.3	4.41 73.4	- 174.8		
D α-Col*p*	4.97 101.5	3.95 64.7	1.93 34.2	3.81 69.6	4.13 68.2	1.13 16.8		
E 6-β-GlcN*p4P*	4.82 99.9	3.07 56.8	3.81 72.9	3.81 75.5	3.70 75.3	3.46 63.7	3.69	
F 5-α-Kdo*p4P*	- 174.2	- 101.0	1.95-2.15 35.5	4.49 71.2	4.20 74.1	3.76 72.8	3.76 70.4	3.64-3.86 64.9

The Kdo (residue **F**) proton and carbon chemical shifts were identified starting from the diastereotopic protons H-3_{ax} and H-3_{eq}. The chemical shifts difference between these protons depends upon the orientation of C-1 carbon, being different for α and β anomers. In this case the $\Delta(H3_{ax}\text{-}H3_{eq})$=0.2 ppm allowed to attribute an α configuration to the residue (Agrawal *et al.*, 1994). Moreover both protons showed a correlation in the DQF-COSY spectrum with a signal at 4.49 ppm, attributed to Kdo H-4, which was in turn correlated to a carbon atom at 71.2 ppm in the DEPT-HSQC spectrum. Both H-4 and C-4 resonances were downfield shifted respect to reference values (Pieretti *et al.*, 2009*b*) and the observed chemical shifts were diagnostic for the presence of a phosphate in that position (Müller-Loennies *et al.*, 2002). The Kdo H-5 proton was identified by vicinal scalar coupling with H-4 in the DQF-COSY spectrum and the corresponding carbon atom was downfield shifted at 74.1 ppm indicating glycosylation at this position. In addition Kdo anomeric carbon showed a long range correlation with H-6 of residue **E**, thus confirming its linkage to the lipid A backbone.

Residue **B** was attributed to a 2-substituted α-*manno*pyranose on the basis of the small $J_{H\text{-}1,H\text{-}2}$ and $J_{H\text{-}2,H\text{-}3}$ coupling constant values. The glycosylation at C-2 position was inferred by comparing the carbon chemical shifts values with those of standard (Bock and Pedersen, 1983), while the α-anomeric configuration was established by the $J_{C\text{-}1,H\text{-}1}$ coupling constant value which measured 176.4 Hz. The HMBC spectrum (Figure 5.6) showed the presence of a long range scalar coupling between H-1 proton of this residue and C-5 of Kdo, thus indicating that this position was substituted by residue **B**. Residue **C**, with H-1/C-1 at 5.16/101.7 ppm was identified as a 2-substituted α-*galacto*pyranuronic acid since its C-6 occurred at 174.8 ppm and its C-2 was downfield shifted at 76.9 ppm. The α-anomeric configuration was inferred by the $J_{C\text{-}1,H\text{-}1}$ coupling constant value of 176.3 Hz. This residue resulted to be linked to residue **B** at position *O*-2, as demonstrated by the

presence of a correlation between H-1 of **C** and C-2 of **B** in the HMBC spectrum (Figure 5.6). The last residue (**D**) of the core oligosaccharidic chain was identified as a terminal α-colitose since its H-3/C-3 and H-6/C-6 occurred at 1.93/34.2 and 1.13/16.8 ppm, respectively. The α-anomeric configuration was inferred by $J_{C\text{-}1,H\text{-}1}$ (173.9 Hz). Its H-1 showed the presence of *inter*-residue NOE connectivities with H-2 of residue **C** in the ROESY spectrum as well as a long range scalar coupling with a carbon atom at 101.7 ppm in the HMBC spectrum (Figure 5.6). Thus it resulted to be linked to residue **C** at position *O*-2.

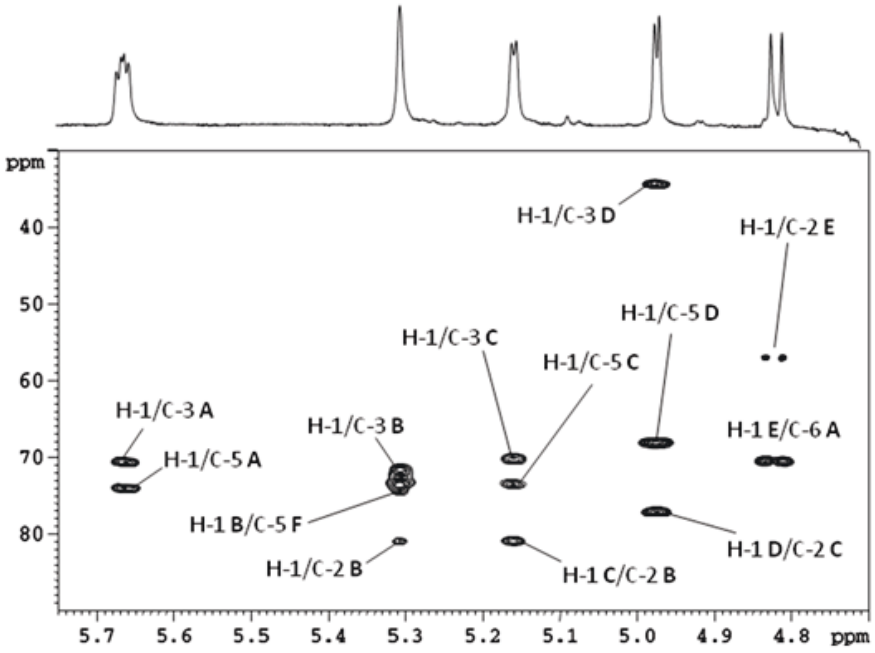

Figure 5.6 - Anomeric region of the ^{1}H-^{13}C HMBC spectrum of **OS**. The spectrum was recorded in D_2O at 302 K at 600 MHz using acetone as internal standard (δ_H 2.225 ppm and δ_C 31.45 ppm). The letters refer to the residues as described in Table 5.1.

To sum up, the above data allowed to identify the main carbohydrate backbone of the lipopolysaccharide from *Colwellia psychrerythraea* as depicted in Scheme 5.1.

α-L-Col-(1→2)-α-D-GalA-(1→2)-α-D-Man-(1→5)-α-D-Kdo4*P*
2
↓
6
β-D-GlcN4*P*-(1→6)-α-D-GlcN1*P*

Scheme 5.1 – *C. psychrerythraea* 34H core structure after KOH treatment.

The ^{31}P-NMR spectrum of **OS** confirmed the presence of only three phosphomonoester signals (Kdo*4P* 3.9 ppm, GlcN*4P* 3.5 ppm, GlcN*1P* 2.6 ppm), in contrast with the results obtained by the analysis of the LOS-OH mass spectra, which indicated four phosphate groups. These results, together with the lack of the glycerol residue in **OS** structure, suggested that these groups did not withstand the alkaline treatment, accordingly to the lability of the diesters towards this hydrolysis (Nummila *et al.*, 1995). In addition the finding of 2,3-disubstituted mannose in the methylation analysis did not fit with the above reported structure.

5.4. NMR analysis of the LOS-OH

To establish the structure of the core oligosaccharide including the labile groups lost during the harsh alkaline treatment, the LOS-OH was analysed by NMR spectroscopy (Figures 5.7). In particular ^{1}H-^{1}H DQF-COSY, ^{1}H-^{1}H TOCSY, ^{1}H-^{1}H ROESY and ^{1}H-^{13}C DEPT-HSQC were acquired. The analysis of all the spectra confirmed that the main carbohydrate backbone was that depicted in Scheme 5.1 (Table 5.2). Moreover, additional signals attributable to glycerol residue were present.

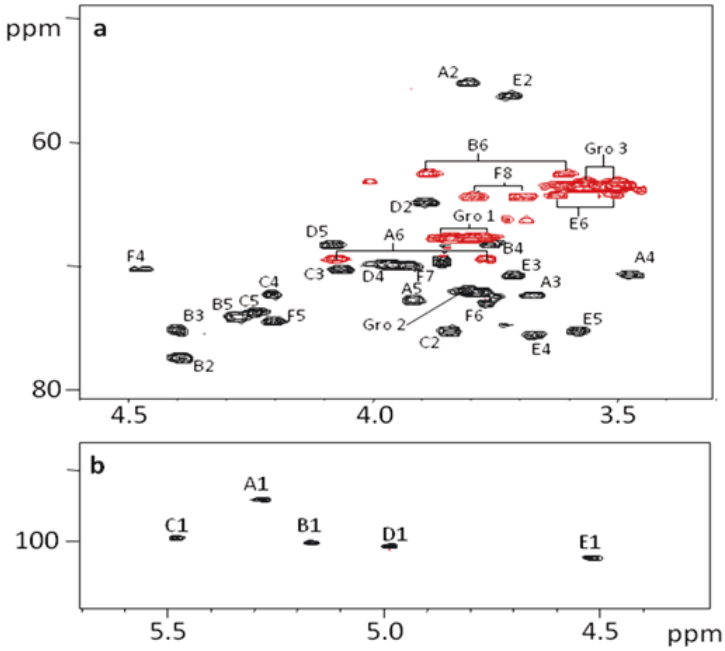

Figure 5.7- Carbinolic (a) and anomeric (b) regions of ^{1}H-^{13}C DEPT-HSQC spectrum of LOS-OH from *Colwellia psychrerytraea* strain 34H. The spectrum was recorded in D_2O at 298 K at 600 MHz using acetone as internal standard (δ_H 2.225 ppm and δ_C 31.45 ppm). The letters refer to the residues as described in Table 5.2 and in Scheme 5.2

More in detail, C-1 of Gro residue occurred at 67.7 ppm in the ^{1}H-^{13}C DEPT-HSQC spectrum (Figure 5.7), thus indicating its phosphorylation at position 1. Furthermore H-3 and C-3 of residue **B** were downfield shifted at 4.40/75.1 ppm, thus indicating that Gro was linked to the mannose residue at position *O*-3 through a phosphodiester linkage, in agreement with the presence of 2,3-disubstituted mannose in the GC-MS methylation analysis. In order to determine the relative configuration of Gro residue, the latter was oxidized to glyceric acid. The product was hydrolyzed and the free gliceric acid was esterified with chiral 2-octanol and then the corresponding octyl ester derivative was analyzed by GC-MS (Rundlöf and Widmalm, 1996).

Table 5.2 - ^{1}H and ^{13}C assignments of the LOS-OH from *Colwellia psychrerythraea* strain 34H. All the values are referred to acetone as internal standard (^{1}H 2.225 ppm; ^{13}C 31.45 ppm). Spectra were recorded at 298 K.

Residue	H1 C1	H2 C2	H3 C3	H4 C4	H5 C5	H6a C6	H6b/H7 C7	H7b/H8 C8
A α-GlcN*p1P*	5.27 94.1	3.80 55.1	3.67 72.4	3.47 70.7	3.91 72.7	3.76 69.4	4.06	
B 2-α-Man*p3P*	5.16 100.2	4.40 77.3	4.40 75.1	3.75 68.1	4.27 74.1	3.87 62.4	3.61	
C 2-α-GalA*p*	5.47 99.7	3.85 75.1	4.06 70.0	4.20 72.2	4.42 73.4	- nd		
D α-Col*p*	4.98 100.3	3.87 64.9	1.88-1.98 34.3	3.97 69.7	4.07 68.2	1.13 17.1		
E 6-β-GlcN*p4P*	4.51 102.5	3.71 56.2	3.67 72.4	3.67 75.5	3.57 75.1	3.49 64.2	3.62	
F 5-α-Kdo*p4P*	- nd	- Nd	1.89-2.16 35.5	4.47 70.1	4.19 74.5	3.76 72.9	3.91 69.8	3.68-3.78 64.3
t-Gro*1P*	3.79-3.83 67.7	3.77 71.9	3.49-3.56 63.4					

By comparison of its retention time with that of a standard sample, it was found to be D-configured.

In conclusion, the complete structure of the core-lipid A saccharidic backbone of the LPS from *Colwellia psychrerythraea* strain 34H resulted to be as depicted in Scheme 5.2.

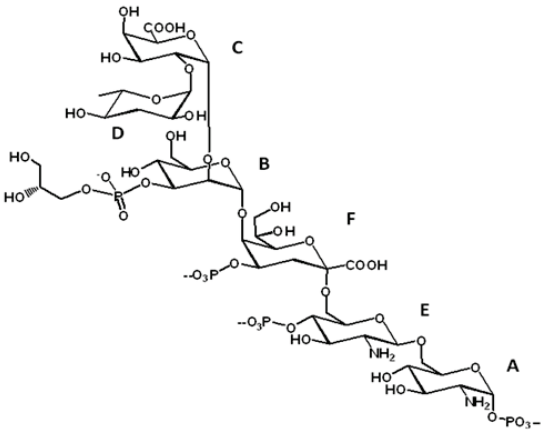

Scheme 5.2 – The structure of core oligosaccharide from *C. Psychrerythraea* 34H

5.5. Lipid A structure elucidation and biological assay

At the time when this thesis has been written down, only a partial study on lipid A structure elucidation has been carried on. However, their peculiarity made the results obtained worth being reported.

The high heterogeneity showed in fatty acids chemical analysis was confirmed by the complexity of negative ion mode ESI FT-ICR charge deconvoluted mass spectrum. Four cluster of signals were present in the spectrum (Figure 5.8, Table 5.3) corresponding to penta-, hexa-, epta- and octa-acylated species. The most abundant species **K3** and **K4,** occurring at 1807.05 *m/z* and 2043.28 *m/z*, respectively, were attributed to the following compositions: $GlcN_2P_2[C12:0(3OH)]_2[C14:1(3OH)]_2C10:0_3$ and $GlcN_2P_2[C12:0(3OH)]_2[C14:1(3OH)]_2C10:0_3C16:1$. To the best of my knowledge this is the first time that an octa-acylated lipid A has been found.

Table 5.3 – The main species of the charge deconvoluted negative ion mode ESI FT-ICR mass spectrum of the lipid A from *C. psychrerythraea* 34H**.**

Species	Observed mass (Da)	Calculated Mass (Da)	Composition
K1	1498.91	1498.91	$GlcN_2P_2[C12:0(3OH)]_2[C14:1(3OH)]_2C10:0$
K2	1652.91	1653.05	$GlcN_2P_2[C12:0(3OH)]_2[C14:1(3OH)]_2C10:0_2$
K3	1807.05	1807.19	$GlcN_2P_2[C12:0(3OH)]_2[C14:1(3OH)]_2C10:0_3$
K4	2043.28	2043.41	$GlcN_2P_2[C12:0(3OH)]_2[C14:1(3OH)]_2C10:0_3C16:1$

Even though the fatty acids distribution has not yet been investigated, its peculiar structure prompted us to investigate *C. psychrerythraea* lipid A biological activity. Preliminary assays were performed by Prof. Francesca Granucci from Milan-Bicocca University. When tested on dendritic cells, *C. psychrerythraea* lipid

A at different concentration resulted to be almost unable to elicit the production of TNFα.

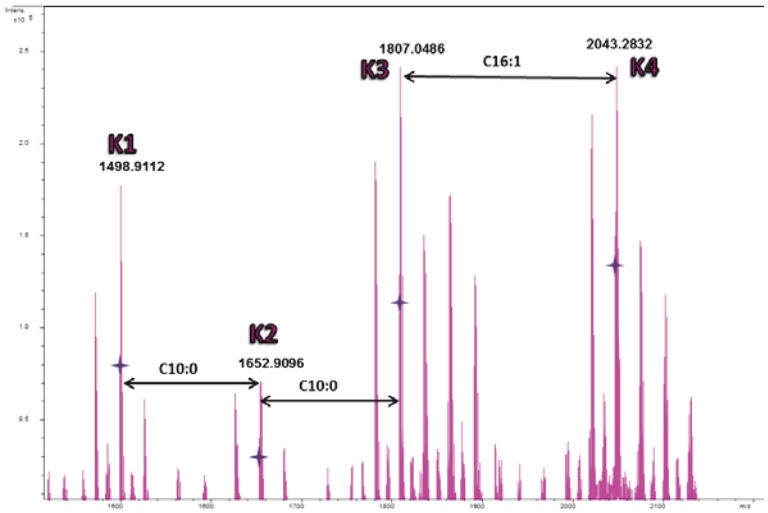

Figure 5.8 – The charge deconvoluted negative ion mode ESI FT-ICR mass spectrum of the lipid A from *C. psychrerythraea* 34H

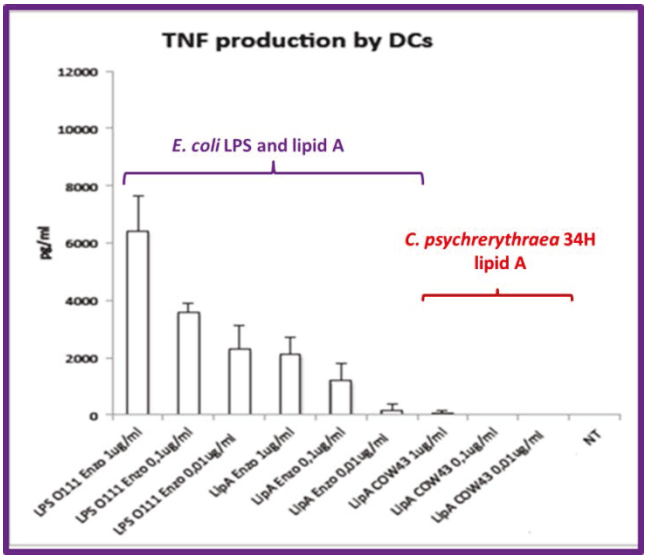

Figure 5.9 – TNFα production in DC cells stimulated with *C. psychrerythraea* 34H lipid A with or without *E. coli* LPS.

However, further experiments are needed to investigate whether this lipid A exerts an inhibitory effect on cytokine up-regulation induced by *E. coli*. In particular, co-incubation of *E. coli* LPS and *C. psychrerythraea* lipid A should show a decreased TNFα production, even if the addition of the antagonist is not simultaneous.

5.6. The capsular polysaccharide of Colwellia psychrerythraea

Colwellia psychrerythraea 34H was grown at 4°C as reported in Section 9.1.5. TEM images for conventionally embedded preparations of the strain used in the present study revealed details of the cell envelope, including the capsular polysaccharides (CPS) around the observed cells (Figure 5.10).

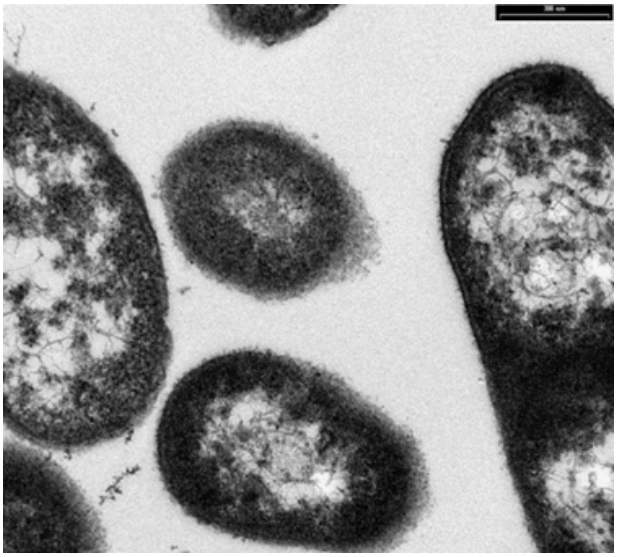

Figure 5.10 - Representative TEM images of thin sections of *Colwellia psychrerythraea* 34H.

In order to isolate the CPS, *C. psychrerythraea* strain 34H cells were extracted with aqueous phenol/water method (Westphal and

Jann, 1965). The water extract (LOS_W) was dialyzed and devoid of contaminants such as proteins and nucleic acids using protease, DNAse and RNAse enzymatic digestion. The purified sample was analyzed by 14% DOC-PAGE experiment, using both silver nitrate and Alcian blue to visualize the sample. The silver nitrate showed the presence of only one band at low molecular mass, corresponding to LOS (see Section 5.1). The Alcian blue staining method allowed us to visualize bands at higher molecular masses (Figure 5.11).

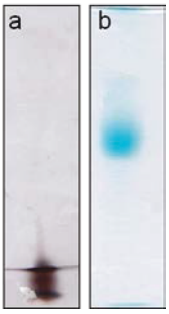

Figure 5.11 – 14% DOC-PAGE of LOS_W after silver staining (a) and Alcian blue staining (b)

Sugar and fatty acid analysis of the sample showed the presence of D-galacturonic acid (GalA), D-glucuronic acid (GlcA), 2-deoxy-2-amino-D-glucose (GlcN) and 2-deoxy-2-amino-D-galactose (GalN), together with 3,6-dideoxyhexose, mannose and 3-hydroxylated dodecanoic acid, which belong to the LOS and then revealed its presence in the aqueous extract. The molecular masses of CPS and LOS species were supposed to be very different on the basis of the DOC-PAGE analysis. Nevertheless the well known ability of the LPS to form micellar aggregates in aqueous solution did not allow the separation of the two macromolecules by size exclusion chromatography. Alternatively the sample was hydrolyzed under mild acid conditions to cleave the glycosidic linkage between the lipid A and the saccharidic region of the LOS. After centrifugation a supernatant containing the CPS and the core oligosaccharidic portion of the LOS was obtained. This mixture

was separated on a Biogel P-10 chromatography column, using pyridinium acetate buffer as eluent. Two fractions were obtained: the first and less retained one (**CPS**) contained the capsular polysaccharide, while the second one (**OS**) contained species with lower molecular mass, corresponding to the core oligosaccharide of the LPS.

Sugar and fatty acids analysis performed on fraction **CPS** revealed the presence of D-GalA, D-GlcA, D-GlcN and D-GalN, while the LPS components were absent. In particular methylation analysis revealed the presence of 2-substituted GalA, 4-substituted GlcA, 3-substituted GlcN and 3-substituted GalN.

CPS polysaccharide was then analyzed by mono- and two-dimensional NMR (DQF-COSY, TOCSY, ROESY, ^{1}H-^{13}C DEPT-HSQC, ^{1}H-^{13}C HMBC) (Figure 5.12, Table 5.4). The analysis of all the 2D-NMR experiment allowed the complete characterization of all the spin systems.

The ^{1}H-^{13}C DEPT-HSQC NMR spectrum (Figure 5.12) displayed the presence of four anomeric cross-peaks at 5.31/98.3 ppm (**A**), 4.54/104.4 (**B**), 4.43/104.2 (**C**) and 4,42/102.4 (**D**). The number of correlations present in the TOCSY and HSQC-TOCSY spectrum allowed to attribute a *gluco*- configuration to residues **B** and **C** and a *galacto*-configuration to residues **A** and **D**. Moreover, two additional spin systems were present (**E**, **F**). The first consisted of three resonances at 1.10/20.0, 4.30/68.8 and 4.40/59.2 ppm, attributed to CH_3, CHOH and CHNH groups of a threonine (Thr), respectively. The second spin system comprised a methyl group at 1.35/17.6 ppm, and a CHNH group at 4.27/50.0, attributed to an alanine residue (Ala).

Residue **A** was assigned to a 2-substituted α-galactopyranuronic acid as its C-2 resonance was shifted downfield (3.74/78.8 ppm) and its $^{1}J_{C1,H1}$ coupling constant measured 181 Hz. Moreover its H5 proton showed a long range scalar connectivity with a carbon atom at 171.9 ppm, which in turn correlated with a proton at 4.40 ppm, that belonged to Thr spin system, thus revealing that the latter was

linked at position C-6 of residue **A**. Residue **C** was assigned to a 4-linked β-glucuronic acid as its $^{1}J_{C1,H1}$ was 169 Hz C-4 resonance was shifted downfield respect to reference value (3.70/81.0 ppm) and both its H-4 and H-5 protons showed a correlation in the HMBC spectrum with a carboxyl signal at 173.3 ppm (Bock and Pedersen, 1983).

Table 5.4. ^{1}H and ^{13}C NMR assignments of CPS. Spectra were recorder in D_2O, using acetone as internal standard.

Residue	H1 C1	H2 C2	H3 C3	H4 C4	H5 C5	H6a,b C6
A	5.31	3.74	3.83	4.12	4.20	-
2-α-D-Gal*p*A6LThr	98.3	78.8	69.0	71.1	72.9	171.9
B	4.54	3.76	3.64	3.41	3.37	3.74-3.67
3-β-D-Glc*p*NAc	104.4	55.9	83.4	69.6	76.6	62.2
C	4.43	3.26	3.55	3.70	3.83	-
4-β-D-Glc*p*A	104.2	73.3	75.0	81.0	75.3	173.3
D	4.42	3.86	3.79	4.21	3.59	3.80-3.64
3-β-D-Gal*p*NLAla	102.4	52.0	79.5	65.9	76.0	61.9

Additional chemical shift:
NAc at 1.89/23.5 ppm (CH3), 176.1 (CO);
Thr at 1.10/20.0 ppm (CH3), 4.30/68.8 (CHOH), 4.40/59.2 (CHNH), 175.3 (COOH);
Ala at 1.35/17.6 ppm (CH3), 4.27/50.0 (CHNH), 177.7 (COOH).

Residue **B** and **D** were identified as a 3-substituted β-glucosamine and β-galactosamine, respectively on the basis of $^{1}J_{C1,H1}$ values (169 Hz both) and of the correlation of their H-2 protons, at 3.76 and 3.86 ppm, with the nitrogen-bearing carbons at 55.9 and 52.0 ppm, respectively. Moreover, both residues showed downfield chemical shifts for their C-3 carbon (83.4 and 79.5 ppm, respectively). Both H-2 protons were shifted downfield indicating the presence of an acyl substituent on the amino groups; in particular, H-2/C-2 of residue **B** bore an acetyl group. In fact it displayed correlations, in the HMBC spectrum, with the carboxylic carbon at 176.1 ppm, in turn correlated to a methyl proton at 1.89 ppm. By exclusion the Ala residue was placed at position *N*-2 of residue **D**.

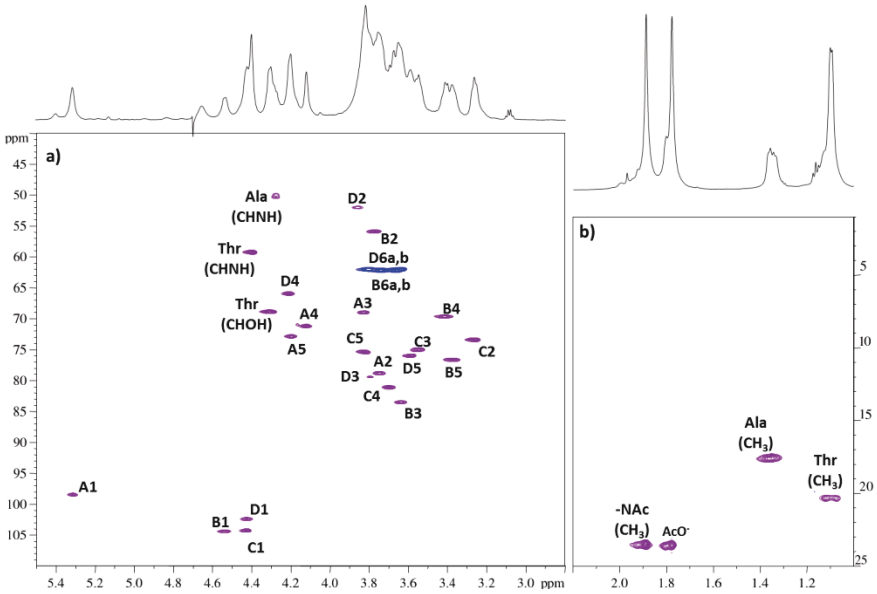

Figure 5.12 – Carbinolic, anomeric(a) and aliphatic (b) regions of ^{1}H-^{13}C DEPT-HSQC spectrum of **CPS** from *Colwellia psychrerytraea* strain 34H. The spectrum was recorded in D_2O at 298 K at 600 MHz using acetone as internal standard (δ_H 2.225 ppm and δ_C 31.45 ppm). The letters refer to the residues as described in Table 5.4.

The sequence of the residues was inferred by long range scalar correlations showed in the HMBC spectrum between H-1 of **A** and C-3 of **D**, H-1 of **B** and C-2 of **A**, H-1 of **C** and C-3 of **B** and H-1 of **D** and C-4 of **C**. These results were confirmed also by *inter*-residue dipolar couplings observed in the ROESY experiment between H-1 of **A** and H-3 of **D**, H-1 of **B** and H-2 of **A**, H-1 of **C** and H-3 of **B** and H-1 of **D** and H-4 of **C**.

The above mentioned data allowed us to attribute a linear structure to the repeating unit of the capsular polysaccharide from *C. psychrerythraea* strain 34H, as illustrated in Scheme 5.3.

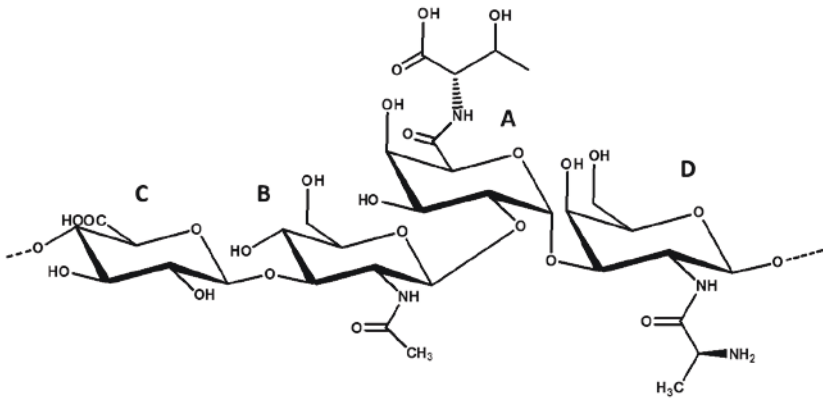

Scheme 5.3 – The repeating unit of the capsular polysaccharide from *C. psychrerythraea* 34H

5.7. Conclusions

In this thesis work the structure of the LOS and CPS from *C. psychrerythraea* 34H was established. As for core region, it is worth nothing the lack of heptoses residues in the inner core of *C. psychrerytraea*. Actually, in place of them an α-mannose residue is linked to the Kdo. This structural feature is commonly found in the *Rhizobiaceae* family, but was never found so far in extremophiles. Moreover in *Colwellia* LOS colitose and glycerol are present. Both these residues have been already found in several O-polysaccharides and K-antigens from Gram-negative bacteria, but to the best of our knowledge this is the first time that they have been found in a core oligosaccharide.

The lipid A moiety, displayed a structure that is new among lipopolysaccharide. In particular, the presence of 3-hydroxy-unsaturated fatty acids was reported only for *Agrobacterium tumefaciens* (Silipo *et al.*, 2004c) and is in agreement with the presence of unsaturated fatty acids in place of saturated ones in psychrophilic membrane bilayers. Moreover, it is hard to speculate about the reason behind the expression of an octa-acylated lipid A,

which maybe reflects the need for an high membrane fluidity. However, even more surprising is the result obtained from biological assay on this molecule. In fact, studies about supramolecular organization of lipid A (Brandenburg *et al.*, 1993) and about the complex lipidA-MD2-TLR4 (Park *et al.*, 2009) showed how acylation degree is important for activation/dimerization of receptorial complex. Generally, hexa-acylated lipid A showed an agonist activity, while under-acylated species showed an antagonist activity (see Section 2.4). As a consequence, would be very important to investigate more in detail the structure of *C. psychrerythraea* 34H lipid A and its biological activity.

As far as we know, the structure of the capsular polysaccharide is also new among bacterial polysaccharides. In fact, most of the EPS produced by marine bacteria, are linear polymers composed of neutral sugars, like pentoses and hexoses, amino sugars or uronic acids. Other components, such as sulphates or organic acids have been found as substituents on the sugar backbone. (Nichols *et al.*, 2005) The structure reported here is composed of a linear tetrasaccharidic repeating unit containing two amino sugars and two uronic acids. It is actually a new glycosaminoglycan polysaccharides. Nevertheless, other Gram-negative and Gram-positive bacteria express glycosaminoglycans as capsule around bacteria cells, and the research for new source of these bioactive compounds is just directed towards microbial production (DeAngelis, 2012). Moreover two α-aminoacids, Thr and Ala, have been found as substituents. They may confer and/or increase a cryoprotective property of the polysaccharide. In fact, AFPs proteins, which are constitutively expressed in psychrophiles, show Thr- and Ala-rich motifs organized into arrays that form the proteins' ice-binding site (Graether *et al.*, 2000; Lin *et al.*, 2011). This result suggests that the saccharidic cryoprotective EPS from *C. psychrerythraea* 34H, tested by Marx *et al.* in 2009, may coincide with this capsular polysaccharide; it could be located

around the cell as a capsule, when the organism is not experiencing a deep worsening of life conditions, or be secreted in the surrounding medium to avoid freezing of its watery environment. This would also explain the finding of *C. psychrerythraea* living cells in brine channels where temperature is very low and salt concentration very high. The process may be supported by the anionic site on the polysaccharide, which might modify the water properties near the cell by binding cations and lowering the freezing temperature, providing a barrier against the environmental stress (Nichols *et al.*, 2005). Moreover, the complete structure bears both negative and positive charged groups, thus it might be classified as a zwitterionic polysaccharide (ZPS) (Tzianabos *et al.*, 1992). Due to this unique structure, ZPSs possess immunomodulatory activities, (Mazmanian *et al.*, 2005) but as far as we know ZPSs from cold-adapted bacteria have never been tested.

All these deductions have to be supported by further analysis on both physicochemical and biological properties of this new unique polysaccharide.

Paper related to this chapter:

Carillo S, Pieretti G, Lindner , Parrilli E, Sannino F, Tutino ML, Lanzetta R, Parrilli M, Corsaro MM.
"Structural characterization of the core oligosaccharide isolated from the lipopolysaccharide of the psychrophilic bacterium *Colwellia psychrerythraea* strain 34H."
Eur J Org Chem. In press.

Psychrophiles: Conclusions

Up to now only few structures of LPSs from other cold-adapted microorganisms have been characterised. By comparing structures from *C. psychrerythraea* 34H LOS, *P. haloplanktis* TAC 125 (Corsaro *et al.*, 2001; Corsaro *et al.*, 2002) and TAB 23 (Carillo *et al.*, 2011), and from *P. arctica* (Corsaro *et al.*, 2008) it turned out that all of them share the lack of the O-chain and the presence of a high charge density in the core region due to the presence of acidic monosaccharides and phosphate groups. In addition, the core region have been found to be constituted by few sugar units. These structural features seem to be common to cold-adapted microorganisms. Recently O-chain polysaccharide was found in LPS from *Psychrobacter muricolla* and *cryohalentis*. Although the latter microorganisms had been isolated at -9°C, the LPS was extracted from bacterial cells grown at 24°C (Kondakova *et al.*, 2012a; Kondakova *et al.*, 2012b). It would be worth investigating the LPS produced at lower growth temperature.

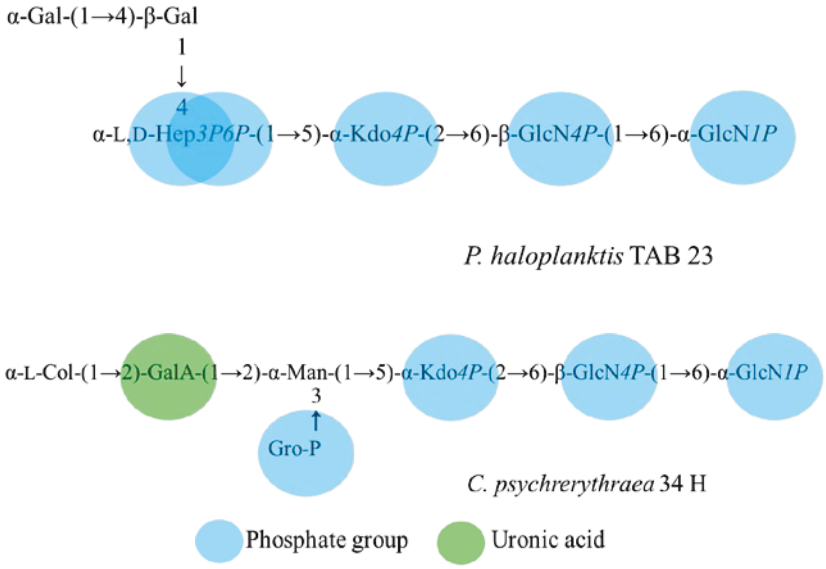

It is tempting to speculate that an evolutionary adaptation of the cell to low temperatures could induce the micro-organism to avoid energy waste and, consequently to produce only rough LPS because the synthesis of the O-chain is an energy-demanding process. However, the gene responsible of O-chain biosynthesis may be irreversibly deleted or not. In fact, although they save the expenditure of unnecessary energy, these mutants may be not able to start the reverse process under changed environmental circumstances (Lukáčová *et al.*, 2008).

Moreover, two very different lipid A were characterized, even if the biological activities carried out were similar. They share shorter and unsaturated fatty acid chains as already found in *P. haloplanktis* TAC 125 lipid A (Corsaro *et al.*, 2002). A similar variation in fatty acids composition has been found in membrane phospholipids and constitutes one of the known cold adaptation mechanisms. Moreover, from biological assays it is clear that the real relationship between structure and activity of lipid A is far to be understood, since a penta-acylated as well as an octa-acylated lipid A were not able to induce inflammatory cytokines production.

Another very interesting point has been the elucidation of the capsular polysaccharide from *C. psychrerythraea*. Its structural peculiarities arise many discussion points about its biological role, its physicochemical properties as well as biological activity.

All the above results make clear that extremophilic microorganisms may be an inexhaustible source of metabolites with a wide range of exploitable properties.

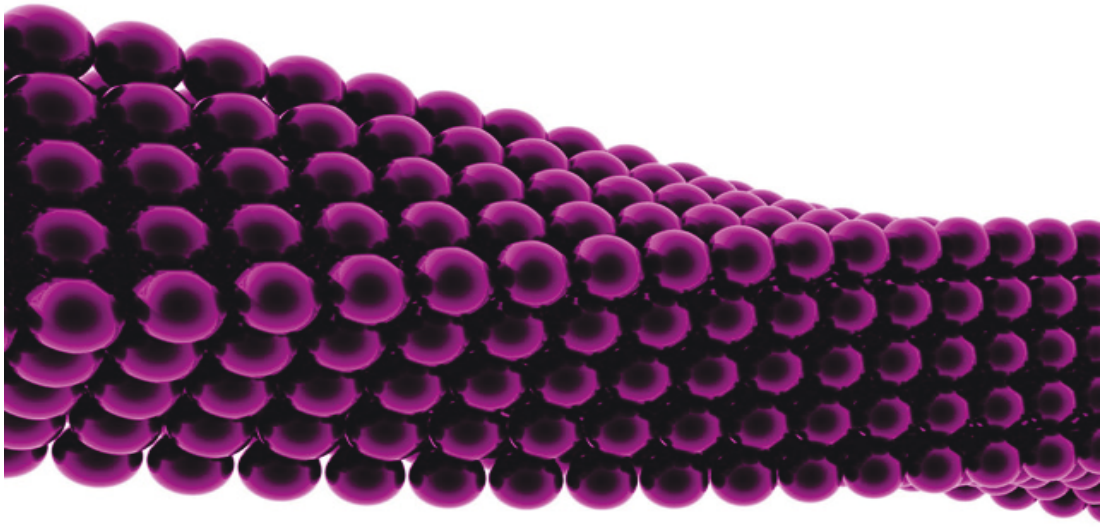

Haloalkaliphiles

In this thesis, the LPS from three haloalkaliphilic bacteria has been investigated; two of them belong to genus *Halomonas*, while the third one to genus *Salinivibrio*.

The *Halomonadaceae* family, which comprise *Halomonas* genus. accommodates moderately halophilic/halotolerant microorganisms that generally thrive in high salt environments (Franzmann *et al.*, 1988). The genus *Halomonas* contains a great number of species (62 species with validly published names; http://www.bacterio.cict.fr/h/halomonas.html) and species belonging to this genus are ubiquitous and typically have been isolated from saline lakes, solar salt facilities, saline soils and marine environments. *Halomonas* genus is extensively exploited both for production of small metabolites, like ectoine and biotechnological relevant exopolysaccharides (see Section 1.3). Beyond the great biotechnological exploitation of bacteria belonging to this genus, they have not previously been reported to be a cause of human infections, but during the last decade, several bacteria belonging to two different *Halomonas* species have been identified (Von Graevenitz *et al.*, 2000; Berger *et al.*, 2007).

Salinivibrio genus is included in the *Vibrionaceae* family, which belongs to the class *Gammaproteobacteria* of the phylum *Proteobacteria*. Besides *S. sharmensis*, up to now, the *Salinivibrio* genus includes *S. costicola* subsp. *costicola* (Smith, 1938; Mellado *et al.*, 1996; Huang *et al.*, 2000), *S. costicola* subsp. *vallismortis* (Huang *et al.*, 2000), *S. costicola* subsp. *alcaliphilus* (Romano *et al.*, 2005), *S. proteolyticus* (Amoozegar *et al.*, 2008) and *S. siamensis* (Chamroensaksri *et al.*, 2009). Members of this genus are moderately halophilic bacteria distributed in salted meats, brines and several hypersaline environments. Lama *et al.* (2005) and Karbalaei-Heidari *et al.* (2008) have studied proteases from species belonging to *Salinivibrio* genus, such as *S. costicola* subsp. *alcaliphilus* and *S. proteolyticus*, respectively. Moreover, *S.*

costicola has been used as model microorganism for studying osmoregulation and other physiological mechanisms in moderate halophiles (Oren, 2002; Amoozegar *et al.*, 2008).

Chapter 6

Halomonas alkaliantarctica CRSS

H. alkaliantarctica was isolated from a salt sediment of a saline lake in Cape Russel in the Antarctic continent (Poli *et al.*, 2007) and has its optimum growth at pH 9, 30°C in 10% NaCl. *Halomonas alkaliantarctica* cells were Gram-negative aerobic rods able to produce exopolysaccharide. The LPS extracted from this bacterium had been already investigated, obtaining the O-chain polysaccharide chemical structure (Pieretti *et al.*, 2009a); it was found to have a trisaccharidic neutral repeating unit formed by rhamnose residues (Scheme 6.1).

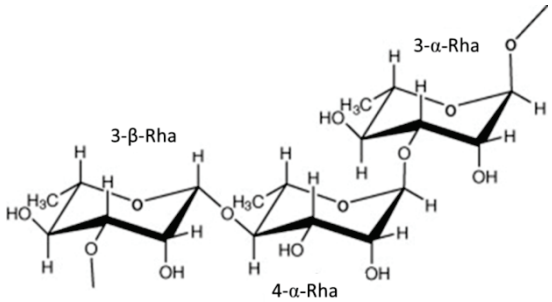

Scheme 6.1 – The structure of the O-chain repeating unit from *H. alkaliantarctica* strain CRSS.

In this thesis the attention has been focused on the structural elucidation of the core oligosaccharidic region from *H. alkaliantarctica* LPS, that was obtained after deacylation in mild acid and alkaline conditions. The obtained products were both analysed by MALDI-TOF mass spectrometry. Moreover the product recovered after alkaline hydrolysis was purified by HPAEC and characterized by means of 2D-NMR spectroscopy.

6.1 Isolation and compositional analysis of LPS

H. alkaliantarctica cells were grown as reported in Section 9.1.1 and the LPS was extracted by both PCP and water/phenol methods (Galanos *et al.*, 1969; Westphal and Jann, 1965). PCP and water extracts were analysed by SDS-PAGE revealing a smooth type LPS. However, only the PCP extract was used for further analysis since it was free from nucleic acids as revealed by UV spectroscopy and sugar analysis, while for LPS_W the contamination was significant. The LPS was acid hydrolysed under mild conditions and the lipid A was removed by centrifugation. The supernatant was fractionated on a Biogel P-10 column. Fraction **a**, eluted in the void volume, was used previously to characterize the O-chain polysaccharide (Pieretti *et al.*, 2009a). Fractions **b** and **c** mainly contained the core oligosaccharide. The sugar analysis performed on these fractions showed the presence of Glc, GlcA, L,D-Hep and Kdo. In addition, fraction **b** still contained rhamnose belonging to the O-chain, therefore its analysis was not convenient for the core structural elucidation. The methylation analysis of fraction **c** was performed after dephosphorylation, and identified the substitution pattern of the core region, i.e. 2-substituted GlcA, terminal Glc, 2-substituted Hep, and 2,3,4-trisubstituted Hep.

Fraction **c** was analysed by both MALDI-TOF MS and ^{1}H-NMR. The reflectron positive ions MALDI-TOF spectrum showed the presence of only two species. The most abundant adduct ion $[M+Na+K]^+$ (**P1**) at *m/z* 1326.6, was attributed to the following composition: $Glc_3GlcAHep_2Kdo$*anhydro* (calculated molecular mass 1327.32 Da). The second one (**P2**) occurred at *m/z* 1164.7, 162 u lower than **P1** and it was then attributed to a molecular species containing one glucose less (calculated molecular mass 1165.27 Da). The ^{1}H-NMR spectrum of the same fraction appeared to be very complex, probably due to the reducing end Kdo present as *anhydro* (Banoub *et al.*, 2004) forms. Therefore the NMR analysis was performed on the deacylated LPS.

6.2 Analysis of the deacylated products

Fully deacylation of the LPS was performed by treating the LPS first with hydrazine and then with KOH (Masoud *et al.*, 1994, Section 9.2.5). The obtained product was desalted on a Sephadex G10 and then partially purified on a Biogel P-10 column. The most abundant fraction (**A**) contained the core oligosaccharide linked to a large number of O-chain repeating units, while the second one (**B**) was mainly constituted by the core oligosaccharides. The reflectron negative ions MALDI-TOF spectrum of this fraction (Figure 6.1) displayed an adduct ion $[M+K-H]^-$ at *m/z* 1883.8 (**M1**, calculated molecular mass 1884.37 Da) which revealed the composition $GlcA(Glc)_3(Hep)_2Kdo(GlcN)_2P_3K$ (GlcN=2-deoxy-2-amino-glucose; $P=PO_4^{3-}$). The signal at *m/z* 1785.9 (calculated molecular mass 1786.53 Da) suggested the presence of a fragment ion which lacks a phosphoric acid molecule, as its mass difference respect to the species **M1** is 98 u (Olsthoorn *et al.*, 1999). In addition a less intense signal at 162 u lower masses (**M2**) indicated a molecular species with one glucose less, in agreement with the data obtained from the MALDI-TOF analysis of fraction **c**.

Fraction **B** was then purified by HPAEC-PAD obtaining a main oligosaccharide, named **OS**. The ^1H NMR spectrum of **OS** (Figure 6.2) showed eight proton anomeric signals, assigned to residues **A-H**, at 5.55-4.36 ppm (Table 6.1).

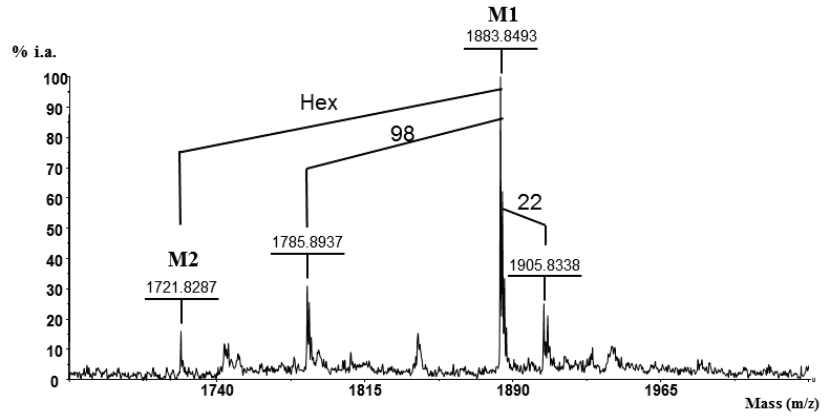

Figure 6.1 - Reflectron MALDI-TOF mass spectrum of fraction **B**. The spectrum was acquired in negative ions mode.
M1: $GlcA(Glc)_3(Hep)_2Kdo(GlcN)_2P_3K$;
M2: $GlcA(Glc)_2(Hep)_2Kdo(GlcN)_2P_3K$; i.a.: ionic abundance)

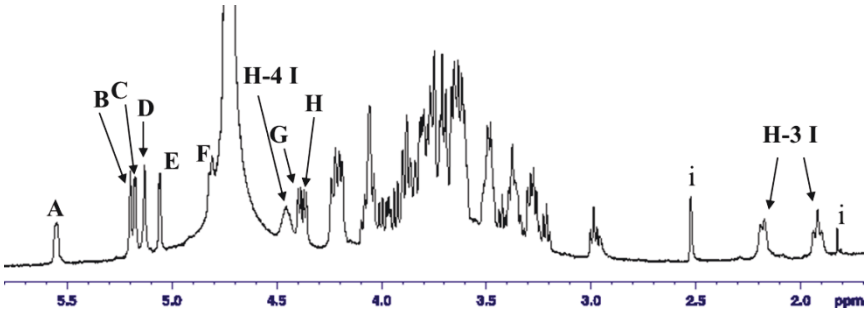

Figure 6.2 - ^{1}H-NMR of **OS** performed at 298K. The spectrum was recorded in D_2O at 600 MHz. The letters refer to the residues as described in Table 6.1. Impurities are indicated by letter i.

The assignment of ^{1}H resonances was achieved by tracing the spin-connectivities, delineated in the DQF-COSY and TOCSY contour maps, from the anomeric and some other diagnostic ring protons, such as axial and equatorial protons (H-3) of Kdo residue at 1.92 and 2.18 ppm. In addition, the spatial proximity of some protons was recognized by NOE contacts measured in a ROESY

spectrum. Carbon chemical shifts were assigned utilizing $^{1}H,^{13}C$-DEPT-HSQC (Figure 6.3) and $^{1}H,^{13}C$-HMBC.

Table 6.1 - ^{1}H-^{13}C NMR assignments of fraction **OS**. All the chemical shifts values are referred to acetone as internal standard (δ_H 2.225; δ_C 31.45). $^{3}J_{H\text{-}1,H\text{-}2}$ - $^{1}J_{C\text{-}1,H\text{-}1}$ are reported in parentheses and given in Hertz. Spectra were recorded in D_2O at 298K.

Residue	H1 ($^{3}J_{H\text{-}1,H\text{-}2}$) C1 ($^{1}J_{C\text{-}1,H\text{-}1}$)	H2 (H3ax) C2	H3 (H3eq) C3	H4 C4	H5 C5	H6a C6	H7a/H 6b C7	H8/H7 b C8
A	5.55 (3.2)	3.29	3.80	3.37	4.07	4.23	3.80	
→6)-α-GlcN*p1P*(1→	92.1 (177)	55.9	71.6	70.9	73.6	70.8		
B	5.19 (<2)	4.19	3.87	3.80	3.71	3.97	3.89	
→2)-α-Hep*p*(1→	102.8 (178)	80.1	72.3	68.8	74.5	69.9	64.7	
C	5.17 (3.0)	3.60	3.81	3.39	3.92	-		
→2)-α-GlcA*p*(1→	99.7 (173)	78.5	72.5	73.9	75.1	177.7		
D	5.13 (<2)	4.06	4.24	3.99	4.05	3.75	3.83	3.65
→2,3,4)-α-Hep*p*(1→	99.6 (173)	80.0	75.6	75.0	69.6	70.8	64.9	
E	5.05 (3.5)	3.48	3.71	3.38	3.85	3.71	3.75	
***t*-α-Glc*p*(1→**	98.3 (173)	72.9	74.5	70.9	73.1	61.9		
F	4.81 (8.1)	2.99	3.77	3.71	3.62	3.49	3.62	
→6)-β-GlcN*p4P*(1→	100.9 (171)	56.9	74.1	73.2	75.5	63.9		
G	4.39 (8.0)	3.28	3.46	3.48	3.61	3.62		
***t*-β-Glc*p*(1→**	103.4(165)	74.1	76.3	72.9	78.7	63.8		
H	4.36 (7.6)	3.26	3.31	3.22	3.35	3.89	3.66	
***t*-β-Glc*p*(1→**	104.3 (166)	74.1	77.1	71.8	77.9	63.2		
I	-	1.92	2.18	4.45	4.20	3.77	4.05	n.d.
→5)-α-Kdo*p4P*(2→	n.d.	n.d.	35.6	70.8	74.5	73.4	73.1	n.d.

Monosaccharide residues were recognised based on their ^{1}H and ^{13}C chemical shifts, which were in agreement with published data of their respective pyranosides (Bock and Pedersen, 1983; Brisson *et al.*, 2002), and on the basis of coupling constant values and *inter*-residue NOE contacts. Anomeric configurations of the *gluco* configured residues, Glc, GlcA and GlcN were suggested from their $^{3}J_{H\text{-}1,H\text{-}2}$ coupling constant values in the ^{1}H NMR spectrum experiment and confirmed by measuring the $^{1}J_{C\text{-}1,H\text{-}1}$ coupling constants in a 2D *F2*-coupled HSQC experiment (Table 6.1).The α–anomeric configuration for heptose residues were deduced from the value of the $^{1}J_{C\text{-}1,H\text{-}1}$ coupling constants of 178 Hz and 173 Hz for **B** and **D**, respectively. The difference (Δ= 0.26) between the proton chemical shifts of H-3_{ax} and H-3_{eq} (Table 6.1) of the Kdo residue indicated the α-configuration for this

monosaccharide (Agrawal *et al.*, 1994). Glucosamine residues **A** and **F** were identified by the correlation of their H-2 protons, at 3.29 and 2.99 ppm, with the nitrogen-bearing carbons at 55.9 and 56.9 ppm, respectively.

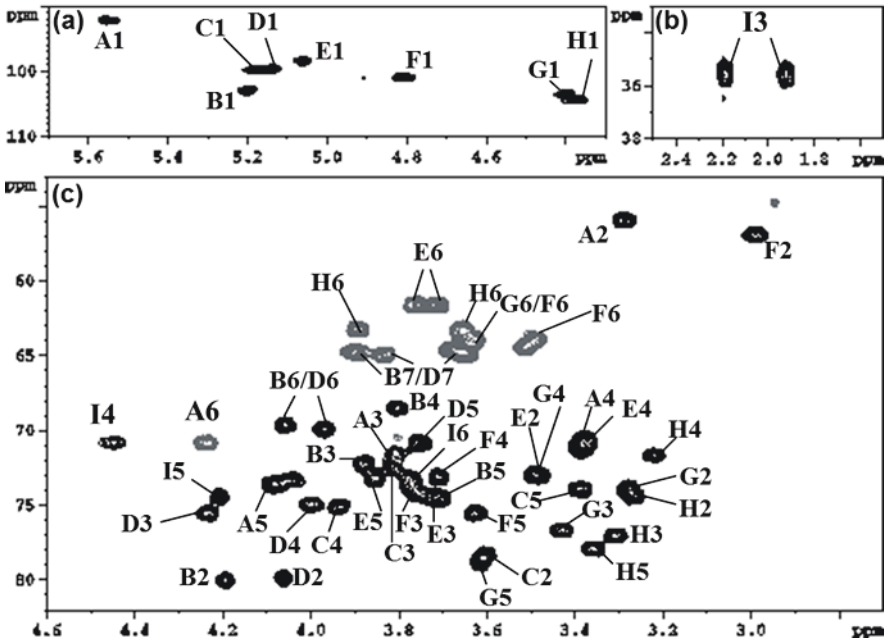

Figure 6.3 –Anomeric region (a), deoxy-group of Kdo (b) and primary and secondary alcohol groups region (c) of $^{1}H,^{13}C$ DEPT-HSQC spectrum of **OS**. Spectrum was performed at 600 MHz in D_2O at 298K. The letters refer to the residues as described in Table 6.1.

All the ^{1}H and ^{13}C chemical shifts of both residues **A** and **F** were in agreement with the presence of the lipid A skeleton disaccharide structure β-GlcN-(1→6)-α-GlcN. The $^{3}J_{H\text{-}1,H\text{-}2}$ of both residues as well as the NOE contact between the anomeric proton of **F** and both H-6 protons of A confirmed this structure. The phosphorylation at position *O*-1 of **A** and at position *O*-4 of **F** were inferred from the multiplicity of the anomeric proton signal ($^{3}J_{H,P}$ =

6.6 Hz) of **A** and from both the C-4 and H-4 downfield shift of **F**, respectively (Holst *et al.*, 1993).

Heptose **B** with C-1/H-1 signals at 102.8/5.19 ppm showed a C-2 downfield glycosylation shift of about 8 ppm, thus indicating that this position was substituted. The assignment of 2,3,4-trisubstituted heptose to residue **D** was deduced by the downfield shift of its C-2, C-3 and C-4, respectively. Residue **C** with C-1/H-1 signals at 99.7/5.17 ppm was attributed to 2-substituted glucuronic acid as its C-2 resonance was shifted downfield. The residues **E**, **G** and **H** were assigned to terminal non-reducing glucose units as none of their carbon atoms were shifted downfield. Phosphorylation at position *O*-4 of Kdo was suggested by its H-4 chemical shift (4.45 ppm) and by the downfield shifted C-4 at 70.8 ppm. Finally, its glycosylation at *O*-5 position was indicated by the shift of its C-5 carbon signal at 74.5 ppm respect to the value of 67.4 ppm for an unsubstituted Kdo residue (Holst *et al.*, 1990).

The ^{31}P NMR spectrum of **OS** confirmed the presence of three phosphates as it displayed (Figure 6.4) three resonances at 2.67, 3.87 and 4.02 ppm, in agreement with the results obtained by MALDI-TOF mass spectrum of the oligosaccharide mixture. The positions of phosphate groups were confirmed by ^{1}H–^{31}P HMQC experiment. More in detail, a ^{31}P signal at 2.67 ppm showed a correlation with H-1 of **A** while the ^{31}P signal at 3.87 ppm was correlated with H-4 of **F**, thus confirming that both glucosamine residues of lipid A were phosphorylated.

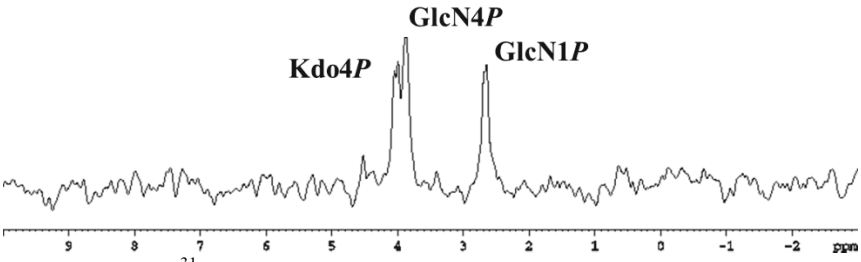

Figure 6.4– ^{31}P NMR spectrum of **OS**. Spectrum was recorded at 400 MHz (298K) in D_2O at pD ~12. H_3PO_4 was used as external standard.

Finally the phosphorylation at position *O*-4 of the Kdo residue was confirmed by the correlations between its H-4 and the ^{31}P signal at 4.02 ppm.

The sequence of the monosaccharides and the linkage positions were deduced from the HMBC and the ROESY experiments. The HMBC revealed the following *inter*-residue correlations: H-1 of **D** with C-5 of Kdo, H-1 of **B** with C-3 of **D**, H-1 of **C** with C-2 of **B**, H-1 of **E** with C-2 of **C**, H-1 of **G** with C-2 of **D,** and H-1 of **H** with C-4 of **D**. In agreement with these results were the *inter*-residue NOE contacts obtained from the ROESY spectrum (Figure 6.5, Table 6.2). In particular dipolar couplings were observed between H-1 of **E** and H-2 of **C**, H-1 of **C** and H-2 of **B**, H-1 of **B** and H-3 of **D**, H-1 of **G** and H-2 of **D**, H-1 of **H** and H-4 of **D**, H-1 of **D** and H-5 of Kdo. The Kdo residue did not show any diagnostic NOE contact or heteronuclear multiple-bond correlation, which may result from the conformation of the Kdo-(2→6)-GlcN (**F**) glycosidic linkage (Olsthoorn*et al.*, 1999). Because the C-6 chemical shift of **F** was in agreement with reported data (Müller-Loennies *et al.*, 2003), the Kdo moiety was placed at C-6 of **F**. Finally the NOE dipolar coupling between H-5 of **D** and H-3_{ax} of Kdo suggested a D configuration for Kdo (Bock *et al.*, 1994).

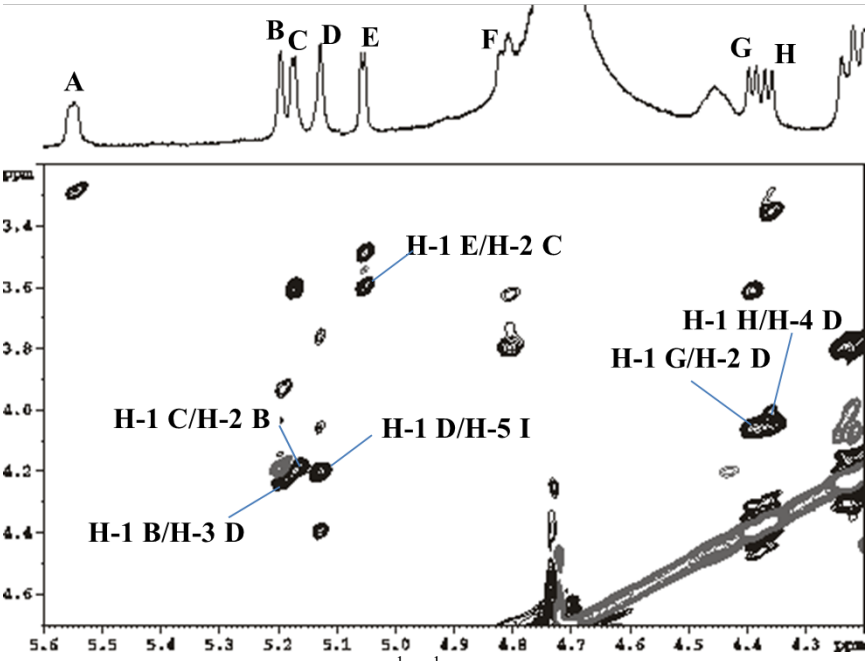

Figure 6.5–Anomeric region of ^{1}H-^{1}H ROESY spectrum of **OS**. Spectrum was recorded at 600 MHz in D_2O (298K). The letters refer to the residues as described in Table 6.2.

Table 6.2 - Nuclear Overhauser Enhancement *intra*- and *inter*-residual connectivities (ROESY) for the anomeric protons of fraction **OS**.

H-1 of sugar residue		*Intra*-residue NOE	*Inter*-residue NOE
→6)-α-GlcN*p1P*(1→	**A**	H-2	
→2)-α-Hep*p*(1→	**B**		**D** H-3, H-4
→2)-α-GlcA*p*(1→	**C**	H-2	**E** H-1 **B** H-2
→2,3,4)-α-Hep*p*(1→	**D**	H-2	**I** H-5, H-6 **G** H-1
t-α-Glc*p*(1→	**E**	H-2	**C** H-1,H-2
→6)-β-GlcN*p4P*(1→	**F**	H-3, H-5	**A** H-6a,b
t-β-Glc*p*(1→	**G**	H-3, H-5	**D** H-1, H-2
t-β-Glc*p*(1→	**H**	H-2, H-3,H-5	**D** H-4

From all these data it was possible to depict the structure of the main core oligosaccharide for the LPS of *H. alkaliantarctica*, which corresponds to the **M1** species (Scheme 6.2).

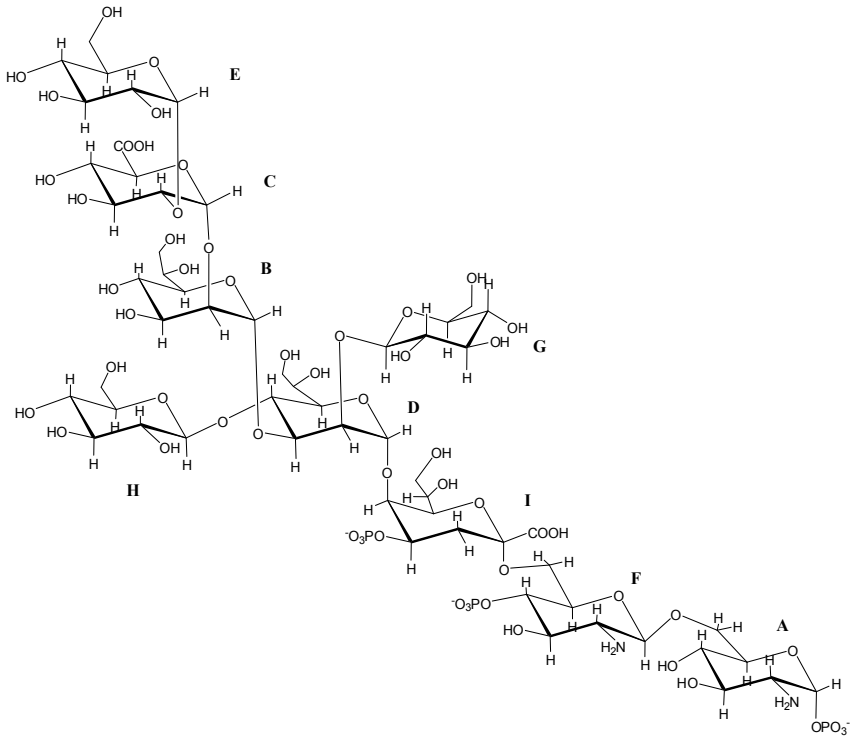

Scheme 6.2 – The core oligosaccharide from *H. alkaliantarctica* strain CRSS. Letters refer to residues as reported in Table 6.1

Nevertheless the MALDI-TOF spectra of the products obtained after mild acid hydrolysis and alkaline hydrolysis showed the presence of two glycoforms, the second of which lacking one glucose unit. This glycoform was recovered in very small amount after HPAEC, precluding its NMR characterization.

In order to identify the non stoichiometric glucose, MALDI-PSD experiments were performed. The best results were obtained on the oligosaccharides released after mild acid hydrolysis. Both the adduct ions **P1** and **P2** were selected for PSD analysis,

obtaining fragment ions for which the Domon and Costello nomenclature was used (Domon and Costello, 1988).

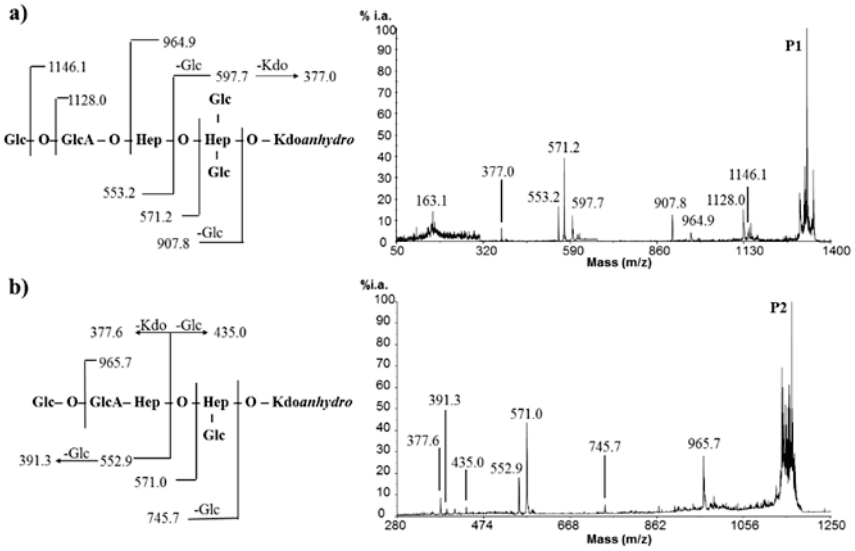

Figure 6.6 –Positive ions MALDI-PSD spectra of **P1** (a) and **P2** (b). i.a. stands for ionic abundance.

In both the spectra (Figure 6.6a,b) the same signals corresponding to the fragment Glc-GlcA-Hep were displayed at *m/z* 553.2 and 552.9 (B ions) and at *m/z* 571.2 and 571.0 (C ions) for **P1** and **P2** respectively, indicating that the glycosylation at GlcA was stoichiometric.

Moreover the ions at *m/z* 907.8 in Figure 6.6a and at *m/z* 745.7 in Figure 6.6b indicated that species corresponding to adduct ion **P2** contained one Glc less in the inner core. This was also confirmed by the presence of the fragment ions at *m/z* 597.7 in Figure 6.6b and at *m/z* 435.0 in Figure 6.6a.

From these data we suggest that the branched heptose is not stoichiometrically substituted.

6.3 Conclusion

Halomonas alkaliantarctica revealed a S-LPS constituted by a rather hydrophobic O-chain, as its repeating unit is formed by three rhamnose residues (Pieretti *et al.*, 2009a). On the contrary, core region is characterized by a negative charge density due to the three phosphate groups (on the two glucosamine and on position *O*-4 of Kdo residue) and to the glucuronic residue.

Paper related to this chapter:

Pieretti G, Carillo S, Nicolaus B, Poli A, Lanzetta R, Parrilli M, Corsaro MM.
"Structural characterization of the core region from the lipopolysaccharide of the haloalkaliphilic bacterium *Halomonas alkaliantarctica* strain CRSS."
Org Biomol Chem. **2010**; 8(23):5404-10.

Chapter 7

Halomonas stevensii S18214

Very recently, 14 bacterial strains (Figure 7.1) have been isolated from the blood of two patients and from the dialysis machines in a Renal Care Center in Santa Clara Valley (California) and classified as three novel *Halomonas* species (Stevens *et al.*, 2009; Kim *et al.*, 2010). The strains were aerobic, moderately halophilic, Gram-negative, motile, non-sporulating rods. Among these, two patient isolates, strains S18214 and T49407, belonged to *H. stevensii* (Kim *et al.*, 2010).

Figure 7.1 – *Halomonas sp.nov.* colonies on blood agar.

The patients developed a bacteraemia, which, in addition to those developed in patients infected by *H. venusta* and *H. phocaeensis* (Von Graevenitz *et al.*, 2000; Berger *et al.*, 2007), highlighted the pathogenic potential of the genus *Halomonas*. The structural motifs at the basis of this pathogenicity are completely unknown and for this reason the complete chemical structure of the LPS from the clinically isolated *H. stevensii* S18214 has been object of my thesis work.

7.1. LPS extraction and purification

H. stevensii cells were grown and extracted first by PCP (Galanos *et al.*, 1969) and then by phenol/water method. (Westphal *et al.*, 1965) The crude extracts were analyzed by SDS-PAGE (Figure 7.2) and showed the presence of LPS both in the PCP extract (LPS_{PCP}, lane B) and in the aqueous layer of the phenol/water extraction (LPS_W, lane A).

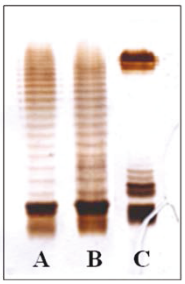

Figure 7.2- 16% SDS-PAGE analysis of the LPS from *H. stevensii* strain S18214. Lanes **A** and **B** represent the water layer of the phenol/water extraction and the PCP extract, respectively. The LPS from *E. coli* O55:B5 serotype (lane **C**) was used as standard.

On the basis of the electrophoretic migration the latter seemed to contain an higher number of O-chain repeating units. UV spectroscopy and sugar analysis showed that LPS_{PCP} was free from nucleic acids, while for LPS_W the contamination was significant. For this reason we used LPS_{PCP} for all the analyses described. The sugar composition was obtained by GC-MS of the acetylated methyl glycosides and revealed the occurrence of Gal, Glc, GlcN, L,D-Hep and Kdo. The presence of the latter residue was revealed only after HF treatment of the LPS, suggesting its phosphorylation (Pieretti *et al.*, 2008). Absolute configurations of the sugar residues were determined by the GC-MS analysis of the corresponding acetylated octyl-glycosides (Leontein *et al.*, 1978).

7.2. O-chain polysaccharide structural determination

In order to obtain the O-chain polysaccharide a mild acid hydrolysis was performed and, after removing the lipid A by centrifugation, the supernatant liquor was purified by a Biogel P-10 column (Biorad) eluting with pyridine/acetate buffer. Three fractions were obtained, the first of which (**PS**) contained high molecular mass O-chain, while the second and the third contained core with several repeating units of the O-chain. The sugar analysis performed on **PS** sample revealed the presence of mainly D-glucose and D-galactose. The methylation analysis indicated the presence of an unsubstituted glucopyranose together with a 4-substituted glucopyranose, and a 3,4-disubstituted galactopyranose.

PS polysaccharide was then analyzed by mono- and two-dimensional NMR (DQF-COSY, TOCSY, ROESY, ^{1}H-^{13}C DEPT-HSQC, ^{1}H-^{13}C HMBC).

The ^{1}H NMR spectrum (Figure 7.3a) displayed three anomeric signals at 4.84 (**A**), 4.59 (**B**) and 4.45 ppm (**C**). For these last two signals a $^{3}J_{H1,H2}$ of 7.5 Hz was observed, which suggested a β configuration for residues **B** and **C**; instead the signal at 4.84 ppm displayed a $^{3}J_{H1,H2}$ of 2.3 Hz, which suggested an α configuration for this residue.

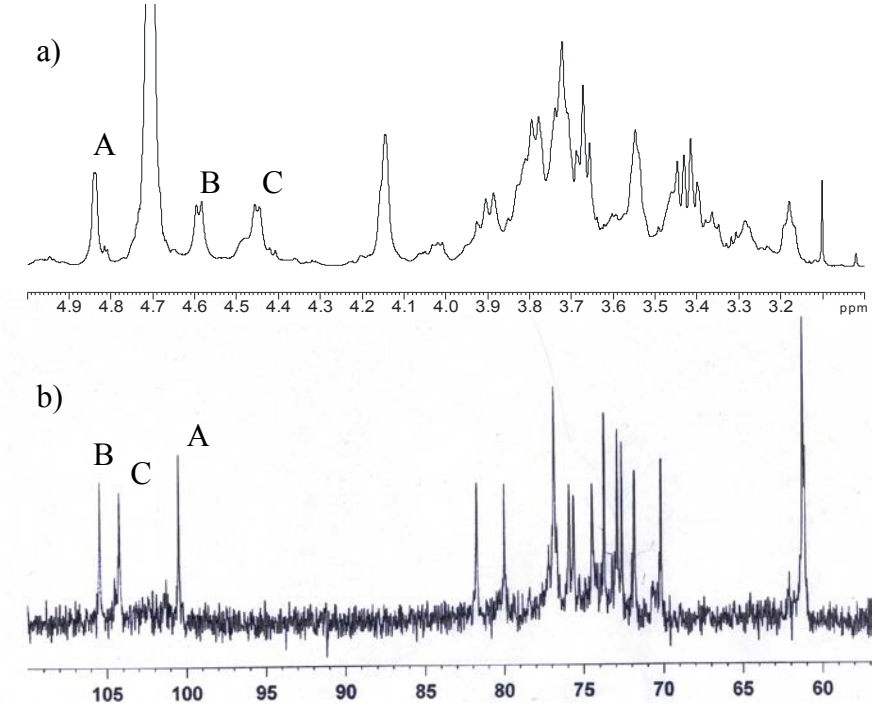

Figure 7.3 - (a) ^{1}H and (b) ^{13}C NMR spectra of the O-chain polysaccharide from *H. stevensii* performed at 298 K. The spectra were recorded in D_2O at 600 and 100 MHz, respectively. The letters refer to the residues as described in Table 7.1.

The ^{13}C NMR spectrum (Figure 7.3b) was in agreement with the presence of a trisaccharidic repeating unit, as it displayed three anomeric carbon signals at 100.5, 104.2 and 105.5 ppm. Residues **A** and **B** were assigned to *gluco*-configured residues because both showed four correlations in the TOCSY spectrum. In particular, for residue **A** it was possible to measure the vicinal coupling constants values $^{3}J_{H2,H3}$, $^{3}J_{H3,H4}$ and $^{3}J_{H4,H5}$ (8–10 Hz) in the DQF-COSY spectrum, which confirmed the configuration. Residue **C** was identified as a galactose unit since the anomeric proton showed only three correlations in the TOCSY experiment. Residue **A** with H-1/C-1 at 4.84/100.5 ppm was assigned to the unsubstituted glucopyranose as none of its carbon chemical shifts was shifted by

glycosylation (Bock and Pedersen, 1983). The C-4 chemical shift of residue **B** was found at 80.0 ppm, thus indicating its *O*-4 substitution. Finally downfield-shifted carbon signals indicated substitutions at *O*-3 and *O*-4 of residue **C** (C-3 at 81.8 ppm and C-4 at 76.9 ppm).

Table 7.1 - ^{1}H and ^{13}C NMR assignments of the O-chain polysaccharide from *H. stevensii*. All the chemical shifts values are referred to acetone as internal standard (^{1}H, 2.225 ppm; ^{13}C, 31.45 ppm). Spectra were recorded at 298 K.

	Residue	H-1 C-1	H-2 C-2	H-3 C-3	H-4 C-4	H-5 C-5	H-6a,b C-6
A	**α-Glc*p***	4.84	3.41	3.67	3.43	4.15	3.78,3.71
		100.5	73.0	73.8	70.2	72.7	61.2
B	**4-β-Glc*p***	4.59	3.18	3.54	3.55	3.46	3.89,3.74
		105.5	74.5	75. 7	80.0	76.0	61.2
C	**3,4-β-Gal*p***	4.45	3.66	3.78	4.14	3.71	3.80,3.73
		104.2	71.9	81.8	76.9	77.0	61.2

The sequence of the three residues was inferred from the HMBC experiment which showed the following correlations: H-1 of **A** with C-4 of **C**; H-1 of **C** with C-4 of **B**; H-1 of **B** with C-3 of **C**. *Inter*-residue NOE contacts (Figure 7.4) confirmed the sequence. The *intra*-residue NOEs of H-1 with H-3 and H-5 supported the β configuration for residues **B** and **C** whereas that between H-1 and H-2 substantiated the α configuration of **A**.

All the above data indicated for the repeating unit of the O-chain from the LPS of *H. stevensii* the structure showed in Scheme 7.1.

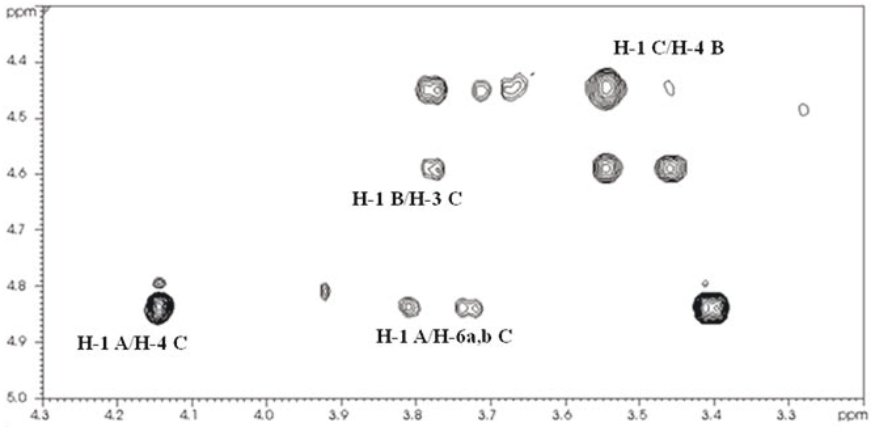

Figure 7.4 - Anomeric region of ^{1}H, ^{1}H ROESY spectrum of the O-chain polysaccharide from *H. stevensii* performed at 298 K. The spectrum was recorded in D_2O at 600 MHz. The letters refer to the residues as described in Table 7.1. Only *inter*-residue correlations are marked.

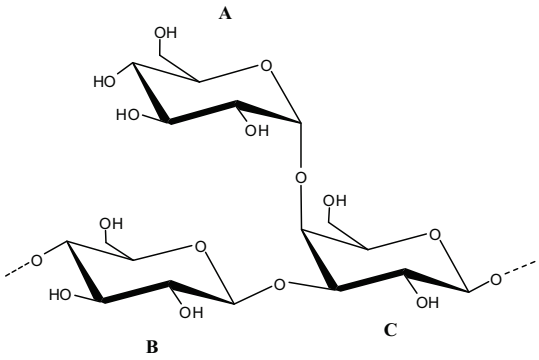

Scheme 7.1 – The structure of the O-chain repeating unit of the LPS from *H. stevensii* strain S18214.

7.3. Mass spectrometric analysis of de-O-acylated LPS

In order to investigate the primary structure of core region, the LPS_{PCP} was first de-*O*-acylated with anhydrous hydrazine. The product was analyzed by ESI FT-ICR mass spectrometry. The

spectrum (Figure 7.5) revealed the presence of three main signal clusters **M1**-**M3** differing for 486 u, corresponding to the mass of the O-chain repeating unit (R.U.).

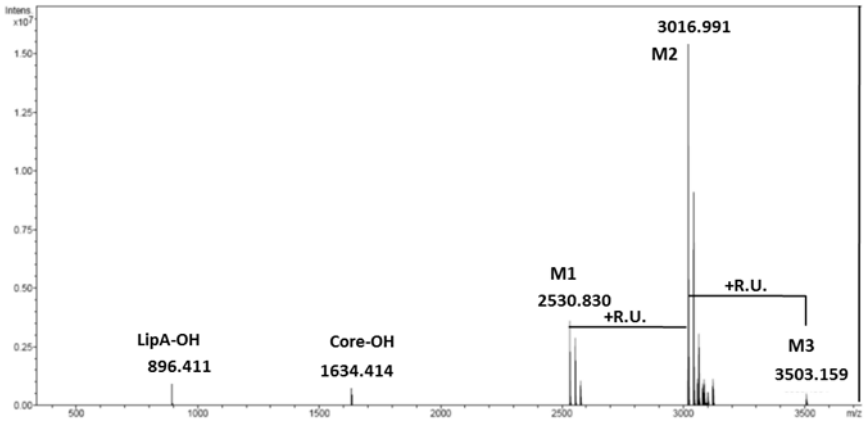

Figure 7.5 –Charge deconvoluted ESI FT-ICR mass spectrum of the de-*O*-acylated LPS fraction isolated from *H. stevensii* bacterium. The spectrum was acquired in negative ion mode. Mass peaks not labelled are sodium and/or potassium adducts. Mass numbers given refer to monoisotopic peak of the neutral molecular species. R.U. stands for repeating unit.

The heterogeneity was then only attributable to the presence of one or two O-chain repeating units, while the core region seemed to be uncommonly constituted by only one oligosaccharide.

The spectrum comprise two further mass peaks at 896.41 *m/z* and 1634.41 *m/z* which are in agreement with lipA-OH consisting of 2 GlcN, 2P, 2 C12:0(3OH) and with the core consisting of $KdoP_2Hep_4Hex_3$-H_2O, respectively (Kondakov and Lindner, 2005). Species **M1** occurring at 2530.83 *m/z* (calculated molecular mass 2530.81 Da) represented the *O*-deacylated lipopolysaccharide (LPS-OH) containing only the lipid A and the core oligosaccharide, whereas **M2** (the most abundant species) and **M3** contained one and two O-chain repeating units, respectively. Further on, the LPS-OH was de-*N*-acylated by strong alkaline hydrolysis and the obtained oligosaccharides mixture was purified by HPAEC-PAD. Two main fractions have been isolated with a high purity, named

OS1 and **OS2**, which were analyzed by ESI FT-ICR MS (Figure 7.6). **OS1** mass spectrum showed the presence of one main species of molecular mass 2620.64 *m/z*, which corresponded to the composition $GlcN_2P_4KdoHep_4Hex_6$ (calculated molecular mass 2620.64 Da), thus containing the core oligosaccharide and one O-chain repeating unit.

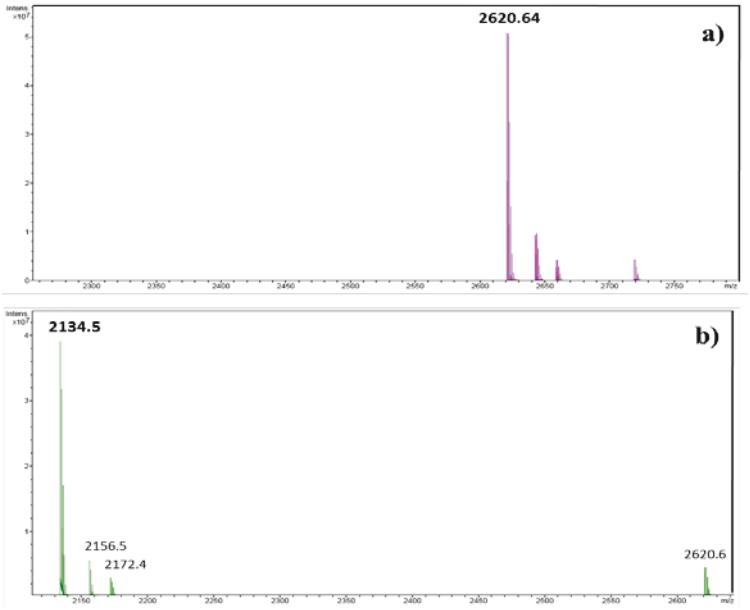

Figure 7.6 – Charge deconvoluted ESI FT-ICR mass spectra of the deacylated **OS1** (a) and **OS2** (b). The spectra were acquired in negative ion mode. Mass peaks not labelled are sodium and/or potassium adducts. Mass numbers given refer to monoisotopic peak of the neutral molecular species.

OS2 mass spectrum showed a peak at 2134.50 *m/z* as main species, which corresponded to a molecular species containing three hexoses (one O-chain repeating unit) less (Pieretti *et al.*, 2011).

7.4. NMR characterization of OS1

The anomeric region of the ^{1}H NMR spectra of **OS1** and **OS2** were compared as shown in Figure 7.7. **OS2** proton spectrum displayed the presence of nine anomeric signals, while **OS1** contained three additional anomeric signals attributable to the O-chain repeating unit, as expected.

Both fractions were analyzed by one- and two-dimensional NMR experiments. In particular ^{1}H-^{1}H DQF-COSY, ^{1}H-^{1}H TOCSY, ^{1}H-^{1}H ROESY, ^{1}H-^{13}C DEPT-HSQC, ^{1}H-^{13}C HSQC-TOCSY, ^{1}H-^{13}C HMBC, ^{1}H-^{31}P HSQC experiments have been performed. Since **OS1** contained the complete information about the core structure and its linkage to the O-antigen, only its structural determination is reported. In particular methylation analysis of **OS1** showed the presence of terminal Glc, 4-substituted Glc, 4-substituted Gal, 6-substituted GlcN, terminal Hep, 7-substituted Hep, 2,6-disubstituted Hep, and 3,4,6-trisubstituted Hep, according to Scheme 7.2.

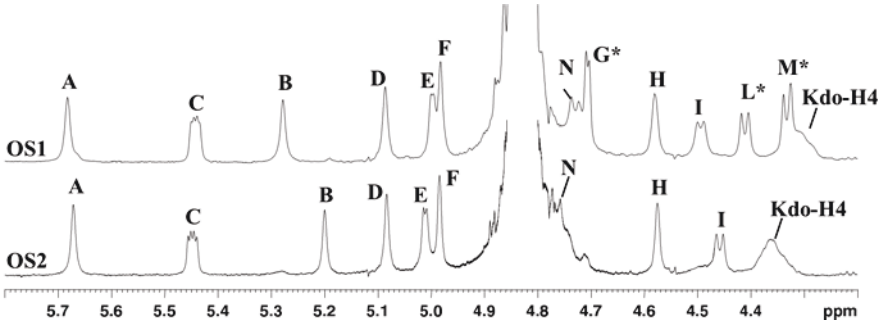

Figure 7.7 –^{1}H NMR anomeric region of **OS1** and **OS2**. The spectra were recorded in D_2O at 280 K at 600 MHz.

The NMR analysis on **OS1** was performed adjusting pD at 12, in order to be able to identify the phosphates positions. The ^{1}H NMR of **OS1**, together with the ^{1}H-^{13}C HSQC spectrum, showed the presence of twelve anomeric signals (**A**-**N**, Figure 7.7). The 2D

homo- and heteronuclear NMR experiments allowed the characterization of the complete structure (Table 7.2, Scheme 7.2). Residues **C** and **N** were attributed to the lipid A GlcN*1P* and GlcN*4P*, respectively, as their H-2 protons showed a correlation with two nitrogen bearing carbon atoms at 56.5 and 56.9 ppm. Moreover H-1 of residue **C** showed the typical multiplicity of a phosphorylated α-anomeric proton signal ($^{3}J_{\text{H-1,H-2}}$ = 3.2 Hz, $^{3}J_{\text{H-1,P}}$ = 8.2 Hz), while glycosylation at position *O*-6 was inferred by the downfield shifted C-6 at 70.4 ppm. As for residue **N** the H-1 proton with a $^{3}J_{\text{H-1,H-2}}$ = 8.1 Hz suggested a β configuration, while its H-4 and C-4 downfield shifts were diagnostic for the presence of a phosphate group linked at position *O*-4.

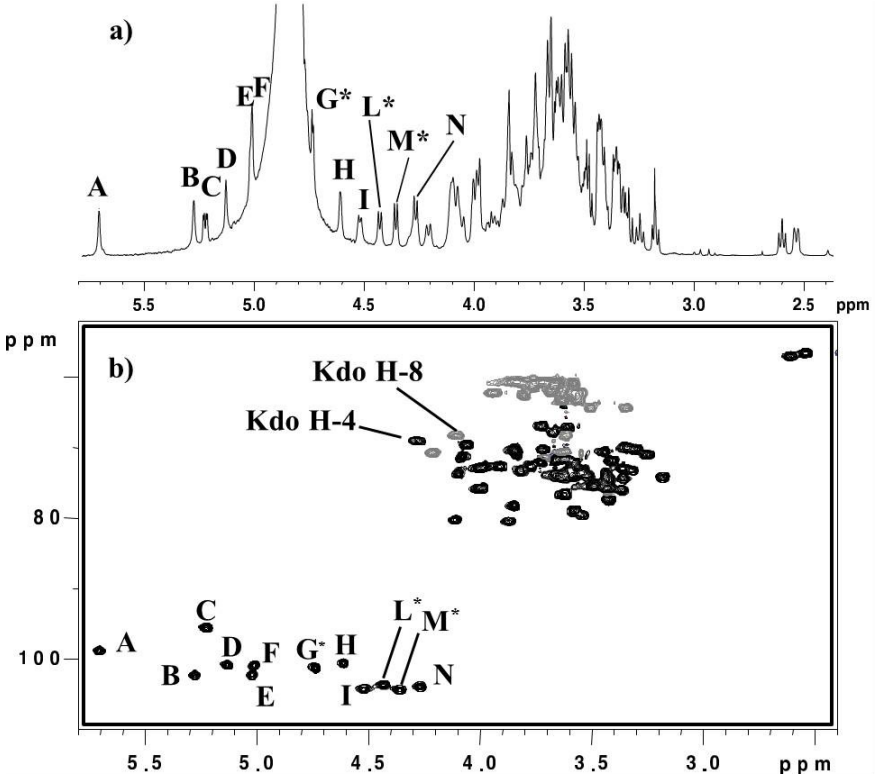

Figure 7.8 - ^{1}H NMR (a) and ^{1}H-^{13}C HSQC (b) spectra of **OS1**. The spectra were recorded in D_2O (pD 12) at 283 K at 600 MHz. The letters refer to the residues as described in Table 7.2 and 7.3 and in Scheme 7.2.

Moreover H-1 of **N** showed correlations with both C-6 and H-6a,b of residue **C** in the HMBC and ROESY experiments, respectively. Starting from the diasterotopic protons H-3_{ax} and H-3_{eq}, the Kdo (residue **O**) was identified. The chemical shift difference between these protons depends upon the orientation of C-1 carbon and then the Δ(H-3_{ax}-H-3_{eq}) = 0.35 value allowed to assign an α configuration to this residue (Agrawal *et al.*, 1994).

Table 7.2 - . ^{1}H and ^{13}C NMR assignments of **OS1**. The chemical shifts were measured in D_2O (pD 12) at 283 K, using acetone as internal standard (δ_H 2.225 ppm δ_C31.45 ppm). Sugars marked with asterisk belong to the O-antigen.

Residue	H1 C1	H2 C2	H3 C3	H4 C4	H5 C5	H6 C6	H7 C7	H8 C8
A 2,6-α-Hep*p*	5.70 98.7	4.10 80.1	3.58 72.1	3.68 67.8	3.83 70.6	4.00 75.7	3.55-3.80 62.5	
B 7-α-Hep*p*	5.27 102.2	3.72 72.0	3.65 71.6	3.72 66.8	3.97 72.5	4.06 69.5	3.70-3.70 71.6	
C 6-α-GlcN*p1P*	5.22 95.4	2.54 56.5	3.42 74.4	3.25 70.9	3.90 72.5	3.62-4.21 70.4		
D 3,4,6-α-Hep*p*	5.13 100.7	4.07 71.1	3.81 73.5	3.99 75.8	3.97 72.4	3.86 80.4	3.93-3.54 62.2	
E *t*-α-Glc*p*	5.02 102.1	3.31 73.1	3.66 73.8	3.34 69.9	3.77 72.5	3.66-3.77 61.1		
F *t*-α-Hep*p*	5.01 100.8	3.71 71.9	3.53 73.2	3.70 67.0	3.55 72.8	3.84 70.1	3.56-3.63 63.1	
G *t*-α-Glc*p**	4.73 101.2	3.35 72.8	3.57 73.6	3.29 70.1	3.99 72.7	nd		
H *t*-α-Glc*p*	4.61 100.5	3.61 71.4	3.43 73.7	3.43 70.5	3.51 73.7	nd		
I 4-β-Glc*p*	4.52 104.2	3.36 74.1	3.42 75.6	3.53 79.4	3.43 77.2	3.84 60.5		
L 4-β-Glc*p**	4.43 103.5	3.17 74.0	3.49 75.2	3.57 78.8	3.43 75.7	3.72-3.84 60.7		
M 4-β-Gal*p**	4.36 104.3	3.40 71.7	3.59 72.9	3.83 78.1	3.61 73.9	nd		
N 6-β-GlcN*p4P*	4.27 103.8	2.60 56.9	3.40 71.7	3.61 76.5	3.48 75.2	3.34-3.50 64.4		
O 5-α-Kdo*p4P8P*	-	-	1.75-2.10 35.6	4.27 68.9	4.09 73.6	3.99 72.8	3.70 70.2	4.10-3.62 68.1

Moreover both H-3 protons showed a correlation, in the DQF-COSY spectrum, with a signal at 4.27 ppm, attributed to H-4, in turn correlated to a proton at 4.09 ppm (H-5 of Kdo). The downfield shift and the broad shape of the H-4 signal revealed the presence of a phosphate group at this position. Besides other ring carbons, H-5 showed in the HSQC-TOCSY a correlation with a carbon atom at 68.1 ppm, attributed to Kdo C-8. The downfield shift of the latter signal revealed the presence of a second phosphate group on Kdo (Brabetz *et al.*, 1997). These data were in agreement with chemical analysis and confirmed by the ^{31}P and ^{1}H-^{31}P HSQC experiments. Actually, the ^{31}P NMR spectrum (Figure 7.9) showed the presence of four phosphate monoester signals attributed to the GlcN*1P* (2.48 ppm), GlcN*4P* (3.53 ppm), Kdo*8P* (4.24 ppm) and Kdo*4P* 4.77 ppm).

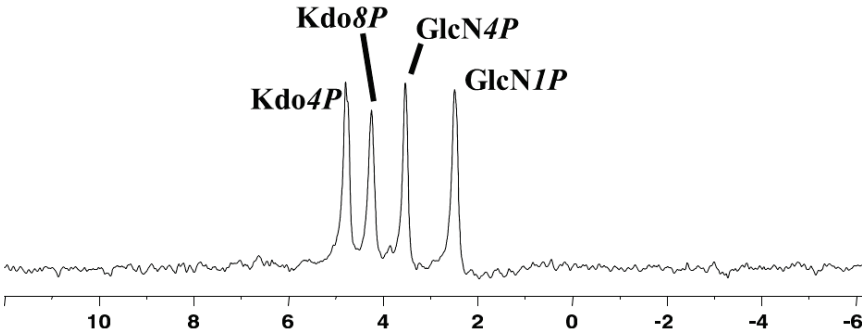

Figure 7.9 – ^{31}P spectrum of fraction **OS1**. Spectrum was recorded in D_2O (pD 12) at 298K. $H_3PO_4$was used as an external reference (δ 0.00 ppm).

Residues **A**, **B**, **D** and **F** were identified as four L-*glycero*-α-D-*manno*-heptopyranoses as their small vicinal coupling constants values of $^{3}J_{H\text{-}1,H\text{-}2}$ and $^{3}J_{H\text{-}2,H\text{-}3}$ indicated the equatorial orientation of H-2. The anomeric configuration for all these residues was inferred by the small $^{3}J_{H\text{-}1,H\text{-}2}$ value and by the *intra*-residue ROE contacts (only the ROE contact between H-1 and H-2 was observed, Table 7.3), while the linkage positions were deduced by

the glycosylation shifts. As for residue **A** the substitution at position *O*-2 was easily identified since, in the HSQC-TOCSY spectrum, beside the anomeric carbon, the H-1 proton showed a correlation with a signal at 80.1 ppm, attributed to C-2. Moreover, through the TOCSY experiment, it was possible to identify the proton H-6, which in turn was correlated to a carbon atom at 75.7 ppm in the ^{1}H-^{13}C HSQC spectrum, thus indicating the substitution at this position (Pieretti *et al.*, 2008). Residue **D** was attributed to a 3,4,6-trisubstituted heptose since its H-3 and H-4 protons, identified by the TOCSY experiment, showed correlations with carbon atoms at 73.5 and 75.8 ppm, respectively (Vinogradov *et al.*, 1995; Cox *et al.*, 1996). Substitution at position *O*-6 was inferred by the long range scalar coupling between H-5 proton and a downfield shifted carbon atom at 80.4 ppm, attributed to C-6 (Vinogradov *et al.*, 1995; Cox *et al.*, 1996). Residue **B** with H-1/C-1 at 5.27/102.2 ppm and residue **F** with H-1/C-1 at 5.01/100.8 ppm were identified as 7-substituted and terminal heptoses, respectively, on the basis of their carbon and proton chemical shifts (Pieretti *et al.*, 2008). In particular C-7 carbon atom of residue **B** was downfield shifted at 71.6 ppm, while none of the carbons belonging to residue **F** was shifted by glycosylation.

E, **H** and **I** were identified as *gluco*-configured hexose residues. In particular residues **E** and **H** were terminal glucopyranoses since none of their carbon was shifted by glycosylation, whereas the α configuration was inferred by the small $^{3}J_{\text{H-1,H-2}}$ values (< 2 Hz) and by the *intra*-residue ROE (Table 7.3).

Table 7.3 - Rotating-framenuclear Overhauser enhancement *intra*- and *inter*-residual connectivities (ROESY) for the anomeric protons of **OS1**. Sugars marked with asterisk belong to the O-antigen.

Residue	*Intra*-residue ROE	*Inter*-residue ROE
A 2,6-α-Hep*p*	H2	H3 **D,** H1 **B**
B 7-α-Hep*p*	H2	H1 and H2 **A**
C 6-α-GlcN*p1P*	H2	-
D 3,4,6-α-Hep*p*	H2	H5 **O**
E*t*-α-Glc*p*	H2	H6 **D**
F*t*-α-Hep*p*	H2	H6 **A**
G*t*-α-Glc*p**	H2	H4 **M**
H*t*-α-Glc*p*	H2	H7 **B**
I 4-β-Glc*p*	H2, H3, H5	H4 **D**
L 4-β-Glc*p**	H2, H3, H5	H4 **I**
M 4-β-Gal*p**	H2, H3, H5	H4 **L**
N 6-β-GlcN*p4P*	H2, H3, H5	H6a,b **C**

Residue **I** was attributed to a 4-substituted glucopyranose, since its C-4 was downfield shifted at 79.4 ppm (Bock and Pedersen, 1983). The β-configuration for this residue was assigned on the basis of $^{3}J_{\text{H-1,H-2}}$ = 7.6 Hz and confirmed by *intra*-residue ROE contacts (Table 7.3). Residues **G**, **L** and **M** were attributed to the unsubstituted α-glucopyranose, the 4-substituted β-glucopyranose and the4-substituted β-galactopyranose, respectively, all belonging to the O-chain repeating unit (Pieretti *et al.*, 2011).

The monosaccharide sequence was inferred by the heteronuclear multiple bond scalar correlations and confirmed by *inter*-residue ROE connectivities (Table 7.3). In particular, the ROE contact between H-5 of **D** and H-3_{ax} of **O** suggests a D configuration for Kdo (Bock *et al.*, 1994).

Moreover, residue **L** resulted to be the primer as its H-1 showed long range scalar correlation with C-4 of residue **I** as well as ROE contact with H-4 of this residue, thus allowing the determination of the linkage between the inner core and the O-chain regions, as well as the biological O-repeating unit. These results were corroborated

by the **OS2** structural characterization: residue **I** in **OS2** was identified as a terminal β-glucopyranose (data not shown).

All the mentioned data allowed to determine the complete structure of the saccharidic region of the LPS from *H. stevensii*, as well as the biological O-antigen repeating unit, as shown in Scheme 7.2.

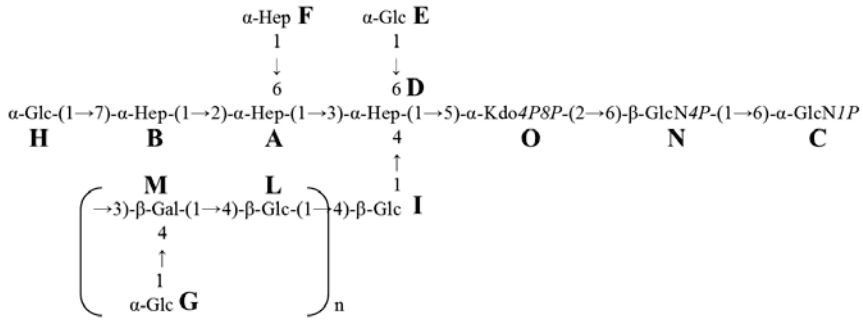

Scheme 7.2 – The complete structure of saccharidic regions from the LPS of *H. stevensii* strain S18214.

7.5. Lipid A structural characterization

Fatty acids of the LPS were analyzed as methyl esters derivatives by GC-MS analysis. The chromatogram showed the presence of 3-hydroxy-dodecanoic [C12:0(3-OH)], tetradecanoic (C14:0), decanoic acid (C10:0) and octadecenoic acid (C18:1). The lipid A from *H. stevensii* LPS was obtained as precipitate after mild acid hydrolysis and was analyzed by ESI FT-ICR mass spectrometry. The charge deconvoluted negative ions ESI FT-ICR mass spectrum showed the presence of six main signals (Figure 7.10, Table 7.4) corresponding to a number of glycoforms differing in their acylation as well as their phosphorylation degree.

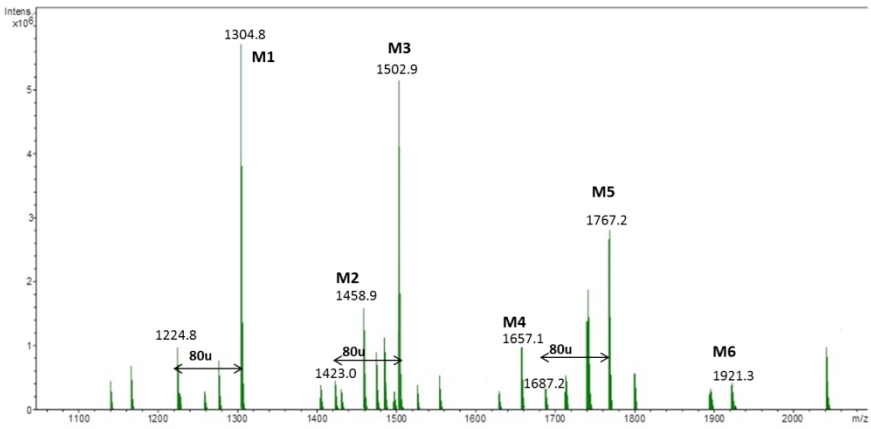

Figure 7.10 – The charge deconvoluted negative ESI FT-ICR mass spectrum of the lipid A from *H. stevensii* strain S18214.

In particular to the species at 1304.8 *m/z* (**M1**) was attributed the following composition: $GlcN_2P_2[C12:0(3OH)]_3C14:0$ (calculated molecular mass 1304.78 Da). Moreover, **M3** species contained an additional C12:0(3OH) while **M5** carries one extra C18:1. Beside these, monophosphorylated species, at 80 u lower were also present, as indicated in the spectrum. Species **M2**, **M4** and **M6** contained one C10:0 more respect to **M1**, **M3** and **M5**, respectively. The actual distribution of the fatty acids on the disaccharidic backbone was investigated by means of MS and MS/MS spectra in the positive ions mode.

The FT-ICR MS (positive ion mode) of lipid A showed the presence of the adduct ion $[M + Et_3N + H]^+$ at *m/z* 1869.28, which corresponded to the hexa-acylated, bis-phosphorylated glycoform **M5** (calculated molecular mass: *m/z* 1869.320). The MS/MS spectrum of this species, obtained by infrared multiphoton dissociation (IRMPD), displayed a B^+ fragment ion (Domon and Costello, 1988; Kondakov and Lindner, 2005) at *m/z* 1112.80, to which the following composition was attributed GlcNP[C12:0(3-OH)]$_2$(C18:1)(C14:0) (calculated mass *m/z* 1112.82). These results

proved that both C18:1 and C14:0 were linked to the distal glucosamine.

Table 7.4 - Composition of the main species present in the charge deconvoluted negative ions ESI FT-ICR mass spectrum of the lipid A from *H. stevensii* S18214.

Species	Observed mass (Da)	Calculated Mass (Da)	Composition
M1	1304,8	1304,78	$GlcN_2P_2[C12:0(3OH)]_3C14:0$
M2	1458,9	1458,92	$GlcN_2P_2[C12:0(3OH)]_3C14:0C10:0$
M3	1502,9	1502,94	$GlcN_2P_2[C12:0(3OH)]_4C14:0$
M4	1657,1	1657,08	$GlcN_2P_2[C12:0(3OH)]_4C14:0C10:0$
M5	1767,2	1767,19	$GlcN_2P_2[C12:0(3OH)]_4C14:0C18:1$
M6	1921,3	1921,33	$GlcN_2P_2[C12:0(3OH)]_4C14:0C18:1C10:0$

Then lipid A was treated with NH_4OH (Silipo *et al.*, 2002); the obtained product (lipA-OH) consists in the disaccharidic backbone devoid of the primary O-linked fatty acids. LipA-OH was analysed by FT-ICR MS and the negative ions mass spectrum showed the presence of three main signals corresponding to species **K1**, **K2** and **K3** (Table 7.5). **K3** signal at 1260.7 *m/z* corresponded to the species $GlcN_2P_2[C12:0(3OH)]_2C14:0C10:0$ (calculated molecular mass: 1260.75Da), while **K2** and **K1** lacked C14:0 or both secondary fatty acids, respectively.

Table 7.5 - Composition of the main species present in the charge deconvoluted negative ions ESI FT-ICR mass spectrum of the LipA-OH from *H. stevensii* S18214.

Species	Observed *m/z*	Calculated *m/z*	Composition
K1	896.4	896.41	$GlcN_2P_2[C12:0(3\text{-}OH)]_2$
K2	1050.5	1050.55	$GlcN_2P_2[C12:0(3\text{-}OH)]_2(C10:0)$
K3	1260.7	1260.75	$GlcN_2P_2[C12:0(3\text{-}OH)]_2(C14:0)(C10:0)$

The lack of C18:1 in these glycoforms demonstrated that C14:0 was linked as acyloxyamide to the distal glucosamine. Moreover, the above data demonstrated that C10:0 was linked as acyloxyamide to the proximal glucosamine.

The positive ions mass spectrum of lipA-OH displayed the presence of the following species: $GlcN_2P_2[C12:0(3OH)]_2C14:0$ as Et_3N adduct (M_{acc} 1208.7 *m/z*), which was selected for fragmentation. The corresponding MS/MS spectrum (Figure 7.11) showed a fragment oxonium ion at 650.4 *m/z* which was attributed to the following composition: GlcNP[C12:0(3OH)]C14:0. Thus, in agreement with previous data, the tetradecanoic acid was determined to be linked as acyloxyamide to the distal glucosamine.

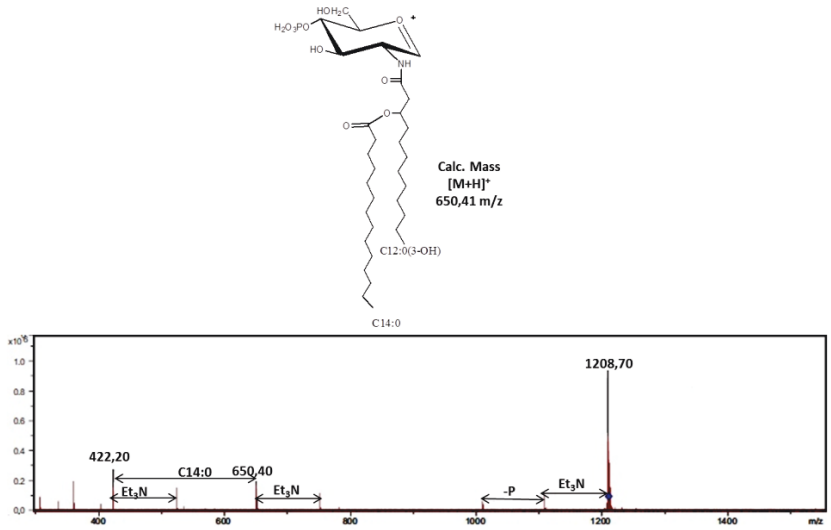

Figure 7.11 – ESI FT-ICR tandem mass spectrum infrared multiphoton dissociation (IRMPD). Product ion scan of the isolated precursor ion 1208.70 *m/z*.

On the basis of all the above data, the general structure for the lipid A of *H. stevensii* S18214 was depicted as shown in Scheme 7.3.

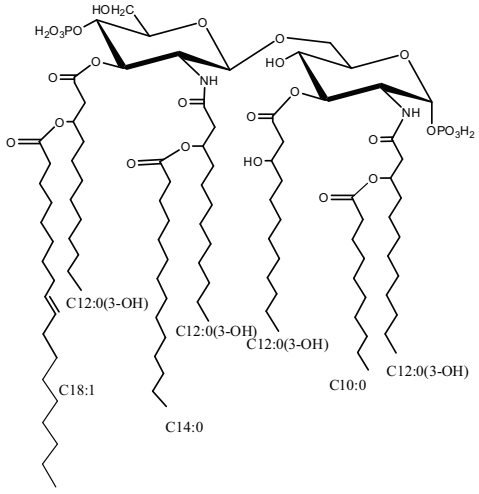

Scheme 7.3 – The structure of the lipid A from *H. stevensii* S18214.

7.6. Conclusion

Halomonas stevensii showed a smooth type LPS where O-chain moiety was characterized by a trisaccharidic branched repeating unit, constituted by neutral sugars. The polysaccharide has been already found in the LPS of *Halomonas magadiensis*, for which two different O-chain were identified (de Castro *et al.*, 2003). This finding is in agreement with the high similarity in the 16S rRNA gene phylogenetic tree between *H. magadiensis* and *H. stevensii* species (Kim *et al.*, 2010).

The core sugar backbone presented here is quite similar to that isolated from the LPS of *H. pantelleriensis* (Pieretti *et al.*, 2008), since both contain the tetrasaccharide α-Glc-(1→7)-Hep-(1→2)-[Hep-(1→6)-]-Hep-(1→ linked to the Hep I of the inner core, even if in *H. pantelleriensis* the 7-substituted Hep is D,D configured. Moreover, besides the phosphorylation at position *O*-4 typical of marine bacteria (Leone *et al.*, 2007), the Kdo residue in *H. stevensii* is phosphorylated also at position *O*-8. Nevertheless, among halophiles, *H. stevensii* is the only human pathogen and it is noteworthy that its core structure is actually closer to those isolated from *Vibrio cholerae* serotype O1 and O139 (Vinogradov *et al.*, 1995; Cox *et al.*, 1996), which are known pathogens. With the latter microorganisms, *H. stevensii* shares the following core portion which represents the almost complete structure:

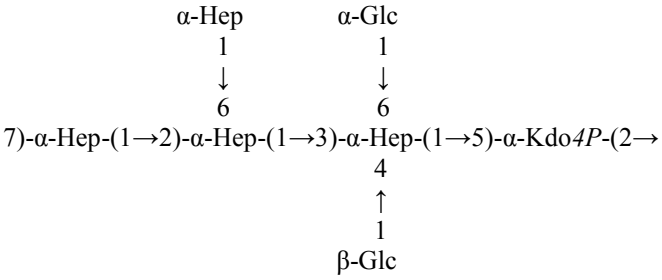

It is tempting to speculate that this similarity can be somehow related to the pathogenicity of *H. stevensii*.

On the basis of the ESI FT-ICR mass spectra it was also possible to assert the lack of heterogeneity in the sugar composition of the core region. This feature is also unusual, since, especially for pathogens, the outer core region shows more structural diversity due to the selective pressure of host responses, bacteriophages and environmental stresses (Raetz and Whitfield, 2002)

The linkage between the O-antigen and the core region has been characterized, which had so far been possible only in few cases. For the majority of bacterial LPS the primer sugar had always been linked to the outer core and it was identified as an amino sugar, with the exception of *Salmonella enteric* serovar Typhimurium (Olsthoorn *et al.*, 2000). In the last case, in fact, the linking sugar was identified as a β-Gal residue.

In this work we demonstrated that for *H. stevensii* the primer sugar is a β-Glc, which is linked to the inner core region at position *O*-4 of the inner core β-Glc.

Other evidences for this structural feature, obtained by genetically modified LPS, had been found for *Yersinia enterocolitica* O:3 and *Vibrio cholerae* O1 (Biedzka-Sarek *et al.*, 2005; Morona *et al.*, 1991), but up to now an oligosaccharide which comprises both the regions has never been isolated and punctually characterized.

Moreover, the lipid A region from *H. stevensii* has been elucidated too. Once again the results were in agreement with the phylogenetic proximity of *H. magadiensis* and *H. stevensii* since the fatty acids distribution on the two glucosamine was found to be the same (Silipo *et al.*, 2004b). Nevertheless, for *H. magadiensis* lipid A an antagonistic activity has been demonstrated (Ialenti *et al.*, 2006). The difference in the biological activity might be explained with a different acylation degree, which is lower in *H. magadiensis* lipid A. In fact, the most abundant species bears only three primary fatty acids and triacylated species are also present. In

H. stevensii the substitution pattern prefers a lipid A with all primary C12:0(3OH) fatty acids and in general with a higher acylation degree. Actually, further studies are needed in order to better understand the molecular reason of this results.

Papers related to this chapter:

Pieretti G, Carillo S, Kim KK, Lee KC, Lee JS, Lanzetta R, Parrilli M, Corsaro MM.
"O-chain structure from the lipopolysaccharide of the human pathogen *Halomonas stevensii* strain S18214.
Carbohydr Res. **2011**; 346(2):362-5.

Pieretti G, Carillo S, Lindner B, Kim KK, Lee KC, Lee JS, Lanzetta R, Parrilli M, Corsaro MM.
"Characterization of the core oligosaccharide and the O-antigen biological repeating unit from *Halomonas stevensii* lipopolysaccharide: the first case of O-antigen linked to the inner core."
Chemistry. **2012**; 18(12):3729-35.

Chapter 8

Salinivibrio sharmensis BAG^T

A novel haloalkaliphilic, facultative anaerobic and Gram-negative microorganism (designated strain BAG^T) was recovered from a saline lake in Ras Mohammed Park (Egypt). It was identified as a novel species of *Salinivibrio* genus, and named *Salinivibrio sharmensis* (Romano *et al.*, 2011).

During this thesis work, the complete structure of LPS from this bacterium has been characterized; core and lipid A regions were investigated by means of NMR spectroscopy and ESI FT-ICR mass spectrometry.

8.1. LPS extraction and purification

S. sharmensis strain BAG^T cells were grown and extracted by PCP to obtain crude LPS (Galanos *et al.*, 1969) The sugar composition was obtained by GC-MS analysis of the acetylated methyl glycosides and revealed the occurrence of GlcA, Glc, GlcN, GalN, L,D-Hep, D,D-Hep and Kdo. The presence of the latter residue was revealed only after HF treatment of the LPS, suggesting its phosphorylation (Pieretti *et al.*, 2008).

Methylation analysis indicated the presence of terminal-GlcA, terminal-Glc, 4-substituted Glc, 2-substituted Hep, 2,3,4-trisubstituted Hep, terminal GalN, 4-substituted GalN and 6-substituted GlcN. The methylation data also revealed a pyranose ring for all the residues.

Absolute configurations of the sugar residues were determined by the GC-MS analysis of the corresponding acetylated octyl-glycosides (Leontein *et al.*, 1978).

8.2. Mass spectrometric analysis of the deacylated LPS

The LPS was first de-*O*-acylated with anhydrous hydrazine. Further on, the LPS-OH was de-*N*-acylated by strong alkaline hydrolysis and the obtained oligosaccharides mixture was analyzed by ESI FT-ICR mass spectrometry.

The charge deconvoluted mass spectrum showed the presence of five main species **M1**-**M5** (Figure 8.1), the composition of which is reported in Table 8.1. The most abundant species occurred at 1859.42 *m/z* (**M3**) and was attributed to the following composition: $HexN_3P_3KdoHep_2HexA_2Hex$ (accurated mass: 1859.41 Da).

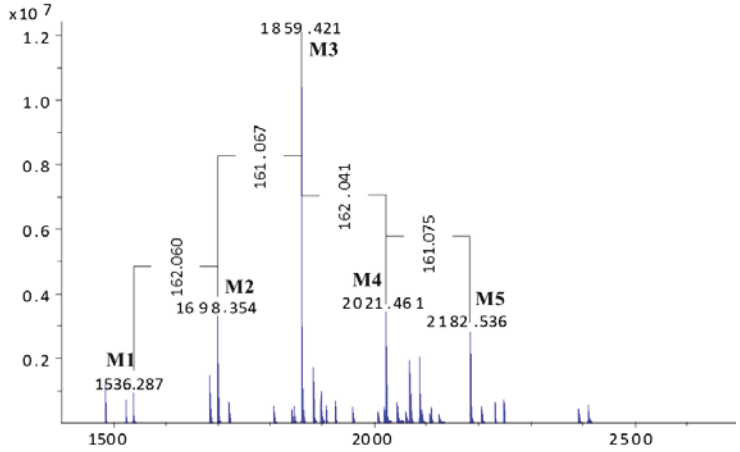

Figure 8.1 – The charge deconvoluted negative ion mode ESI FT-ICR mass spectrum of the deacylated LPS from *S. sharmensis* strain BAG^T.

Species **M2** and **M4** contained one hexosamine less and one hexose more, respectively. Species **M1** and **M5** contained one hexose and one hexosamine less and one hexose and one hexosamine more compared to **M3**, respectively.

Table 8.1 - Composition of the main species observed in the charge deconvoluted ESI FT-ICR mass spectrum of the deacylated LPS from *S. sharmensis* (see Fig. 8.1).

Species	*Observed mass (Da)*	*Calculated mass (Da)*	*Composition*
M1	1536.29	1536.28	$HexN_2P_3KdoHep_2HexA_2$
M2	1698.35	1698.35	$HexN_2P_3KdoHep_2HexA_2Hex$
M3	1859.42	1859.41	$HexN_3P_3KdoHep_2HexA_2Hex$
M4	2021.46	2021.47	$HexN_3P_3KdoHep_2HexA_2Hex_2$
M5	2182.54	2182.54	$HexN_4P_3KdoHep_2HexA_2Hex_2$

The ^{1}H-NMR spectrum of the deacylated product appeared quite complex, so it was purified by HPAEC-PAD (Figure 8.2). After recover and desalting of HPAEC-PAD fractions, only **E** and **C** provided satisfying yield and purity, as shown from ^{1}H-NMR and ESI FT-ICR mass spectra (Figure 8.3-4). Fractions **E** and **C** were named $\mathbf{OS_E}$ and $\mathbf{OS_C}$, and were analyzed by NMR spectroscopy (Figure 8.5).

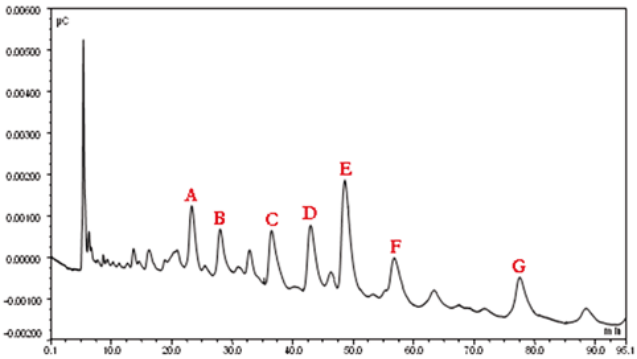

Figure 8.2 – HPAEC chromatogram on deacylated LPS. The gradient used was 43%→50% of B over 90 min (A: 0.1M NaOH, B: 1M NaOAc/0.1M NaOH) at 1 mL/min.

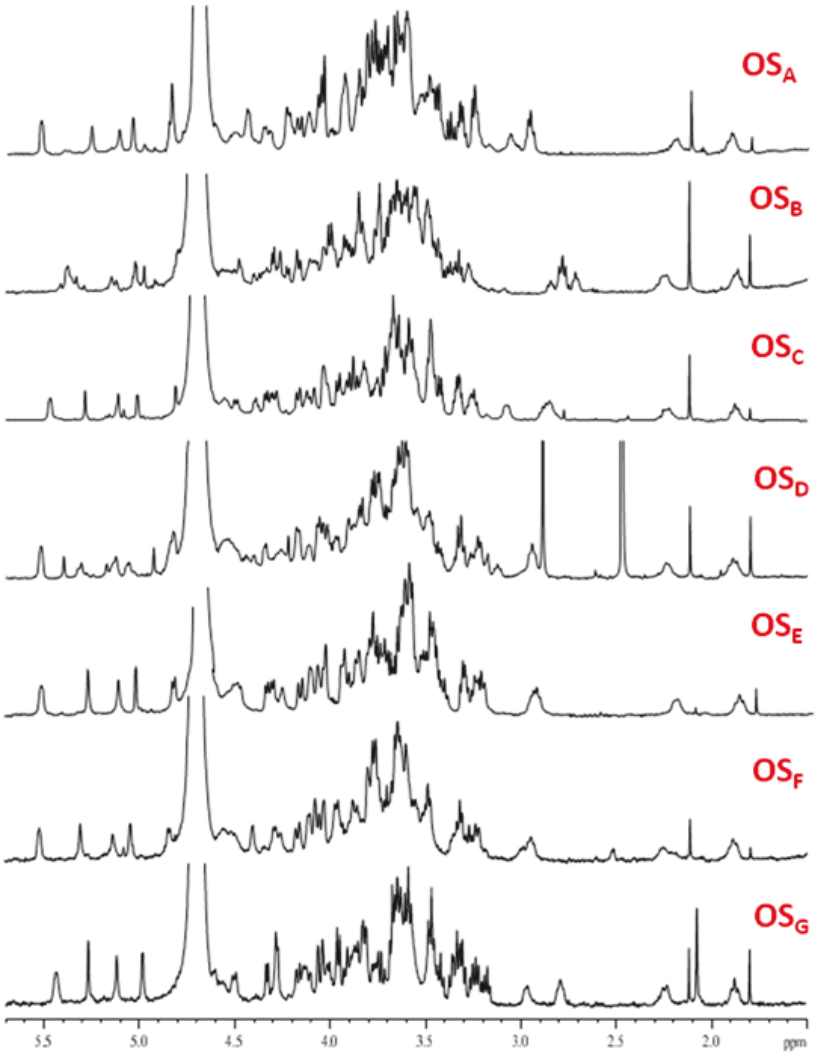

Figure 8.3 – ^{1}H NMR of fractions obtained from HPAEC-PAD purification of the deacylated LPS from *S. sharmensis*.

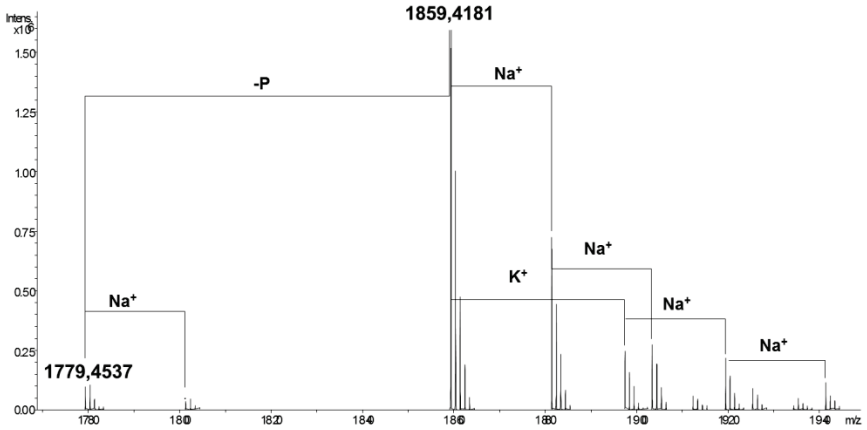

Figure 8.4 - The charge deconvoluted negative ion mode ESI FT-ICR mass spectrum of fraction $\mathbf{OS_E}$ obtained from HPAEC-PAD chromatography. To the main species at 1859.4181 *m/z* was attributed the following composition $HexN_3HexKdoHep_2HexA_2P_3$, calculated molecular mass 1859.42 Da.

8.3. NMR characterization of OS_E and OS_C

$\mathbf{OS_E}$ fraction was analyzed by one- and two-dimensional NMR experiments (Figure 8.5a, 8.6, Table 8.2). In particular ^{1}H-^{1}H DQF-COSY, ^{1}H-^{1}H TOCSY, ^{1}H-^{1}H ROESY, ^{1}H-^{13}C DEPT-HSQC, ^{1}H-^{13}C HSQC-TOCSY, ^{1}H-^{13}C HMBC and 2D *F2*-coupled HSQC. The ^{1}H-NMR spectrum of the oligosaccharide $\mathbf{OS_E}$ (Figure 8.5a) showed the presence of eight anomeric signals (**A-H**) between 4.3 and 5.6 ppm.

Residue **A** was attributed to the 6-substituted α-GlcpN*1P* of lipid A on the basis of the multiplicity of the anomeric proton signal due to its phosphorylation ($^3J_{H,P}$= 7.8 Hz). Moreover the C-2 chemical shift occurred at 55.7 ppm, which indicated a nitrogen-bearing carbon while the C-6 chemical shift was downfield shifted by glycosylation at 70.3 ppm.

Residue **E** with C-1/H-1 signals at 100.8/4.84 ppm ($^1J_{C1,H1}$= 169 Hz) was attributed to the lipid A 6-substituted β-GlcpN*4P* residue

as a result of its C-2 chemical shift at 56.6 ppm and its linkage to *O*-6 of **A**.

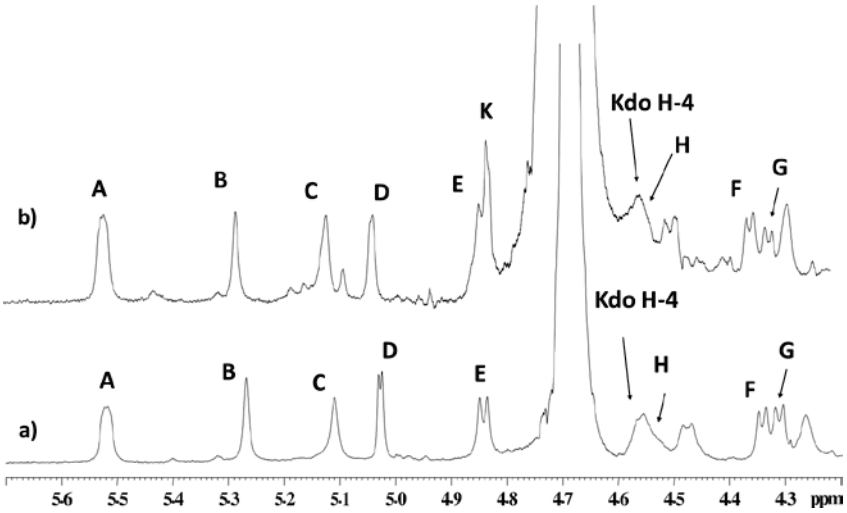

Figure 8.5 – ^{1}H NMR anomeric region of $\mathbf{OS_E}$ (a) and $\mathbf{OS_C}$ (b). The spectra were recorded in D_2O at 298K at 600 MHz.

Table 8.2. ^{1}H and ^{13}C NMR assignments of $\mathbf{OS_E}$ and $\mathbf{OS_C}$. Spectra were recorded in D_2O, using acetone as internal standard. Spectra were recorded at 298 K.

Residue	H1 C1	H2 C2	H3 C3	H4 C4	H5 C5	H6a C6	H6b/H7 C7	H7b/H8a-b C8
A **6-α-GlcN*p1P***	5.52 92.0	3.23 55.7	3.77 71.2	3.32 71.2	4.06 73.7	3.77 70.3	4.19	
B **2-α-Hep*p***	5.27 102.1	4.08 80.9	3.82 72.2	3.73 68.3	3.59 73.0	3.95 69.7	3.47 64.4	3.64
C **2,3,4-α-Hep*p***	5.11 98.4	4.04 79.0	4.11 74.4	3.92 76.2	4.48 75.0	4.11 70.6	3.62 62.4	3.80
D ***t*-α-GlcA*p***	5.03 102.3	3.48 73.3	3.66 74.1	3.32 73.7	3.95 74.9	- 176.4		
E **6-β-GlcN*p4P***	4.84 100.8	2.94 56.6	3.74 74.1	3.88 74.1	3.61 75.0	3.53 63.0	3.53	
F ***t*-β-GlcA*p***	4.35 103.3	3.23 73.8	3.41 76.6	3.45 73.0	3.60 78.7	- 177.0		
G **4-β-Glc*p***	4.32 103.8	3.26 74.5	3.50 74.9	3.54 78.2	3.49 76.6	3.72 62.4	3.72	
H ***t*-β-GalN*p***	4.56 100.8	3.01 54.7	3.64 71.9	3.80 69.1	3.64 77.2	3.86 62.2	3.68	
I **5-α-Kdo*p***	- 177.2	- n.d.	1.89-2.22 35.5	4.54 69.7	4.27 73.2	3.82 73.0	3.60 71.2	3.87-3.65 64.8
K* ***t*-α-Glc*p***	4.82 101.2	3.43 73.0	3.65 73.8	3.34 70.5	4.05 73.2	3.69 61.4	3.69	
H* **4-β-GalN*p***	4.56 100.8	2.99 54.6	3.66 70.8	3.91 77.5	3.70 77.3	3.92 62.2	3.71	

*These residues belong to $\mathbf{OS_C}$

This structural feature was inferred by the *inter*-residue connectivity between H-1 of **E** and H-6a,b of **A** identified in the ROESY experiments. Moreover, the H-4 and C-4 downfield shifts were diagnostic for the presence of a phosphate group linked at *O*-4 (Holst *et al.*, 1993).

Starting from the diastereotopic protons H-3_{ax} and H-3_{eq}, the Kdo (residue **I**) was identified. The sugar was present in pyranose form. The chemical shifts difference between these protons depends upon the orientation of C-1 carbon, being different for α and β anomers. In this case the $\Delta(H3_{ax}\text{-}H3_{eq})$=0.33 ppm allowed to attribute an α configuration to the residue (Agrawal *et al.*, 1994). Moreover, both protons showed a correlation in the DQF-COSY spectrum with a signal at 4.54 ppm, attributed to Kdo H-4, which was in turn correlated to a carbon atom at 69.7 ppm in the DEPT-HSQC spectrum, indicating phosphorylation at this position. The proton at 4.27 ppm displayed a vicinal scalar coupling with Kdo H-4 in the DQF-COSY spectrum and was then attributed to Kdo H-5 proton, which showed a correlation in the DEPT-HSQC spectrum with a carbon atom at 73.2 ppm. This last, in turn, was downfield shifted respect to the reference value, indicating glycosylation at this position.

Residues **B** and **C,** with C-1/H-1 signals at 102.1/5.27 ppm and 98.4/5.11 ppm, were identified as two *manno*-configured heptopyranoses due to their small $J_{H\text{-}1,H\text{-}2}$ and $J_{H\text{-}2,H\text{-}3}$ values. In addition an α–anomeric configuration for both residues was established, as their $^{1}J_{C\text{-}1,H\text{-}1}$ were found to be 181 and 177 Hz, respectively (Bock and Pedersen, 1983). The substitution positions were inferred by comparing the carbon chemical shifts values with those of standard unsubstituted heptoses, taking into account the methylation results. Residue **B** was attributed to a 2-substituted heptopyranose as its C-2 carbon atom occurred at 80.9 ppm, while **C** was identified as a 2,3,4-trisubstituted heptopyranose as its C-2, C-3 and C-4 carbon atoms occurred at 79.0, 74.4 and 76.2 ppm, respectively. L,D- and D,D- configurations for heptoses **B** and **C**

were inferred by comparing the GC retention time of each partially methylated alditol acetate with that of authentic standards.

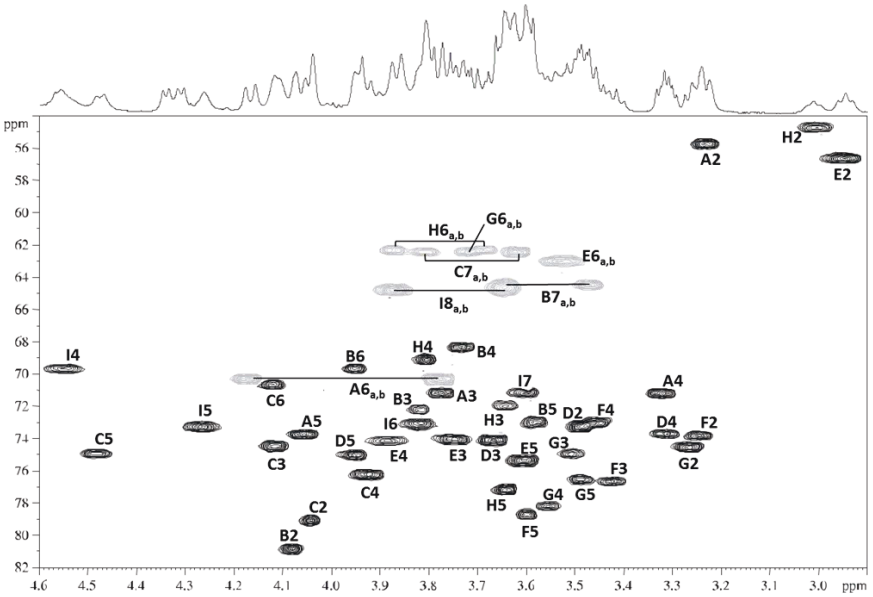

Figure 8.6 – ^{1}H-^{13}C HSQC spectrum of **OS$_E$**. The spectrum was recorded in D_2O at 298 K at 600 MHz using acetone as internal standard (δ_H 2.225 ppm and δ_C 31.45 ppm). The letters refer to the residues as described in Table 8.2 and in Scheme 8.1.

Residues **D** and **F** were identified as terminal glucopyranuronic acids since their C-6 occurred at 176.4 and 177.0 ppm, respectively and none of their carbon was shifted by glycosylation. In particular to residue **D** was attributed an α anomeric configuration while to residue **F** a β one, on the basis of their $^{1}J_{C\text{-}1,H\text{-}1}$ coupling constant values, of 175 and 166 Hz, respectively. Moreover the ROESY spectrum displayed correlations between H-1 proton and H-3 and H-5 protons of residue **F**, confirming its β configuration in the $^{4}C_1$ ring conformation.

Residue **G** with C-1/H-1 signals at 103.8/4.32 ppm was attributed to a 4-substituted β-glucopyranose, as its $^{1}J_{C\text{-}1,H\text{-}1}$ was 168 Hz and its C-4 carbon atom was downfield shifted at 78.2 ppm.

Residue **H** was identified as a terminal β-galactopyranosamine since its H-2 proton showed a correlation in the DEPT-HSQC spectrum, with a nitrogen bearing carbon, which occurred at 54.7 ppm, while none of the remaining carbon was downfield shifted by glycosylation. The β anomeric configuration was inferred by the *intra*-residue NOE contacts.

The monosaccharides sequence was deduced by the long range scalar coupling correlations displayed in the HMBC spectrum and supported by the *inter*-residues ROE contacts in the ROESY spectrum (Table 8.3). More in details, heptose **C** was linked to the *O*-5 position of the Kdo residue, in turn linked to the lipid A backbone. Heptose **B** H-1 displayed a correlation with C-3 of residue **C**. The latter residue was also glycosylated at position *O*-2 by the terminal β-glucuronic acid residue **F** and at position *O*-4 by the β-glucose residue **G**, which was in turn glycosylated at position *O*-4 by the β-galactosamine residue **H**. Finally, residue **D** H-1 showed a correlation with the C-2 of residue **B** in the HMBC spectrum.

Table 8.3 - Main nuclear Overhauser enhancement *intra*- and *inter*-residual connectivities for the anomeric protons of $\mathbf{OS_E}$ and $\mathbf{OS_C}$.

Residue	*Intra*-residue ROE	*Inter*-residue ROE
A 6-α-GlcN*p1P*	H2	
B 2-α-Hep*p*	H2	H3 C
C 2,3,4-α-Hep*p*	H2	H5 I, H1 F
D *t*-α-GlcA*p*	H2	H1 B, H2 B
E 6-β-GlcN*p4P*	H3, H5	H6 A
F *t*-β-GlcA*p*	H3, H5	H1 C, H2 C
G 4-β-Glc*p*	H3	H4 C
H *t*-β-GalN*p*	H3	H4 G
K* *t*-α-Glc*p*	H2	H4 H* H5 H*
H* 4-β-GalN*p*	H3, H5	H4 G

*These residues belong to $\mathbf{OS_C}$

As for the $\mathbf{OS_C}$ oligosaccharide, the ^{1}H-NMR proton spectrum (Figure 8.5b) showed the presence of an additional anomeric proton signal (residue **K**) at 4.82 ppm. Also $\mathbf{OS_C}$ was completely characterized by 2D NMR spectroscopy and residue **K** was identified as a terminal α-glucopyranose residue, on the basis of its carbon and proton chemical shifts, which were in agreement with those of an unsubstituted α-glucose. The analysis of the HMBC and ROESY spectra allowed to determine its position in the oligosaccharide; it resulted to be linked at position *O*-4 of residue **H**.

It was then possible to conclude that $\mathbf{OS_E}$ and $\mathbf{OS_C}$ oligosaccharides correspond to **M3** and **M4** species, revealed in the ESI FT-ICR mass spectrum of the fully deacylated product.

Reasonably, from these data the punctual structures of species **M1** and **M2** can be defined too, while it had been not possible to elucidate the position of the fourth GlcN residue present in **M5** species, because the latter was not obtained in an amount sufficient for a complete characterization.

Successively, the de-*O*-acylated LPS fraction (LPS-OH) was also analyzed by ESI FT-ICR MS. The spectrum showed the presence of four main signals (**N1**-**N4**, Table 8.4).

The composition of the species was in agreement with the results obtained after KOH treatment. In particular, to the most intense signal was attributed the following composition: $HexN_2[C14(3\text{-}OH)]_2P_3KdoHep_2HexA_2Hex_2HexNAc$, which revealed the presence of a HexNAc residue. Actually hydrazinolysis treatment kept the amide linkages intact, allowing us to determine that the galactosamine residue **H** bears an *N*-acetyl group at C-2 in the native LPS.

Table 8.4 - Composition of the main species observed in the charge deconvoluted ESI FT-ICR mass spectrum of the LPS-OH from *S. sharmensis* (spectrum not shown).

Species	*Observed mass (Da)*	*Calculated mass (Da)*	*Composition*
N1	1988.68	1988.69	$HexN_2[C14(3\text{-}OH)]_2P_3KdoHep_2HexA_2$
N2	2150.73	2150.74	$HexN_2[C14(3\text{-}OH)]_2P_3KdoHep_2HexA_2Hex$
N3	2353.81	2353.82	$HexN_2[C14(3\text{-}OH)]_2P_3KdoHep_2HexA_2HexHexNAc$
N4	2515.83	2515.87	$HexN_2[C14(3\text{-}OH)]_2P_3KdoHep_2HexA_2Hex_2HexNAc$

On the basis of all the above mentioned data, the structure of the core-lipid A backbone of the LPS from *S. sharmensis* was depicted as described in Scheme 8.1.

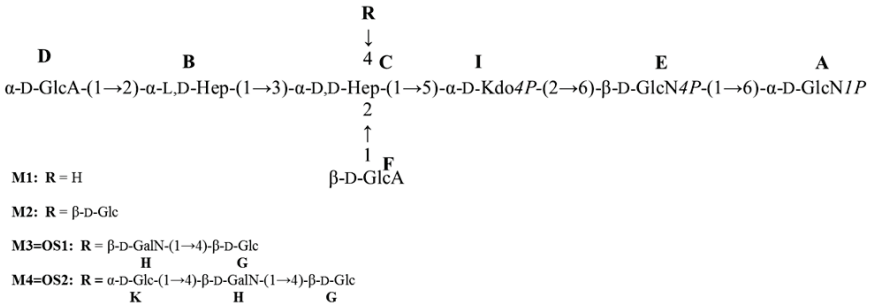

Scheme 8.1 – Core structure of the LPS from *S. sharmensis* BAG^T. Letter refer to residues as described in Table 8.2.

8.4. Lipid A characterization

The lipopolysaccharidic fraction was hydrolyzed under mild acidic condition, with 5% acetic acid. The gas chromatography mass spectrometry (GC-MS) analysis of the fatty acids methyl esters derivative, obtained after the LPS methanolysis, showed the presence of 3-hydroxy-dodecanoic [C12:0(3-OH)] and 3-hydroxy-tetradecanoic acids [C14:0(3-OH)] as the most abundant species, together with dodecanoic (C12:0), tetradecanoic (C14:0) and hexadecenoic (C16:1) acids.

Lipid A was analyzed by ESI FT-ICR mass spectrometry. The charge deconvoluted negative ions ESI FT-ICR mass spectrum showed the presence of nine signals (**M1**–**M9**, Figure 8.7, Table 8.5) corresponding to a number of glycoforms differing in their acylation as well as their phosphorylation degree. In particular, they ranged from hexa-acylated to di-acylated glycoforms and, except for **M9**, were mono or bis-phosphorylated.

In particular **M1**, **M3**, **M5** and **M7** corresponded to the bis-phosphorylated glycoforms. The following composition was attributed to the species **M1**, with the mass 1741.14 *m/z*, $GlcN_2P_2[C12:0(3\text{-}OH)]_2[C14:0(3\text{-}OH)]_2(C12:0)(C14:0)$ (calculated molecular mass: 1741.17 Da). Species **M3** was identified as penta-acylated lipid A since it carries no C12:0 fatty acid, while the **M5** species was missing a C12:0 and 3-hydroxy dodecanoic acid. The tri-acylated species **M7** contained only one 3-hydroxy dodecanoic and two 3-hydroxy tetradecanoic acids. Finally **M9** was the only di-acylated species corresponding to the following composition $GlcN_2P[C14:0(3\text{-}OH)]_2$.

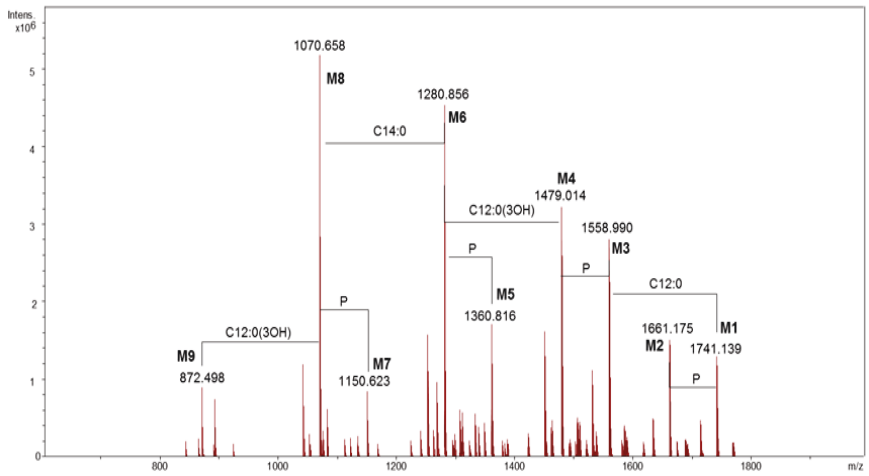

Figure 8.7. The charge deconvoluted negative ion electrospray ionization Fourier transform ion cyclotron (ESI FT-ICR) mass spectrum of the lipid A from *S. sharmensis* strain BAG^T.

Table 8.5. Composition of the main species present in the charge deconvoluted negative ions ESI FT-ICR mass spectrum of the lipid A from *S. sharmensis* strain BAG^T.

Species	M_{obs}	M_{acc}	Composition
M1	1741.14	1741.17	$GlcN_2P_2$[C12:0(3-OH)]$_2$[C14:0(3-OH)]$_2$(C12:0)(C14:0)
M2	1661.18	1661.21	$GlcN_2P$[C12:0(3-OH)]$_2$[C14:0(3-OH)]$_2$(C12:0)(C14:0)
M3	1558.99	1559.00	$GlcN_2P_2$[C12:0(3-OH)]$_2$[C14:0(3-OH)]$_2$(C14:0)
M4	1479.01	1479.04	$GlcN_2P$[C12:0(3-OH)]$_2$[C14:0(3-OH)]$_2$(C14:0)
M5	1360.82	1360.84	$GlcN_2P_2$[C12:0(3-OH)][C14:0(3-OH)]$_2$(C14:0)
M6	1280.86	1280.87	$GlcN_2P$[C12:0(3-OH)][C14:0(3-OH)]$_2$(C14:0)
M7	1150.62	1150.64	$GlcN_2P_2$[C12:0(3-OH)][C14:0(3-OH)]$_2$
M8	1070.66	1070.67	$GlcN_2P$[C12:0(3-OH)][C14:0(3-OH)]$_2$
M9	872.50	872.51	$GlcN_2P$[C14:0(3-OH)]$_2$

Less abundant species, due to the replacement of the C14:0 with a C16:1 (+26 u) or a C12:0 (−28 u) fatty acid, were also present. In order to obtain the detailed information on the distribution of fatty acids on the disaccharidic backbone, MS and MS/MS spectra in the positive ion mode were generated.

The FT-ICR-MS (positive ion mode) of lipid A showed the presence of the adduct ion $[M + Et_3N + H]^+$ at *m/z* 1843.31, which corresponded to the hexa-acylated, bis-phosphorylated glycoform (calculated molecular mass: *m/z* 1843.303). The MS/MS spectrum of this species, obtained by infrared multiphoton dissociation (IRMPD) (see Section 9.4), displayed a B^+ fragment ion (Domon and Costello, 1988; Kondakov and Lindner, 2005) at *m/z* 1058.76, to which the following composition was attributed: GlcNP[C12:0(3-OH)][C14:0(3-OH)](C12:0)(C14:0) (calculated mass *m/z* 1058.77). These results proved that both the secondary fatty acids (C12:0 and C14:0) were linked to the distal non-reducing end glucosamine.

By treating the sample with NH_4OH (Silipo *et al.*, 2002), the lipid A was devoid of primary *O*-linked fatty acids. The product was analyzed again in the positive ion mode. The mass spectrum revealed the presence of four main signals corresponding to [M +

H]$^+$ adducts with one or two Et_3N molecules, followed by the signals of the corresponding monophosphorylated species at 80 u lower (**N1**–**N6**, Figure 8.8, Table 8.6).

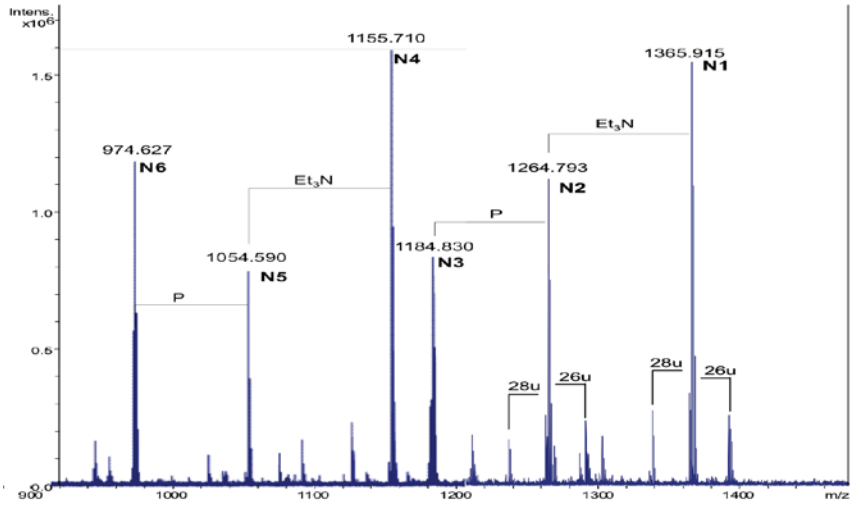

Figure 8.8. The charge deconvoluted positive ion ESI FT-ICR mass spectrum of the NH_4OH product from the lipid A of *Salinivibrio sharmensis* strain BAG^T.

Table 8.6. Composition of the main species present in the positive ions ESI FT-ICR mass spectrum of the NH_4OH product of the lipid A from *S. sharmensis* strain BAG^T.

Species	Observed *m/z*	Calculated *m/z*	Composition
N1	1365.91 [a]	1365.92	$GlcN_2P_2$[C14:0(3-OH)]$_2$(C14:0)
N2	1264.79 [b]	1264.80	$GlcN_2P_2$[C14:0(3-OH)]$_2$(C14:0)
N3	1184.83 [b]	1184.84	$GlcN_2P$[C14:0(3-OH)]$_2$(C14:0)
N4	1155.71 [a]	1155.72	$GlcN_2P_2$[C14:0(3-OH)]$_2$
N5	1054.59 [b]	1054.60	$GlcN_2P_2$[C14:0(3-OH)]$_2$
N6	974.63 [b]	974.64	$GlcN_2P$[C14:0(3-OH)]$_2$

[a] This signal corresponds to the adduct $[M + 2Et_3N + H]^+$; [b]This signal corresponds to the adduct $[M + Et_3N + H]^+$.

The $[M + 2Et_3N + H]^+$ adduct ion at 1365.91 *m/z* (**N1**) was selected for fragmentation. The MS/MS spectrum showed the presence of a B^+ fragment ion at *m/z* 678.4 (GlcNP[C14:0(3-OH)]C14:0, calculated *m/z* 678.3, Figure 8.9a), thus revealing that C14:0 was linked as acyloxyamide to the GlcN II. As a consequence, C12:0 resulted to be linked as acyloxyacyl to the GlcN II. In Figure 8.8, starting from the **N1** signal, a species at 26 u higher masses was found (*m/z* 1391.90), which corresponded to the replacement of the C14:0 with C16:1, as already found.

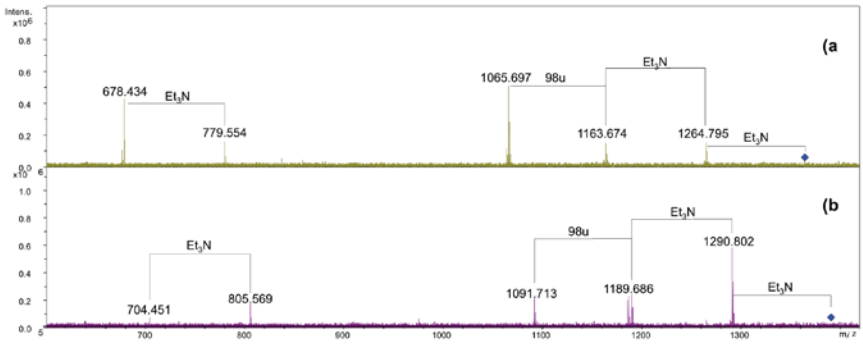

Figure 8.9. ESI FT-ICR tandem mass spectrum infrared multiphoton dissociation (IRMPD). (**a**) Product ion scan of the isolated precursor ion 1365.9 *m/z*. (**b**) Product ion scan of the isolated precursor ion 1391.9 *m/z*.

The MS/MS spectrum of the signal at *m/z* 1391.9 (Figure 8.9b) displayed the presence of a B^+ fragment ion at *m/z* 704.4 confirming that C16:1 occupies the same position of C14:0. The MS/MS spectrum of **N3** showed the presence of a B^+ fragment ion at 678.4 *m/z*, the same as obtained by **N1** fragmentation (data not shown). This pointed out that the phosphate group on the proximal glucosamine was not stoichiometric. The lack of the phosphate group was a consequence of the 5% acetic acid hydrolysis. In fact during the structural characterization of the oligosaccharidic portion, after mild and strong alkaline treatment of the LPS, the

phosphate group was found to be stoichiometric. On the basis of all the data obtained from the mass spectra as well as from the chemical analysis, the structure of the lipid A from the *S. sharmensis* strain BAG^T is depicted in Scheme 8.2.

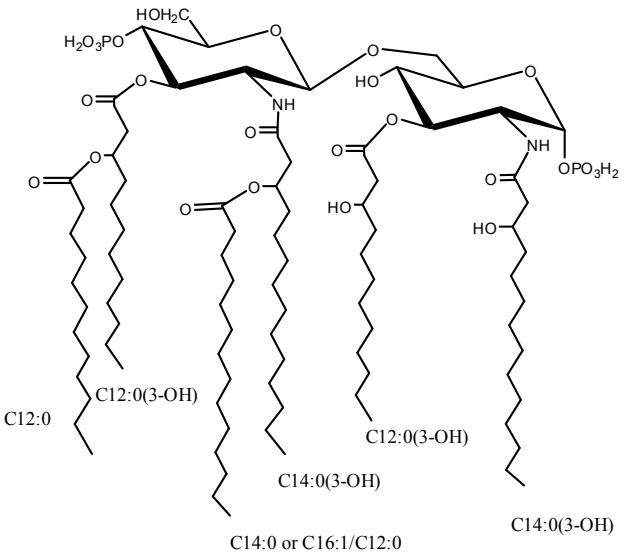

Scheme 8.2. Structure of the Lipid A from *Salinivibrio sharmensis* strain BAG^T

8.5. Conclusion

The LPS obtained from *S. sharmensis* dried cells was found to be rough and the core structural identification was performed.

It resulted to be very heterogeneous, as already found in many Gram-negative bacteria. These core structures share some similarities with those of the lipopolysaccharides of phylogenetically closely related *Vibrio vulnificus* (Vinogradov *et al.*, 2009) and *V. parahaemolyticus* (Hashii *et al.*, 2003). In both these strains, as well as in *Salinivibrio*, the Kdo residue in the inner core region is glycosylated at position *O*-5 substituted by the D,D-Hep, which in turn was glycosylated at the *O*-4 position by D-Glc

and at the *O*-3 position by L,D-Hep. D,D-Hep has already been found in the outer LPS core region of halophilic bacteria (Pieretti *et al.*, 2008) but its presence in the inner core region is rather unique.

The presence of two glucuronic acids in the core structure of *S. sharmensis* lipopolysaccharide, together with the occurrence of one phosphate groups on the Kdo residue, increase the negative charge density on the external membrane.

The lipid A from *S. sharmensis* was characterized as well. It is composed of a family of molecules with different acylation patterns; the fatty acid C14:0(3-OH) is always found to be acyloxyamide linked to both glucosamines of the saccharidic backbone, while position 3 and 3′ are substituted with C12:0(3-OH). The distribution of secondary acyl chains in the hexa-acyl species is asymmetric (4 + 2), since C12:0 and C14:0 are both linked to the primary fatty acids of the distal glucosamine. In addition C14:0 can be replaced by C16:1 or C12:0. The overall fatty acid distribution resembles that of *E. coli* lipid A (Holst *et al.*, 1993), even though the chain length of primary *O*-linked fatty acids is different. On the contrary, *Neisseria meningitidis* lipid A (Kulshin *et al.*, 1992) shows the same distribution of primary fatty acids, but its hexa-acylated lipid A species displays an overall symmetric (3 + 3) fatty acids distribution, since C12:0 secondary fatty acids are linked as acyloxyamide at position 2 and 2′, respectively. *N. meningitidis* lipid A is not toxic and shows little agonist behavior (Zughaier *et al.*, 2007), so it is a good candidate to be used as vaccine adjuvant. On this basis the biological activity of the lipid A from *Salinivibrio sharmensis* is also worth being investigated.

Papers related to this chapter:

Carillo S, Pieretti G, Lindner B, Romano I, Nicolaus B, Lanzetta R, Parrilli M, Corsaro MM.
"The lipid A from the haloalkaliphilic bacterium *Salinivibrio sharmensis* strain BAG^T."
Marine Drugs. **2013**; 11(1): 184-93.

Carillo S, Pieretti G, Lindner B, Romano I, Nicolaus B, Lanzetta R, Parrilli M, Corsaro MM.
"Structural characterization of the core oligosaccharide isolated from the lipopolysaccharide of the haloalkaliphilic bacterium *Salinivibrio sharmensis* strain BAG^T."
Carbohydr Res. **2013**; 368: 61-7.

Haloalkalophiles: Conclusions

During this thesis work three LPSs from haloalkalophilic bacteria were structurally characterized. In particular, two bacteria belonging to genus *Halomonas* and one belonging to genus *Salinivibrio* were investigated and each structural motif has shown its own peculiarity.

The main common feature was found to be the presence of a phosphate group linked at position *O*-4. All marine bacteria seems to share this structural feature (Leone *et al.*, 2007). Moreover, additional negative charges are always found to be present, as phosphate groups or uronic acid residues. This feature may be an haloadaptation. In fact, it was already found in proteins (Coquelle *et al.*, 2010) and phospholipids from this bacteria (Nicolaus *et al.*, 2001; Hart *et al.*, 1988) and matches the well known accumulation of osmolytes inside the cytoplasm (Beales, 2004; Russell *et al.*, 1995). Moreover, such structural elements contribute to the tightness of the outer-membrane and decrease the ion permeability, due to the association of LPS molecules through divalent cations (Ca^{2+} and Mg^{2+}) (Leone *et al.*, 2007; Alexander and Rietschel, 2001).

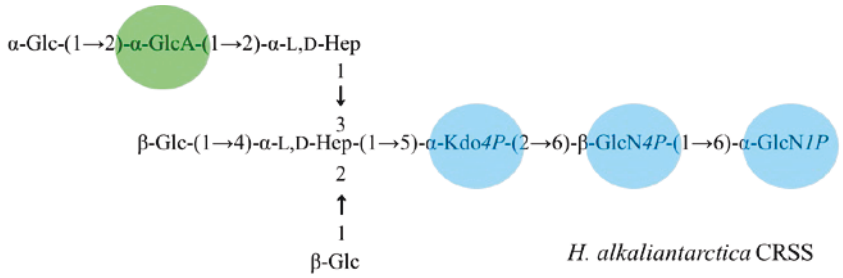

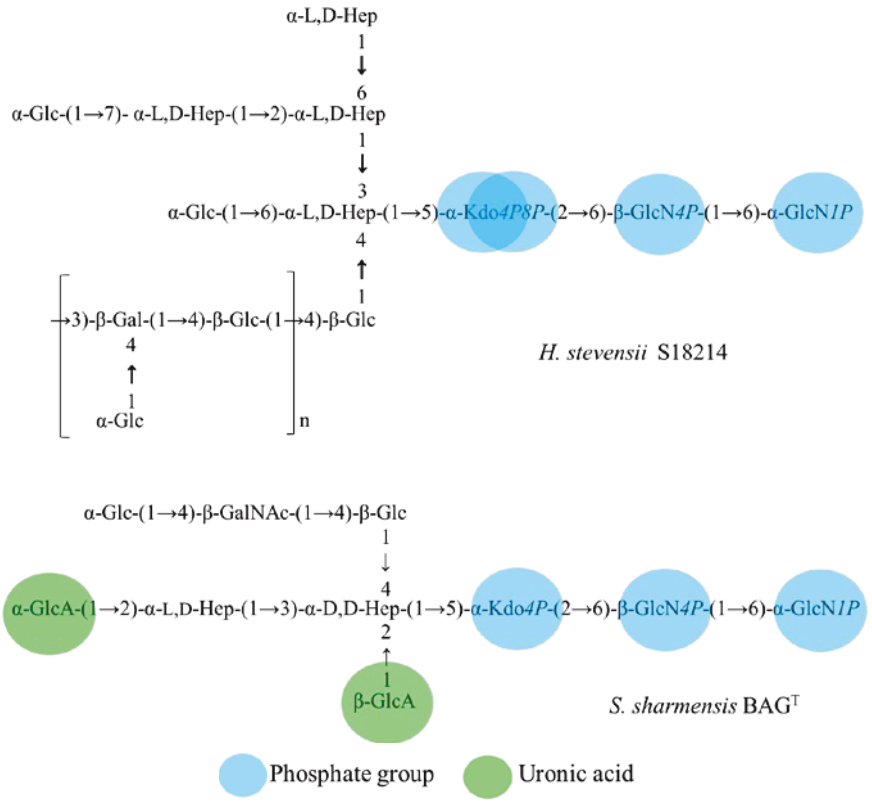

Finally, even if *H. stevensii* highlighted the pathogenic potential of *Halomonas* genus, haloalkaliphilic bacteria are rarely found to be pathogen. As a consequence, biological active molecules derived from these extremophiles are worth being investigated from a structural and a biological point of view.

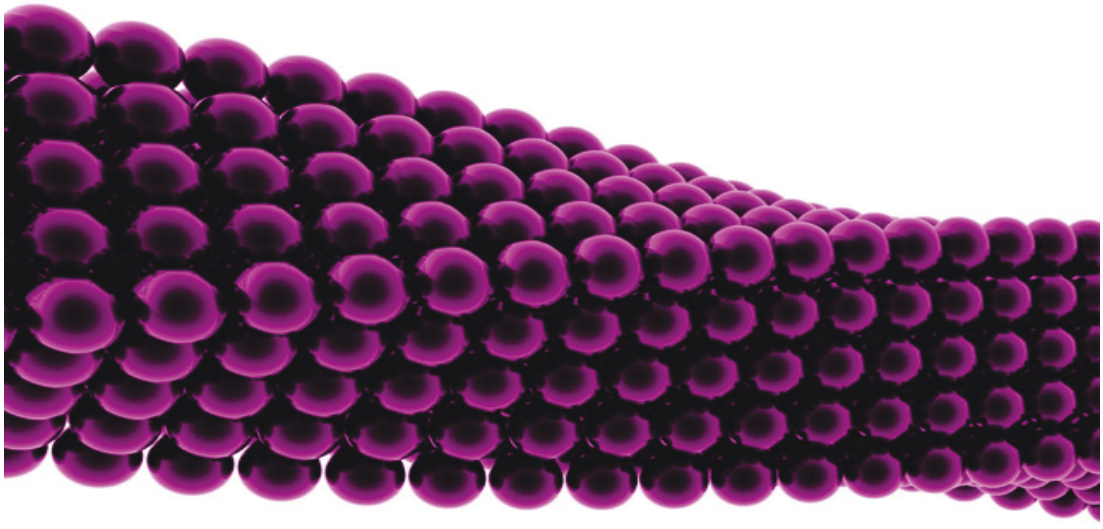

Experimental part

Chapter 9

Materials and Methods

9.1 Bacteria growth

9.1.1 Halomonas alkaliantarctica strain CRSS

Halomonas alkaliantarctica strain CRSS was isolated from salt sediments in a saline lake of Cape Russell, Antarctica (Poli *et al.*, 2007). Cells were grown by Dott. Barbara Nicolaus research group of the Istituto di Chimica Biomolecolare ICB-CNR, Naples. It was routinely grown at 30°C in a rotary shaker incubator with stirring at 100 rpm in 5 L flasks filled with 1000 cm^3 of the following enrichment medium (g/L): yeast extract 10, NaCl 100, trisodium-citrate 3, KCl 2, $MgSO_4.7H_2O$ 1, $MnCl_2.4H_2O$ 0.00036, $FeSO_4$ 0.050, Na_2CO_3 3 in distilled water, pH 9.0 (Na_2CO_3 and NaCl were autoclaved separately). The inoculum was 5% of total volume and aerobic condition was used. Cell growth was monitored by measuring the turbidity at 540 nm. The cultures were grown until the late exponential phase and harvested by centrifugation (10000 g). The cells were washed once with a saline solution and lyophilised.

9.1.2 Halomonas stevensii strain S18214

Halomonas stevensii strain S18214 was grown by Prof. Jung-Sook Lee research team at the Korea Research Institute of Bioscience and Biotechnology. Cells were grown for 4 days at 35°C in brain heart infusion broth (3% NaCl added) adjusted to pH 8.0; cells were checked for purity, harvested by centrifugation and lyophilized.

9.1.3 Salinivibrio sharmensis strain BAG^T

S. sharmensis strain BAG^T (=ATCC BAA-1319^T = DSM 18182^T), isolated from samples collected in a small permanent saline lake in Ras Mohammed Park, located at Sharm el-Sheikh, Egypt (Romano *et al.*, 2011). Cells were grown by Dott. Barbara Nicolaus research group of the Istituto di Chimica Biomolecolare ICB-CNR, Naples. It was grown, at 35 °C and at pH 9.0, using a medium containing the following components (g/L): yeast extract 10.0, NaCl 100.0, Na_3-citrate 3.0, Na_2CO_3 3.0, KCl 2.0, $MgSO_4$ x 7 H_2O 1.0, $MnCl_2$ x 4 H_2O 0.00036, $FeSO_4$ 0.05 (NaCl and Na_2CO_3 were autoclaved separately). The medium was autoclaved for 20 min at 121 °C. The inoculum was prepared using a dilution of 1:50 v/v. Bacterial growth was directly monitored in a UV/Vis spectrophotometer DU 730 (Beckman Coulter) by utilizing the change in optical density at 540 nm. After incubation of 24 h at an absorbance of 2.0, the cells were collected by centrifugation at 10.000 g and lyophilized.

9.1.4 Pseudoalteromonas haloplanktis strain TAB23

P. haloplanktis TAB 23 was grown by Prof. Gennaro Marino research team in Dipartimento di Scienze Chimiche, University "Federico II", in Naples. Cells were grown at 15°C in aerobic conditions in TYP medium (16 g/L Bactotryptone, Difco; 16 g/L yeast extract Difco; 16 g/L sea salt, pH 7.5).

The large scale biomass production was carried out in shaken flasks (2.5 L total volume) containing 500 mL of liquid broth. When the liquid culture reached the late exponential phase (D_{600} 12), cells were harvested by centrifugation (15 min, 5000 rpm) and lyophilized.

9.1.5 Colwellia psychrerythraea strain 34H

C. psychrerythraea 34H was grown by Prof. Gennaro Marino research team in Dipartimento di Scienze Chimiche, University "Federico II", in Naples. Cells were grown aerobically growth at

4°C in Marine Broth medium (DIFCO™ 2216). When the liquid culture reached the late exponential phase (OD_{600} = 2), cells were harvested by centrifugation for 20 min, 3000 *g* at 4 °C.

9.2 General and analytical methods

9.2.1 LPS extraction and purification

PCP was performed on dried cells as described by Galanos et al (Galanos *et al.*, 1969). The cells were extracted three times with a mixture of aqueous phenol 90%/chloroform/light petroleum ether (2:5:8 v/v/v, ~10ml/g of dry cells). After removal of the organic solvents under vacuum, LPS was precipitated from phenol with drops of water, then washed once with aqueous phenol 80% and three times with cold acetone and then lyophilized. The yields obtained for each bacterium are summarized in Table 9.1.

Water/phenol extraction for LPS and capsular polysaccharide was performed according to Westphal *et al.* procedure (Westphal and Jann, 1965). Dried cells or PCP residual were suspended in aqueous phenol 90%/water (1:1 v/v, ~10ml/g of dry cells) at 68°C. After three extraction with hot water the supernatant were collected and the phenol phase diluted with water; both were dialysed against water (cut-off 3500 Da). The fractions were purified from proteic and nucleic material with enzymatic digestion with DNase, RNase and protease K (Sigma-Aldrich) and then dialysed again.

Table 9.1 – Yield obtained for each strain after PCP extraction.

Bacterium	Dried cells	LPS_{PCP}
H. alkaliantarctica	21 g	396 mg
H. stevensii	11 g	330 mg
S. sharmensis	7 g	103 mg
P. haloplanktis	5 g	45 mg
C. psychrerythraea	4.8 g	52 mg

9.2.2 Electrophoretic analysis

Sodium dodecyl sulphate and deoxycholate polyacrylamide gel electrophoresis (SDS- and DOC-PAGE) were performed as already described. Silver staining was performed according to Kittelberger et. al. (Kittelberger, 1993). Alcian blue staining was performed with Alcian blue dye 0.05% in MeOH (40%) and AcOH (5%).

9.2.3 Chemical analysis

Sugar and fatty acids analysis - Monosaccharides were analysed as acetylated methyl glycosides obtained from each LPS (0.5 mg) as follows: the samples were first dephosphorylated with 48% HF (100 μL), then the methanolysis was performed in 1 M HCl/MeOH (0.5 cm^3, 80°C, 20 h). The obtained product was extracted twice with hexane and the methanol layer was dried and acetylated with Ac_2O (50 μL) and Py (50 μL) at 100°C for 30 min. The hexane layer containing fatty acids methyl esters was analysed by GC-MS to obtain fatty acids composition.

Alditol acetates were obtained from each LPS (1 mg) as follows: the LPS was hydrolysed with 2 M trifluoroacetic acid (120°C, 2 h), reduced with $NaBD_4$ and acetylated with Ac_2O (50 μL) and pyridine (50 μL). The monosaccharides were identified by EI mass spectra and GC retention times by comparison with those of authentic standards.

Absolute configuration - The absolute configuration of the sugars was determined by gas-chromatography of the acetylated (*S*)-2-octyl glycosides (Leontein *et al.*, 1978). Absolute configuration of Gro was determined by GC-MS analysis of its 2-octyl ester derivative. Briefly it was oxidized using 2,2,6,6 tetramethylpiperidine-1-oxyl (TEMPO), then hydrolyzed with 2M TFA and esterified with chiral 2-octanol (Rundlöf and Widmalm, 1996). The absolute configuration of amino acids residues was inferred analyzing their butyl esters derivatives (Leontein *et al.*, 1978)

Linkage analysis - The linkage positions of the monosaccharides were determined by GC-MS analysis of the partially methylated alditol acetates. Briefly, the deacylated LPS (1 mg) was methylated with CH_3I (300 µL) in DMSO (1.0 mL) and NaOH powder (20 h) (Ciucanu and Kerek, 1984). The product was hydrolyzed with 2 M TFA (100 µL, 120°C, 2 h), reduced with $NaBD_4$ and finally acetylated with Ac_2O and Py (50 µL each, 100°C, 30 min). If uronic acids were present in the sample, acid hydrolysis was preceded by reduction of carboxymethyl with $NaBD_4$. When phosphorylated sugars were present 48% HF treatment was performed before.

Table 9.2 – Temperature programs for sugar derivatives.

Derivatives	Temperature program
Acetylated methyl glycosides	150°C for 3 min, 150°C→240°C at 3°C/min
Alditol acetates	150°C for 3 min, 150°C→240°C at 3°C/min
Acetylated octyl glycosides	150°C for 5 min, 150°C→240°C at 6°C/min, 240°C for 5 min
Partially methylated alditol acetates	90°C for 1 min, 90°C→140°C at 25°C/min, 140°C→200°C at 5°C/min, 200°C→280°C at 10°C/min, 280°C for 10 min.
Fatty acids methy esters	140 °C for 3 min, 140 °C→280 °C at 10 °C/min
Aminoacids acetylated butyl esters	100°C for 2 min, 100°C→180°C at 3°C/min, 180°C→300°C at 15°C/min
Glyceric acid octyl ester	80°C for 5 min, 80°C→200°C at 5°C/min, 200°C→300°C at 10° C/min

All of these sugar derivatives were analysed on a Agilent Technologies gas chromatograph 6850A equipped with a mass selective detector 5973N and a Zebron ZB-5 capillary column

(Phenomenex, 30 m x 0.25 mmi.d., flow rate 1 mL/min, He as carrier gas) according to temperature program as described in Table 9.2.

9.2.4 Mild acid hydrolysis

The LPSs were hydrolysed with 1% or 5% aqueous CH_3COOH (10mg/mL, 100°C, ~3-6h); each sample was treated as already reported (Carillo *et al.*, 2011; Pieretti *et al.*, 2010; Pieretti *et al.*, 2011). The obtained suspensions were then centrifuged (10.000 *g*, 4°C, 30 min.). The pellet were washed twice with water and the supernatant layers were combined and lyophilized. The precipitate (lipid A) were also lyophilized. The polysaccharide portions were then fractionated on a Biogel P-10 column (Biorad, 1.5 x 130 cm, flow rate 17 mL/h, fraction volume 2.5 mL) eluted with water buffered (pH 5.0) with 0.05 M pyridine and 0.05 M sodium acetate.

9.2.5 de-O and de-N-acylation of LPSs

The LPS were first dried under vacuum over phosphoric anhydride and then incubated with hydrazine (20-30 mg/mL, 37°C, 1.5 h). To precipitate the O-deacylated LPSs cold acetone was added. The pellet were recovered after centrifugation (4°C, 10.000 *g*, 30 min), washed 3 times with acetone and finally suspended in water and lyophilized (Masoud *et al.*, 1994).

The O-deacylated LPSs were dissolved in 4 M KOH and incubated at 120°C for 16 h. KOH was neutralized with 2 M HCl until pH 6 and the mixtures were extracted three times with $CHCl_3$. The water phases were recovered and desalted on a column Sephadex G-10 (Amersham Biosciences, 2.5 × 43 cm, 35 mL/h, fraction volume 2.5 mL, eluent NH_4HCO_3 10 mM). The eluted oligosaccharide mixtures were then lyophilized.

9.2.6 Ammonium hydroxide hydrolysis of lipid A

The lipid A (~1 mg) were incubated with conc. NH_4OH (100 µL), as reported (Silipo *et al.*, 2002). The sample was simply dried and analyzed by mass spectrometry.

9.2.7 CPS isolation and purification

Water extract was hydrolyzed with 1% aqueous CH_3COOH (9 mL, 100 °C, 5 h). The obtained suspension was then centrifuged (10,000*g*, 4 °C, 30 min). The pellet was washed twice with water and the supernatant layers were combined and lyophilized. Polysaccharide portion was then fractionate on a Biogel P-10 column (Biorad, 1.5x130 cm, flow rate 17 mL/h, fraction volume 2.5 mL), eluted with water buffered (pH 5.0) with 0.05 M pyridine, and 0.05 M sodium acetate obtaining two fractions named CPS and OS.

9.3 HPAEC-PAD

Separation of the oligosaccharides mixture obtained after deacylation of the LPSs were performed by HPAEC-PAD on a semi-preparative column (9 × 250 mm) of Carbopac PA-100 eluted with the following gradient:

H. alkaliantarctica: 25%→31% of B over 55 min, 31%→50% of B over 30 min (A: 0.1 M NaOH and B: 2 M NaOAc/ 0.1 M NaOH) at 1 mL/min.

H. stevensii: 38%→45% of B over 35 min (A: 0.1 M NaOH, B: 1 M NaOAc/ 0.1 M NaOH) at 1 mL/min.

S. sharmensis: 43%→50% of B over 90 min (A: 0.1 M NaOH, B: 1 M NaOAc/ 0.1 M NaOH) at 1 mL/min.

P. haloplanktis: 45% → 55% of B over 50 min, 55% → 70% of B over 45 min (A: 0.1 M NaOH and B: 1 M NaOAc/ 0.1 M NaOH) at 0.8 mL/min.

The main fractions were desalted on a column (1.5 × 100 mm) of Sephadex G-10 (Amersham Biosciences, 2.5 × 43 cm, 39 mL/h, fraction volume 2 mL, eluent NH_4HCO_3 10 mM).

9.4 Mass spectrometry

Negative ions reflectron MALDI-TOF mass spectra were acquired on a Voyager DE-PRO instrument (Applied Biosystems) equipped with a delayed extraction ion source. Ion acceleration voltage was 20 kV, grid voltage was 17 kV, mirror voltage ratio 1.12 and delay time 200 ns. Samples were irradiated at a frequency of 5 Hz by 337 nm photons from a pulsed nitrogen laser. Mass calibration was obtained with a hyaluronan oligosaccharides mixture. A solution of 2,5-dihydroxybenzoic acid in 20% CH_3CN in water at a concentration of 25 mg/mL was used as the MALDI matrix. Spectra were calibrated and processed under computer control by using the Applied Biosystems Data Explorer software. Postsource decay was performed using an acceleration voltage of 20 kV. The reflectron voltage was decreased in 10 successive 25% steps.

Electrospray ionization Fourier transform ion cyclotron (ESI FT-ICR) mass spectrometry was performed by Dott. Buko Lindner from Research Center in Borstel. Mass spectra were performed in negative ion mode using an APEX Qe, BrukerDaltonics, equipped with a 7 Tesla actively shielded magnet and a dual ESI/MALDI ion source. Samples were dissolved in a 50:50:0.001 (v/v/v) mixture of 2-propanol, water, and triethylamine at a concentration of ~ 10 ng/µL and were sprayed at a flow rate of 2 µl/min. Capillary entrance voltage was set to 3.8 kV, and dry gas temperature to 200°C. The mass spectra were charge deconvoluted and mass numbers given refer to the monoisotopic masses of the neutral molecules. Mass calibration was done externally by similar compounds of know structure.

The MS/MS lipid species were analyzed in the positive ion mode using a 50:50:0.03 (v/v/v) mixture of 2-propanol, water, and 30 mM ammonium acetate (pH 4.5). Small amounts of triethylamine were added to generate triethylamine adduct ions, which are favorable as precursor ions for MS/MS (Kondakov and Lindner, 2005). Precursor ions were isolated in the ICR-cell and then fragmented by infrared multiphoton dissociation (IRMPD). For this, the unfocused beam of a 35-watt, CO_2 laser (Synrad) was directed through the center of the trap. The duration of laser irradiation was adapted for optimal fragmentation and varied between 50 and 200 ms, and fragment ions were detected after a delay of 0.5 ms.

9.5 NMR spectroscopy

For structural assignments of oligosaccharides 1D ^{1}H and 2D ^{1}H- ^{13}C NMR spectra were recorded using a Bruker 600 MHz spectrometerequipped with a cryo-probe. All two-dimensional homo- and heteronuclear experiments (COSY, TOCSY, ROESY, HSQC-DEPT, *F2*-coupled HSQC, HSQC-TOCSY and HMBC) were performed using standard pulse sequences available in the Bruker software. The mixing time for TOCSY, ROESY and HSQC-TOCSY experiments was 100 ms. Chemical shifts were measured in D_2O using acetone as internal standard (δ 2.225 and 31.45 for CH_3 proton and carbon, respectively).

The ^{13}C NMR spectrum were recorded in D_2O at 100 MHz with a Bruker DRX 400 Avance spectrometer equipped with a 5-mm BBO (Observe Broadband) probe at 298 K.

^{31}P NMR spectra were recorded on a Bruker DRX-400MHz spectrometer. Phosphoric acid was used as an external reference (δ 0.00) for ^{31}P NMR spectroscopy. NaOD was added to the sample prior to one- and two-dimensional ^{31}P spectroscopy as described (Holst *et al.*, 1990).

9.6 Biological assays

Biological assay were performed in collaboration with Dott. Monica Molteni from BlueGreen Biotech s.r.l. in Milan.

Cell culture: THP-1, a human monocytic cell line (Istituto Zooprofilattico della Lombardia e dell'Emilia Romagna), was grown in RPMI 1640 (Euroclone Ltd, West York, U.K.) containing 10% of heat-inactivated Fetal Bovine Serum (FBS) (Euroclone), 2mM L-glutammine (Euroclone) and 0,05 mM β-mercaptoethanol (Sigma-Aldrich, St. Louis, MO), at 37°C in a humidified atmosphere with 5% CO_2. For each experiment, cells were harvested, seeded in 24-well tissue culture plates at a density of $5 \cdot 10^5$ cellmL^{-1} and incubated with lipid A obtained from *P. haloplanktis* strain TAB 23 at the final concentrations of 1, 10, 20 µgmL^{-1}, respectively. Similar cultures were performed co-incubating the cells with *P. haloplanktis* lipid A, at different concentrations, and LPS from *E. coli*, strain O111:B4 (Sigma-Aldrich, St. Louis, MO), at 1 µgmL^{-1}. Cultures were maintained at 37°C in 5% CO_2 for 18 hours and then supernatants were collected, centrifuged, and stored at -80°C for subsequent analyses.

TNFα and IL-6 ELISA: The amounts of TNFα and IL-6 in the cell culture supernatants were measured by solid-phase sandwich ELISA using Human TNFα and IL-6 Eli-pairs (Diaclone; Gen-Probe incorporated, San Diego, CA), respectively. Samples were tested in triplicate according to manufacturer's instructions.

Bibliography

Agrawal PK, Bush A, Qureshi N, Takayama K, *Adv. Biophys. Chem.* **1994**. 4, 179-236.

Alexander C, Rietschel ET*, J. Endotox. Res.*, **2001**. 7, 167-202.

Amoozegar MA, Schumann P, Hajighasemi M, Fatemi AZ, Karbalaei-Heidari HR, *Int. J. Syst. Evol. Microbiol.,* **2008**. 58, 1159–1163.

Arias S, del Moral A, Ferrer MR, Tallon R, Quesada E, Béjar V, *Extremophiles* **2003**. 7, 319–326.

Auzanneau F I, Charon D, Szabo L, *J. Chem.Soc., Perk. Trans. 1* **1991**, 509-17.

Banoub J, Cohen A, El Aneed A, LeQuart V, Martin P, *Eur. J. Mass Spectrom.* **2004**. 10*,* 715-554.

Bazaka K, Crawford RJ,. Nazarenko EL, Ivanova EP, *Bacterial Adhesion*, Advances in Experimental Medicine and Biology. D. Linke, A. Goldman (eds.). **2011**. 213-226.

Beales N, *Comp. Rev. Food Sci. Food Safety*, **2004**. 3, 1-20.

Berger P, Barguellil F, Raoult D, Drancourt M, *J. Hosp. Infect*. **2007**. 67, 79-85.

Biedzka-Sarek M, Venho R, Skurnik M, *Infect. Immun.* **2005**. 73, 2232-2244.

Black S, Shinefield H, Fireman B, Lewis E, Ray P, Hansen JR, Elvin L, Ensor KM, Hackell J, Siber G, Malinoski F, Madore D, Chang I, Kohberger R, Watson W, Austrian R, Edwards K, *Pediatr. Infect. Dis. J.* **2000**. 19, 187–195.

Bock K, Pedersen C, *Adv. Carbohydr. Chem. Biochem.* **1983**. 41, 27-66.

Bock K, Vinogradov EV, Holst O, Brade H, *Eur. J. Biochem.* **1994**. 225, 1029-1039.

Bogaert D, de Groot R, Hermans PWM, *Lancet Infect. Dis.* **2004**. 4, 144–154.

Bowman JP, Gosinkt JJ, McCammon SA, Lewis TE,Nichols DS, Nichols PD, Skerratt JH, Staley JT, McMeekin TA. *Int. J. Syst. Bacteriol.,* **1998**. 48, 1171-1180.

Brabetz W, Muller-Loennies S, Holst O, Brade H, *Eur. J. Biochem.*, **1997**. 247, 716-724.

Brade H, Zähringer U, Rietschel ET, Christian R, Schulz G, Unger FM, *Carbohydr. Res.,* **1984**. 134, 157-166.

Brandenburg K, Mayer H, Koch MHJ, Weckesser J, Rietschel ET, Seydel U, *Eur. J. Biochem*. **1993**. 218, 555-563.

Brisson JR, Crawford E, Uhrín D, Khieu NH, Perry MB, Severn WB. Richards JC, *Can. J. Chem.* **2002**. 80, 949-963.

Brock TD, Freeze H, *J. Bacteriol*. **1969**. 98, 289–297.

Calvo C, Martínez-Checa F, Toledo FL, Porcel J, Quesada E, *Appl. Microbiol. Biotechnol.* **2002**. 60, 347–351.

Canganella F, Wiegel J, *Naturwissenschaften*, **2011**. 98, 253–279.

Carillo S, Pieretti G, Parrilli E, Tutino ML, Gemma S, Molteni M, Lanzetta R, Parrilli M, Corsaro MM, *Chem. Eur. J.* **2011**. 17, 7053-7060.

Caroff M, Karibian D, *Carbohydr. Res.* **2003**. 338, 2431-2447.

Casanueva A, Tuffin M, Cary C, Cowan DA *Trends in Microbiology*, **2010**. 18, 374-381.

Cavicchioli R, Siddiqui KS, Andrews D, Sowers KR *Current Opinion in Biotechnology* **2002**. 13, 253-261.

Chamroensaksri N, Tanasupawat S, Akaracharanya A, Visessanguan W, Kudo T, Itoh T. *Int. J. Syst. Evol. Microbiol*. **2009**. 59, 880–885.

Chattopadhyay MK, *J. Biosci.* **2006**. 31, 157–165.

Ciucanu I, Kerek F, *Carbohydr. Res.* **1984**. 131, 209-217.

Coombs JM, Brenchley JE, *Appl. Environ. Microbiol.* **1999**. 65, 5443-5450.

Coquelle N, Talon R, Juers DH, Girard E, Kahn R, Madern DJ, *Mol. Biol.* **2010**. 404, 493-505.

Corsaro MM, Dal Piaz F, Lanzetta R, Parrilli M, *J. Mass Spectrom*. **2002**. 37, 481-488.

Corsaro MM, Lanzetta R, Parrilli E, Parrilli M, Tutino ML, *Eur. J. Biochem*. **2001**. 268, 5092-5097.

Corsaro MM, Pieretti G, Lindner B, Lanzetta R, Parrilli E, Tutino ML, Parrilli M. *Chemistry*. **2008**. 14, 9368-9376.

Cox D, Brisson J-R, Varma V, Perry MB, *Carbohydr. Res.* **1996**. 290, 43-58.

de Castro C, Molinaro A, Nunziata R, Grant W, Wallace A, Parrilli M. *Carb. Res.*, **2003**. 338, 567–570.

de Castro C, Parrilli M, Holst O, Molinaro A, *Methods in Enzymology*, **2010**. 480, 89-115.

DeAngelis PL, *Appl. Microbiol. Biotechnol.*, **2012**. 94, 295-305.

DeLong EF, Franks DG, Yayanos AA. *Appl. Environ. Microbiol*. **1997**. 63, 2105-2108.

DeLong EF, Yayanos AA. *Appl Environ Microbiol.*, **1986**. 51, 730-737.

Domon B, Costello CE, *Glycoconjugate J.* **1988**. 5, 397-409.

Erridge C, Bennett-Guerrero E, Poxton IR, *Microbes and Infection* **2002**. 4, 837-851.

Feller G, Lonhienne T, Deroanne C, Libioulle C, Van Beeumen J, Gerday C, *J. Biol. Chem.* **1992**. 267, 5217-5221.

Franzmann PD, Wehmeyer U, Stackebrandt E, *Syst. Appl. Microbiol*. **1988**. 11, 16-19.

Freitas F, Alves VD, Reis MAM, *Trends in Biotechnology*, **2011**. 29, 388-398.

Fujinami S, Fujisawa M, *Environ Technol.* **2010**. 31, 845-56.

Galanos C, Lüderitz O, Westphal O*, Eur. J. Biochem.* **1969**. 9, 245-249.

Georlette D, Jonsson ZO, Petegem FV, Chessa J-P, Beeumen JV, Hubscher U, Gerday C, *Eur. J. Biochem.*, **2000**. 267, 3502-3512.

Ghosh T, Chattopadhyay K, Marschall M, Karmakar P, Mandal P, Ray B, *Glycobiology*, **2009**. 19, 2–15.

Graether SP, Kuiper MJ, Gagné SM, Walker VK, Jia Z, Sykes BD, Davies PL, *Nature*, **2000**. 406, 325-328.

Grzeszczyk B, Holst O, Müller-Loennies S, Zamojski A, *Carbohydr. Res.* **1998**. 307, 55-67.

Grzeszczyk B, Holst O, Zamojski A, *Carbohydr. Res.* **1996**. 290, 1-15.

Hall-Stoodley L, Costerton JW, Stoodley P. *Nature Reviews Microbiology,* **2004**. 2, 95-108.

Hardy MR, Townsend RR, Lee YC. *Analytical Biochemistry*, **1988**. 170, 54-62.

Hart DH, Wreeland RH, *J. Bacteriol.*, **1988**. 270, 132-135.

Hashii N, Isshiki Y, Iguchi T, Kondo S, *Carbohydr. Res.* **2003**. 338, 1063–1071.

Holmström C, Kjelleberg S, *FEMS Microbiology Ecology*, **1999**. 30, 285-293.

Holst O, in *Methods in Molecular Biology*, Vol. 145, (ed. O. Holst) Humana Press, Totowa, NJ, **2000**, 345-353.

Holst O, Molinaro A *Microbial Glycobiology: Structures, relevance and applications*, **2009**. Academic Press (Eds. Moran AP, Holst O, Brennan PJ, von Itzstein M), 29-55.

Holst O, Müller-Loennies S, Lindner B, Brade H, *Eur. J. Biochem*. **1993**. 214, 695-701.

Holst O, Rohrscheidt-Andrzejewski E, Brade H, Charon D, *Carbohydr. Res.*, **1990**. 204, 93-102.

Horrocks LA, Yeo YK. *Pharmacological Research* **1999**. 40, 211–225.

Hough DW, Danson MJ, *Curr Opin Chem Biol.* **1999**. 3(1):39-46.

Huang CY, Garcia JL, Patel BKC, Cayol JL, Baresi L, Mah RA. *Int. J. Syst. Evol. Microbiol.,* **2000**. 50, 615–622.

Huston AL, Krieger-Brockett BB, Deming JW*, Environ. Microbiol.* **2000**. 2, 383-388.

Huston AL, Ph.D. thesis, **2003** (Univ. of Washington, Seattle).

Ialenti A, Di Meglio P, Grassia G, Maffia P, Di Rosa M, Lanzetta R, Molinaro A, Silipo A, Grant W, Ianaro A, *Eur. J. Immunol.* **2006**. 36, 354-360.

Janeway CA, Travers P, Walport MS (eds) (2001) Immunobiology. Garland, New York, NY

Junge K, Eicken H, Deming JW, *Appl. Environ. Microbiol*., **2003**. 69, 4282–4284.

Kim KK, Lee KC, Oh HM, Lee JS. *Int. J. Syst. Evol. Microbiol*., **2010**. 60, 369-377.

Kittelberger R, Hilbink FJ, *Biochem Biophys Methods*. **1993**. 26, 81-86.

Knirel YA. *Microbial Glycobiology: Structures, relevance and applications*, **2009**. Academic Press (Eds. Moran AP, Holst O, Brennan PJ, von Itzstein M), 57-73.

Kondakov A, Lindner B, *Eur. J. Mass Spectrom*., **2005**. 11, 535-546.

Kondakova AN, Novototskaya-Vlasova KA, Arbatsky NP, Drutskaya MS, Shcherbakova VA, Shashkov AS, Gilichinsky DA, Nedospasov SA, Knirel YA, *J. Nat. Prod.* **2012a**. 75, 2236-2240.

Kondakova AN, Novototskaya-Vlasova KA, Drutskaya MS, Senchenkova SN, Shcherbakova VA, Shashkov AS, Gilichinsky DA, Nedospasov SA, Knirel YA, *Carbohydr. Res.* **2012b**. 349, 78-81.

Krasikova IN, Kapustina NV, Isakov VV, Gorshkova NM, Solov'eva TF, *Russ. J. Bioorgan. Chem.* **2003**. 30, 367-373.

Krembs C, Deming JW, Junge K, Eicken H, *Deep-Sea Res.* **2002**. 49, 2163–2181.

Kulshin VA, Zaehringer U, Lindner B, Frasch CE, Tsai CM, Dmitriev BA, Rietschel ET. *J. Bacteriol.* **1992**. 174, 1793–1800.

Leone S, Silipo A, Nazarenko EL, Lanzetta R, Parrilli M, Molinaro A, *Mar. Drugs*, **2007**. 5, 85-112.

Leontein K, Lindberg B, Lönngren J, *Carbohydr. Res.*, **1978**. 62, 359-362.

Lin F-H, Davies PL, Graham LA. *Biochemistry* **2011**. 50, 4467–4478.

Lipsitch M, O'Hagan JJ. *J. Royal Soc. Interf.* **2007**. 4, 787–802.

Loppnow H, Libby P, Freundenberg M, Krauss JH, Weckesser J, Mayer H, *Infect. Immun.* **1990**. 58, 3743-3750.

Lukáčová M, Barák I, Kazár J, *Clin. Microbiol. Infect.* **2008**. 14, 200-206.

Macelroy RD. *Biosystems,* **1974**. 6, 74–75.

Mancuso Nichols CA, Garon S, Bowman JP, Raguenes G, Guezennec J,. *J. Appl. Microbiol*. **2004**. 96, 1057–1066.

Martin DD, Bartlett DH, Roberts MF, *Extremophiles,* **2002**. 6, 507–514.

Marx JG, Carpenter SD, Deming JW. *Can. J. Microbiol.* **2009**. 55, 63–72.

Masoud H, Altman E, Richards JC, Lam JS, *Biochemistry*, **1994**. 33, 10568-10578.

Mata-Haro V, Cekic C, Martin M, Chilton PM, Casella CR, Mitchell TC, *Science,* **2007**. 316, 1628–1632.

Mazmanian SK, Cui HL, Tzianabos AO, Kasper DL, *Cell*, **2005**. 122, 107–118.

Mellado E, Moore ERB, Nieto JJ, Ventosa A. *Int. J. Syst. Bacteriol.*, **1996**. 46, 817–821.

Methé BA, Nelson KE, Deming JW, Momen B, Melamud E, Zhang X, et al. *Proc. Natl. Acad. Sci.* USA. **2005.** 102*,* 10913-10918.

Morita RY. *Bacteriol. Rev*. **1975**. 39, 144–167.

Morona R, Brown MH, Yeadon J, Heuzenroeder MW, Manning PA, *FEMS Microbiol. Lett.*, **1991**. 82, 279-285.

Müller-Loennies S, Brade L, Brade H, *Eur. J. Biochem.* **2002**. 269, 1237-1242.

Müller-Loennies S, Lindner B, Brade H, *J. Biol. Chem.*, **2003**. 278, 34090-34101.

Nagata S, Wang Y, Oshima A, Zhang L, Miyake H, Sasaki H, Ishida A, *Biotechnol. Bioeng*. **2007**. 99, 941–948.

Nevot M, Deroncele` V, Montes MJ, Mercade E. *J. Appl. Microbiol.* **2008**. 105, 255–263.

Nichols CM, Guézennec J, Bowman JP. *Mar Biotechnol* (NY). **2005**. 7, 253-271.

Nicolaus B, Manca MC, Lama L, Esposito E, Gambacorta A, *Pol. Biol.*, **2001**. 24, 1-8.

Nummila K, Kilpeläinen I, Zähringer U, Vaara M, Helander IM, *Mol. Microbiol*. **1995**. 16, 271-278.

Olsthoorn MMA, Haverkamp J, Thomas-Oates JE, *J. Mass Spectrom*. **1999**. 34, 622-636.

Olsthoorn MMA, Petersen BO, Duus J, Haverkamp J, Thomas-Oates JE, Bock K, Holst O, *Eur. J. Biochem.*, **2000**. 267, 2014-2027.

Oren A. *Environ. Technol.* **2010**. 31, 825–834.

Oren A. *J. Ind. Microbiol. Biotechnol*., **2002**. 28:56–63.

Park BS, Song DH, Kim HM, Choi B-S, Lee H, Lee J-O, *Nature* **2009**. 458, 1191-1196.

Pieretti G, Carillo S, Kim KK, Lee KC, Lee JS, Lanzetta R, Parrilli M, Corsaro MM, *Carbohydr. Res.* **2011**. 346, 362-365.

Pieretti G, Carillo S, Nicolaus B, Poli A, Lanzetta R, Parrilli M, Corsaro MM. *Org Biomol Chem*. **2010**. 8, 5404-5410.

Pieretti G, Corsaro MM, Lanzetta R, Parrilli M, Nicolaus B, Gambacorta A, Lindner B, Holst O, *Eur. J. Org. Chem.* **2008**. 721-728.

Pieretti G, Corsaro MM, Lanzetta R, Parrilli M, Vilches S, Merino S, Tomàs JM, *Eur. J. Org. Chem.* **2009b**. 1365-1371.

Pieretti G, Nicolaus B, Poli A, Corsaro MM, Lanzetta R, Parrilli M, *Carbohydr. Res*., **2009a**. 344, 2051-2055.

Poli A, Esposito E, Orlando P, Lama L, Giordano A, de Appolonia F, Nicolaus B, Gambacorta A, *System. Appl. Microbiol*., **2007**. 30, 31-38.

Quillaguamán J, Delgado O, Mattiasson B, Hatti-Kaul R, *Enz. Microb. Technol.,* **2006**. 38, 148–154.

Raetz CRH, Whitfield C, *Annu Rev Biochem*. **2002**. 71, 635–700.

Raj R, Hemaiswarya S, Rengasamy R, *Appl. Microbiol. Biotechnol.* **2007**. 74, 517–523.

Rehm BHA. (ed.) Caister Academic Press, **2009**.

Rietschel ET, Kirikae T, Schade FU, Mamat U, Schmidt G, Loppnow H, Ulmer AJ, Zähringer U, Seydel U, Di Padova F, Schreier M, Brade H, *The FASEB Journal,* **1994**. 8, 217-225.

Rietschel ET, Kirikae T, Schade FU, Ulmer AJ, Holst O, Brade H, Schmidt G, Mamat U, Grimmecke HD, Kusumoto S, Zähringer U. *Immunobiology*, **1993**. 187, 169–190.

Romano I, Gambacorta A, Lama L, Nicolaus B, Giordano A. *Syst. Appl. Microbiol.*, **2005**. 28, 34–42.

Romano I, Orlando P, Gambacorta A, Nicolaus B, Dipasquale L, Pascual J, Giordano A, Lama L, *Extremophiles* **2011**. 15, 213–220.

Rose JR, Christ WJ, Bristol JR, Kawata T, Rossignol DP, *Infect. Immun*. **1995**. 63, 833-839.

Rothschild LJ, Mancinelli RL, *Nature*, **2001**. 409, 1092-1101.

Rundlöf T, Widmalm G, *Anal. Biochem.* **1996**. 243, 228-233.

Russell NJ, Evans RI, terSteeg PF, Hellemons J, Verheul A, Abee T, *Int. J. Food Microbiol.*, **1995**. 28, 255-261.

Sauer T, Galinski EA, *Biotechnol. Bioengin*. **1998**. 57, 306–313.

Shivanand P, Mugeraya G. *Current Science*, **2011**. 100, 1516-1521.

Silipo A, De Castro C, Lanzetta R, Molinaro A, Parrilli M, *Glycobiology* **2004c** . 14, 805-815.

Silipo A, Lanzetta R, Amoresano A, Parrilli M, Molinaro A, *J. Lipid. Res.* **2002**. 43, 2188-2195.

Silipo A, Leone S, Lanzetta R, Parrilli M, Sturiale L, Garozzo D, Nazarenko EL, Gorshkova RP, Ivanova EP, Gorshkova NM, Molinaro A, *Carbohydr. Res.* **2004a**. 339, 1985-1993.

Silipo A, Sturiale L, Garozzo D, de Castro C, Lanzetta R, Parrilli M, Grant WD, Molinaro A. *Eur. J. Org. Chem.* **2004b**. 2263-2271.

Smith FB. *Proc. Royal Soc. Qld.* **1938**. 49, 29–52.

Stevens DA, Hamilton JR, Johnson N, Kim KK, Lee JS. *Medicine*, **2009**. 88, 244-249.

Suesskind M, Brade L, Brade H, Holst O, *J. Biol. Chem.* **1998**. 273, 7006-7017.

Takeda K, Akira S, *Seminars in Immunology*, **2004**. 16, 3–9

Takeuchi A, Kamiryou Y, Yamada H, Eto M, Shibata K, Haruna K, Naito S, Yoshikai Y. *Int. Immunopharmacol.* **2009**. 9, 1562–1567.

Townsend RR, Hardy MR, Hindsgaul O, Lee YC, *Analytical Biochemistry* **1988**. 174, 459-470.

Tsigos I, Velonia K, Smonou I, Bouriotis V. *Eur J Biochem,* **1998**. 254, 356-362.

Turkiewicz M, Gromek E, Kalinowska H, Zielinska M, *J Biotechnol* **1999**. 70, 53-60.

Tzianabos AO, Pantosti A, Baumann H, Brisson J-R, Jennings HJ, Kasper DL, *J. Biol. Chem.* **1992**. 267, 18230–18235.

Uma S, Jadhav RS, Seshu-Kumar G, Shivaji S, Ray MK, *FEBS Lett,* **1999**. 453, 313-317.

Ventosa A, Nieto JJ, Oren A, *Microbiol. Mol. Biol. Rev.*, **1998**. 62, 504-b544.

Verde C, Vergara A, Mazzarella L, di Prisco G, *Current Protein and Peptide Science*, **2008**. 9, 578-590.

Vinogradov EV, Bock K, *Carbohydr. Res.* **1999**. 320, 239-243.

Vinogradov EV, Bock K, Holst O, Brade H, *Eur. J. Biochem.* **1995**. 233, 152-158.

Vinogradov EV, Wilde C, Anderson EM, Nakhamchik A, Lam JS, Rowe-Magnus DA. *Carbohydr. Res.* **2009**. 344, 484–490.

Von Graevenitz A, Bowman J, Del Notaro C, Ritzler M. *J. Clin. Microbiol*. **2000**. 38, 3123-3124.

Welsh DT, *FEMS Microbiol Rev*, **2000**. 24, 263-290.

Westphal O, Jann K. *Methods Carbohydr. Chem.* **1965**. 5, 83-91.

Zughaier S, Steeghs L, van der Ley P, Stephens DS. *Vaccine,* **2007**. 25, 4401–4409.

E anche stavolta è arrivato il momento dei ringraziamenti. Solo che stavolta scrivere queste poche righe mi consente di fare un resoconto di una fase importantissima della mia vita.

Un enorme grazie va ovviamente a tutto il gruppo CSS che mi ha accolto e proprio come una grande famiglia, con i suoi alti e bassi, mi ha sostenuto sempre. In particolare grazie ai professori; Prof. Parrilli, Prof. Lanzetta, Prof. Adinolfi.

Un grazie anche a Cristina e Alfonso per esserci sempre nei momenti del bisogno!

Un grazie ancora più grande va a Tony: mi hai vista crescere e diventare prima donna, poi tua "collega" e poi mamma in questi anni. Non dimenticherò mai due momenti in particolare e in entrambi avevi una lacrimuccia ferma con uno spillo sull'occhio: quando hai visto me e Roberta a Siena, al nostro primo convegno, ed eri fiero di noi, e quando ti sei reso conto che ero diventata mamma. Ti voglio bene!

Grazie anche a Alba e Emiliano e tutti quelli che sono passati nei laboratori in questi anni: Flaviana, Alberto, Concetta, Valentina, Teresa, Eleonora, Mary e Antonello.

Ma un ruolo importantissimo negli ultimi 4 anni lo ha avuto Liana. Sei stata quasi una seconda mamma per me e una guida importante nel lavoro e nella vita. Grazie mille di tutto tutto tutto.

Peppa…che dire!!! Mi hai supportato e sopportato! Ma è anche nata una meravigliosa amicizia! Ti prego…pensa a queste parole dolci e affettuose quando troverai i miei guai sparsi nei quaderni e negli scatoli!!!! Ti voglio bene assaje!!!

Lo stesso vale anche e forse di più per Angela…a cui lascio il testimone! Tu più di tutti mi vorrai maledire! Nei momenti di sconforto che inevitabilmente arriveranno non dimenticare mai il mio numero di telefono…sono a tua completa disposizione per sfoghi, varie ed eventuali….ma non pretendere che ricordi dove ho messo quel campione!

A tutti gli altri che hanno reso belli questi anni, anche se forse alcuni non leggeranno mai queste righe: Marco Meoli, Marco

Evidente, Sara Basso, Luca Unione, Diego Tufano, Gennaro Franzese, Carlotta Ciaramelli.

Una menzione speciale va a Cirillo! Siamo stati per troppo poco tempo vicini di laboratorio…ma il tuo modo di essere (bello o brutto che sia, io lo adoro!) mi tiene ancora compagnia!!!

A tutti i miei grandi amici: Veronica e Gianna, Rossella e le salviette, Greta e i gatti, Marco e la sua Elisa, Pas e i panorami, Valentina e i pezzettini di colla di pesce, Nadia e…qualsiasi cosa sia commestibile, Franz e avanti e indietro da Roma, Stefano e il fantacalcio, Rosa e il kebab di Menilmontant, Annarita e casa Bellavista, Mena e le serate fuori al terrazzino, alla piccola India che ci guarda da lassù e chissà quanti ne sto dimenticando!

E ora arriviamo alla parte difficile! Difficile perché non si può semplicemente ringraziare i pilastri della propria vita!

Roberta…non riesco neanche a descrivere quello che mi lega a te…penso che nella vita sono stata fortunata perché oltre al vero amore ho incontrato anche la vera amicizia. Ci siamo sempre state l'una per l'altra e so che dovunque mi condurrà la vita questa cosa non cambierà mai. Ecco…le lacrime mi stanno scendendo già ora…figuriamoci all'esame! Mettere un punto a questa tesi vuol dire anche mettere un punto a una fase della mia vita in cui ci sei sempre stata, ogni singolo giorno…e forse non avere più questa quotidianità con te è la cosa che mi pesa di più. Ti auguro tutto il bene possibile e di andare sempre avanti, sia nella tua vita che nel lavoro. Un grazie anche a zio Marco!

Alla mia famiglia a cui come sempre è toccato il compito più gravoso, ossia sopportare il mio caratteraccio nei momenti "no" (perché? Ci sono stati dei momenti "si"??). Spero di non avervi mai deluso e di continuare a non farlo mai, perché avendo avuto tutto devo restituirvi tutto, prima o poi.

All'amore della mia vita! Tore, questi anni sono stati complicati, pieni di avvenimenti…ne abbiamo passato la gran parte distanti, ma i nostri cuori, dal momento in cui ci siamo conosciuti, non

hanno fatto altro che avvicinarsi…fino ad unirsi per dare vita alla parte più importante di noi…la piccola Rebecca.

Piccola mia…ti auguro di raggiungere tutti i tuoi obiettivi come ho fatto io finora, di avere sempre tanta passione per quello che fai, di avere sempre il sorriso sulle labbra e anche nel cuore. Anche se mi hai costretto a scrivere questa tesi con una mano sola, questo lavoro, questo mio successo è solo per te!